NASA TECHNICAL NOTE

NASA TN D-2069

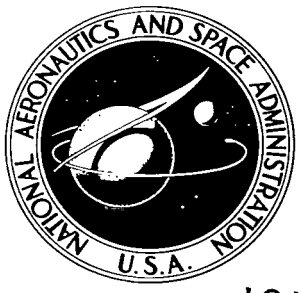

NASA TN D-2069

PROSPECTS FOR OBTAINING AERODYNAMIC HEATING RESULTS FROM ANALYSIS OF METEOR FLIGHT DATA

by H. Julian Allen and Nataline A. James

Ames Research Center

Moffett Field, Calif.

NATIONAL AERONAUTICS AND SPACE ADMINISTRATION • WASHINGTON, D. C. • JULY 1964

PROSPECTS FOR OBTAINING AERODYNAMIC HEATING RESULTS FROM ANALYSIS OF METEOR FLIGHT DATA

By H. Julian Allen and Nataline A. James

Ames Research Center
Moffett Field, Calif.

NATIONAL AERONAUTICS AND SPACE ADMINISTRATION

For sale by the Office of Technical Services, Department of Commerce,
Washington, D.C. 20230 -- Price $2.75

TABLE OF CONTENTS

PROSPECTS FOR OBTAINING AERODYNAMIC HEATING RESULTS FROM ANALYSIS OF METEOR FLIGHT DATA

By H. Julian Allen and Nataline A. James

Ames Research Center
Moffett Field, Calif.

SUMMARY

Analyses of velocity and luminosity records of meteor flight obtained from ground based cameras provide a means for increasing our knowledge on aerodynamic heating of bodies entering the atmosphere at earth hyperbolic speeds. The principles of the dynamical and photometrical methods of analysis are reviewed. Results from records of six bright meteors are compared with expected behaviors for these meteors. Reasons for departure from expected behavior are discussed and future prospects are treated.

INTRODUCTION

For over a decade, now, aerodynamicists in this country have been intimately concerned with the return to earth of man-made objects propelled into space by rockets. The first interests in the problems of entry into the earth's atmosphere were confined to the aerodynamic stability, loading, and heating of ballistic missiles. Later these interests were concerned with higher speed bodies, such as Mercury. Now our attentions are focused on the Apollo vehicle, and in time we shall need to understand atmosphere entry phenomena associated with interplanetary vehicles which, on return to earth, may approach the atmosphere at speeds well in excess of earth parabolic speed. It would be foolish to attempt to say what limit on entry speed will ultimately be established as practicable. It is only important here to note that we must, from the research standpoint, obtain, from theory and experiment, proper understanding of all the phenomena of atmospheric entry up to speeds as high as can be realized.

Theory, as in the scientific delineations of all natural philosophy, is vital to our understanding of the phenomena of high-enthalpy air flow. In hypersonic flow problems experimental results are also vital because many of the basic physical concepts involved are not well understood. Thus, it is the partnership of theoretical and experimental research from our ground-based laboratories that has accounted for the rapid progress in this scientific field.

Progress in the laboratory is fraught with difficulties. The tools of the experimentalist are high-performance shock tubes and shock-tube wind tunnels, ballistic ranges, and combinations of such facilities to provide the

required test environment. The testing is exacting because of the short time available for observations but, more important, there is justified concern that we may not be able to provide the test speeds and enthalpies we will need in the future because of strength limitations of the materials of which our laboratory facilities are constructed. Present facilities have provided environments appropriate to free flight at speeds somewhat in excess of 13 km/sec. We expect, from present knowledge, that we may extend these to 15 km/sec or thereabouts. However, there are no assurances that further improvement will be forthcoming.

One, then, turns to rockets in free flight as tools for research at higher speeds. One finds them unattractive in the main because of their great cost in both money and time. Practically, we can hope they will confirm results obtained in ground tests, in particular as regards scaling laws, but will probably not contribute importantly to our basic fund of knowledge.

On the other hand observations of meteors in flight can possibly provide valuable experimental data. At first glance these look unusually attractive because the rate of influx of extraterrestrial debris into the earth's atmosphere is very great. However, the concern of the aerodynamicist is with hypersonic continuum flow and but a small fraction of the meteoric bodies experience any but free molecular flow. In addition, of those which are observed by properly instrumented observatories, the resulting meteorite has been recovered only in one case (the fragments from the Czechoslovakian meteor Příbram), so that with this exception the meteor density is not known nor can the body shape during descent be inferred. Nonetheless, the flight data from meteor observations may provide useful results. The purpose of this paper is to acquaint aerodynamicists with the methods of analyzing flight data of meteors and to apply these methods to six meteors for which published data are available in order to indicate to what extent such sources can provide useful information to aerodynamicists in the future.

METEOR PHENOMENA

Although man has certainly been awed by the meteor phenomenon since the earliest times, it is strange that only within the last several centuries has the phenomenon been appreciated in its proper perspective. Chladni is credited (ref. 1) with being the first modern scientist to demonstrate that meteoric bodies were, in fact, extraterrestrial in origin. Öpik in 1922 (ref. 2) seems to have been the first to have attempted to formulate theory to understand quantitatively the behavior of meteoric bodies in their descent through the atmosphere. He showed that if the mass loss from the body per unit of distance traveled was proportional to the instantaneous kinetic energy, then simple relations could be obtained for expressing the mass in terms of velocity. Lindemann and Dobson, in the following year, published a remarkable paper (ref. 3) in which they proposed physical models of the heating processes in an effort to determine the fraction of the total kinetic energy involved in the mass loss by ablation. Although their analysis contained some basic errors (ref. 4), it is significant in that it correctly distinguished between

the direct air-molecule-impact process, applicable to the many small meteoric bodies, and the shielded impact process, which occurs for the relatively few large bodies, in continuum flow, when a protective gas cap forms ahead of the body. Öpik (ref. 5), Hoppe (ref. 6), and others laid the foundation for the photometrical method of analysis of meteor data in which the rate of mass loss by ablation could be related to the intensity of observable radiation. The current state of meteor theory is summarized by Öpik in reference 7.

Near the turn of this century, Elkin (e.g., refs. 8 and 9; for review see ref. 10), Director of the Yale Observatory, photographed over 100 meteors with two cameras located at the ends of a base line. The cameras were equipped with rotating shutters. The triangulation permitted the determination of the meteor trajectories while the shutters, rotating at a constant rate, occulted the moving images and provided the time-distance records for evaluating velocity and acceleration as a function of time and altitude. Although the accuracy of the early results was not good because of the short base line, the principles employed are the same as those presently used. The philosophy of the data reduction methods currently used for evaluating heights and velocities from meteor photographs was described by Fisher (ref. 11) and the accurate methods now employed are due, in a large measure, to the efforts of the staff of the Harvard Observatory (Dr. Fred Whipple, Dr. Luigi Jacchia, et al.). There are, at the present time, at least three groups engaged in essentially continuous observations of meteors in North America and Europe: the Smithsonian Astrophysical Observatory group at Harvard University under Dr. Fred Whipple, the group under Dr. Zdenek Ceplecha at the Ondřejov Observatory in Czechoslovakia, and the group at the Canadian Dominion Observatory in Ottawa headed by Dr. Peter Millman of the National Research Council.

Several facts concerning meteors that are important to this paper are the following: First, photographic observations have shown that the speeds at entry into the earth's atmosphere range from about earth parabolic speed (11 km/sec) to about the highest speed a body may have and still be a member of the solar system (72 km/sec). Second, the meteoric bodies may have a variety of compositions. As is well known, meteorites (which are meteoric bodies recovered on the earth's surface) as seen in museums are stony or metallic in composition. However, there are wide variations in these two classes (ref. 1). Many stony meteorites (e.g., chondrites) are of greater density than the surface rocks of the earth, but many are of more normal density. The metallic meteorites are most commonly composed of iron and nickel. It should be emphasized that these museum meteorites, which apparently come from the asteroid belt and have relatively low speeds at atmosphere entry, are assuredly of extraterrestrial origin, but almost certainly are not the only materials which arrive on earth from space. Chapman (ref. 12) has convincingly demonstrated that the glassy objects known as tektites are also meteoritic and most probably of lunar origin. Some fast meteoroids, which appear to be of cometary origin (refs. 13 and 14), are much less dense than water, as indicated by their behavior during atmosphere entry (e.g., refs. 15 and 16). It is probable that hosts of materials found on the surface of the

earth are meteoric but, because they are the same or similar in composition to terrestrial materials, are not recognized to be extraterrestrial in origin.

ANALYSIS

Two methods are currently employed for analyzing meteor tracking data to obtain the size and heat-transfer characteristics as a function of altitude. The first method discussed herein, termed the dynamical method, employs the velocity history along with the equation of motion and the equation for heat transfer to determine the desired quantities. The second, termed the photometrical method, employs the velocity history and a relation between luminosity and mass loss. For all but one of the meteors considered in this report both analyses are required since the meteor density is not known because the meteorites were not recovered. The symbols used in this report (see appendix A) are, for the most part, the convention of aerodynamicists. (The meteor astronomers employ other symbols but these are related in the appendix.)

The Dynamical Method of Analysis

In this method the inputs are velocity and acceleration as a function of time or altitude, the trajectory angle, and the density of the meteoric body.

The equation of motion of an arbitrary body descending through the earth's atmosphere, and acted upon only by the gravitational force and the aerodynamic drag if the earth is assumed flat (see ref. 17), is[1]

$$m \frac{dV}{dt} = mg \sin \theta - \frac{1}{2} C_D \rho V^2 A \qquad (1)$$

wherein

m	mass
V	velocity
t	time
g	acceleration of gravity
θ	angle measured below the local horizontal to the trajectory
C_D	drag coefficient
ρ	air density
A	reference area upon which the drag coefficient is based

[1]In this development, the gravity terms are retained for completeness, but in practice they may generally be ignored as trivial.

In reality, all of the quantities are variables as we proceed along the trajectory. For purposes of the analysis to follow, certain restrictions are imposed. The assumptions are made that:

1. The trajectory is a straight line ($\sin \theta$ is constant).

2. The acceleration of gravity, g, is constant.

3. The body is spherical throughout the descent (for justification see ref. 18).

4. The drag coefficient is constant (assumed unity).

Then if r is the radius of the sphere and ρ_m is the density of the meteoric body, the mass is

$$m = \frac{4}{3} \pi \rho_m r^3 \tag{2}$$

and the reference area is

$$A = \pi r^2 \tag{3}$$

and if the air density is

$$\rho = \rho_o \bar{\rho} \tag{4}$$

then equation (1) becomes

$$\frac{dV}{dt} = g \sin \theta - \frac{3 C_D \rho_o}{8 \rho_m} \left(\frac{\bar{\rho} V^2}{r} \right) \tag{5}$$

Also,

$$dt = - \frac{dh}{V \sin \theta} \tag{6}$$

So equation (5) can be expressed as

$$\frac{d}{dh} (V^2 + 2gh) = \frac{3 C_D \rho_o}{4 \rho_m \sin \theta} \left(\frac{\bar{\rho} V^2}{r} \right) \tag{7}$$

From equation (5) the radius is

$$r = - \frac{3 C_D \rho_o}{8 \rho_m} \left[\frac{\bar{\rho} V^2}{(dV/dt) - g \sin \theta} \right] \tag{8}$$

and from equation (7) is

$$r = \frac{3C_D\rho_o}{4\rho_m \sin\theta}\left[\frac{\bar{\rho}V^2}{(d/dh)(V^2 + 2gh)}\right] \tag{9}$$

It is customary in analysis of the aerodynamic heating of meteors to assume that

1. The rate at which heat is radiated from the body is trivial compared to the total heat input rate, and

2. The rate of heat storage within the body can be ignored compared to the total heat input rate.

The first of these is permissible at the high speeds of meteors if the body is not very small, which covers the cases of interest in this report, and if the trajectory is reasonably steep (say, $\theta > 10^o$). The second is permissible when the thermal conductivity is low. This is certainly the case for meteoric stones and generally acceptable for meteoric irons as well.

With these assumptions, then, the rate of heat input must equal the rate at which heat is lost as a result of surface ablation so that

$$\zeta \frac{dm}{dt} = -\frac{1}{2} C_H \rho V^3 A \tag{10}$$

wherein

ζ the heat of ablation expressed in units of the kinetic energy equivalent per unit mass (i.e., V^2 units) is the energy required to heat the surface from the cold state to the state at which ablation occurs. If a fluid is ablated, then ζ must include the latent heat of fusion; if a vapor is ablated, then it must include both the latent heats of fusion and vaporization.

C_H the mean heat-transfer coefficient based on the cross-sectional area

Now, since

$$\frac{dm}{dt} = \frac{d}{dt}\left(\frac{4}{3}\pi\rho_m r^3\right) = 4\pi r^2 \rho_m \frac{dr}{dt} = 4\rho_m A \frac{dr}{dt} \tag{11}$$

equation (10) becomes (with eq. (4))

$$\frac{dr}{dt} = -\frac{C_H \rho_o}{8\zeta\rho_m}(\bar{\rho}V^3) \tag{12}$$

and with altitude rather than time as the independent variable (see eq. (6))

$$\frac{dr}{dh} = \frac{C_H \rho_o}{8\zeta \rho_m \sin \theta} (\bar{\rho} V^2) \tag{13}$$

The radius of the body can be calculated from equation (9) as a function of altitude if V and dV/dt (or dV/dh) are given, if the air density ratio $\bar{\rho}$ is assumed to be a known function of altitude. For all the calculations of this report the ARDC 1959 Standard Atmosphere (ref. 19) was chosen. Generally, however, the density of the meteoric body is not known because the meteorite is not recovered on the ground so that we shall usually know, in the end, only the product

$$\rho_m r = \frac{-3C_D \rho_o}{8} \left[\frac{\bar{\rho} V^2}{(dv/dt) - g \sin \theta} \right] \tag{14}$$

or

$$\rho_m r = \frac{3C_D \rho_o}{4 \sin \theta} \left[\frac{\bar{\rho} V^2}{(d/dh)(V^2 + 2gh)} \right] \tag{15}$$

In the event the density is known, the mass can be calculated from equation (2).

Differentiation of equation (8) gives

$$\frac{dr}{dt} = - \frac{3C_D \rho_o}{8\rho_m} \frac{d}{dt} \left[\frac{\bar{\rho} V^2}{(dV/dt) - g \sin \theta} \right] \tag{16}$$

while differentiation of equation (9) gives

$$\frac{dr}{dh} = \frac{3C_D \rho_o}{4\rho_m \sin \theta} \frac{d}{dh} \left[\frac{\bar{\rho} V^2}{(d/dh)(V^2 + 2gh)} \right] \tag{17}$$

Thus equations (16) and (12) give

$$\frac{C_H}{C_D \zeta} = \frac{3}{\bar{\rho} V^3} \frac{d}{dt} \left[\frac{\bar{\rho} V^2}{(dV/dt) - g \sin \theta} \right] \tag{18}$$

or from equations (17) and (13)

$$\frac{C_H}{C_D \zeta} = \frac{6}{\bar{\rho} V^2} \frac{d}{dh} \left[\frac{\bar{\rho} V^2}{(d/dh)(V^2 + 2gh)} \right] \tag{19}$$

Note that if C_D is presumed known (for a sphere it is assumed as unity for continuum flow), the heat-transfer coefficient cannot be determined unless ζ is known, which it is not. There is an upper limit to the possible values of ζ, however, which is the total energy required to bring the

surface material from the cold solid state to the vapor state.[2] Thus, an upper limit for C_H can be found in any event. For stone meteors one expects that vaporization would be the usual ablation process. That is to say, liquid stone is highly viscous so that ablation in the liquid state should generally not occur if the heating rates are high. For low-speed meteors or for nearly flat trajectories, this will not be the case. Chapman (refs. 12 and 20) has made a very detailed analysis of the ablation of tektites. He has indicated to us that for the stagnation point of tektites entering the atmosphere at $\theta = 20^\circ$ the ratio of vapor-to-total ablation will be

V, km/sec	Mass vaporized / Total mass ablated
7	0.08
9	.15
11	.22
15	.38

Since liquid stone is probably less viscous than liquid tektite, even more extensive liquid run-off would be expected. For these low heating-rate cases one must expect a considerable mass loss in the fluid state.

On the other hand, when air loads and heating rates are sufficiently high one expects that ablation in the solid state may occur. Stone is a weak material so that projecting segments may be torn from it when air loads are high. Because the thermal conductivity is low, it may also spall as a result of excessive thermal stress when heat rates are very great. Nininger (ref. 1) notes that such structural failure is common for brilliant meteors.

For stone meteors, then, one expects ablation by vaporization; however, when the speed of entry is low or the trajectory is nearly flat, fluid ablation will predominate, or when the speed of entry is high and the body is large and in steep descent, structural failure and spalling occur so solid ablation may predominate. Also when the stone is weak, as we shall see appears to be the case for several examples, solid ablation will be prevalent.

For iron meteors, thermal conductivity is reasonably high and the material is strong. Ablation in the solid state would not be expected at all except, perhaps, for huge bodies. On the other hand, liquid iron has a very low viscosity (about one order of magnitude lower than for cold water) so that when the melting point is reached, the melted layer should be rapidly sluffed off by the aerodynamic shear. Thus one expects for iron a value of ζ corresponding more closely to fusion (i.e., the energy required to bring a unit mass from the cold solid state to the liquid state).

---

[2]Note that ζ as used herein is not the so-called "effective" heat of ablation commonly used by aerodynamicists, but rather the actual heat of ablation since C_H is the actual heat-transfer coefficient because it includes the blockage of convective heat input due to ablation.

Appropriate values for vapor and fluid ablation of stone and iron are given in table I.

For the low density cometary types, which are presumably of a weak porous stone, one expects profuse ablation in the solid state. Results of heat-transfer analysis for such bodies, accordingly, will not be very useful in attempting to assess heat-transfer coefficients.

An additional equation we shall find of value is obtained from equations (1), (6), and (10)

$$\frac{dm}{m} = \frac{C_H}{2C_D\zeta} d(V^2 + 2gh) \tag{20}$$

If one may substitute a mean value of $C_H/2C_D\zeta$ in this expression it can be integrated to give

$$\frac{m}{m_E} = e^{-(C_H/2C_D\zeta)[V_E^2-V^2+2g(h_E-h)]} \cong e^{-(C_H/2C_D\zeta)(V_E^2-V^2)} \tag{21}$$

where subscript E denotes values at entry to the atmosphere.

Two computation procedures have been used to apply the dynamical method of analysis to a number of meteors to be discussed later. These procedures are detailed in appendix B.

The Photometrical Method of Analysis

In this method to find the mass variation during entry to the atmosphere one must know velocity and luminosity as a function of time or of altitude, provided one also knows flight-path angle. To determine size and heat-transfer characteristics as a function of time or altitude one must know the density of the meteoric body as well.

Historically the photometrical method was developed for application to small meteoric bodies entering the atmosphere at high meteor speeds. Such bodies experience free molecular flow, so that no bow shock layer exists. Thus the molecular collisions which occur are only the result of the air molecules colliding with the molecules on and from the surface of the meteoric body. The luminosity observed must result from the collisions of air molecules with the molecules of vapor from the surface and hence be proportional to the rate of loss of mass and the collision energy per unit mass. Thus Öpik (ref. 7) gave the relation

$$I = -\tau \left(\frac{V^2}{2}\right) \frac{dm}{dt} \tag{22}$$

where

I luminous intensity, defined in meteor astronomy as the amount of light received on a surface of 1 square meter area at a distance of 100 km from the source (in units of kilowatts/square meter in this report)

τ so-called luminous efficiency

The luminous efficiency varies with velocity. Jacchia (ref. 21) after examining Öpik's calculation found that τ varied very nearly directly with velocity over the speed range from 20 to 70 km/sec. He therefore proposed the presently accepted mass-loss equation

$$\frac{dm}{dt} = -\frac{2I}{\tau_o V^3} \tag{23}$$

For known luminosity and speed as a function of time one could, from integration of equation (23), then find the mass if the constant of integration were known. For fast meteors in free molecule flow, the factor

$$\frac{C_H V_E^2}{2C_D\zeta} \tag{24}$$

is very large and the final velocity at the earth surface V_o is trivial; then from equation (21)

$$\frac{m_o}{m_E} = e^{-C_H V_E^2/2C_D\zeta} \ll 1 \tag{25}$$

so one can obtain the meteor mass as a function of time from

$$m = \frac{2}{\tau_o}\int_t^{t_o} \frac{I}{V^3}\,dt \tag{26}$$

where t_o may correspond to any time near the end of the trajectory after which I has become trivially small.

When the meteor entrance speed, V_E, is low then even for meteoric bodies in free molecular flow the assumption that the end mass, m_o, is trivial cannot be made. Cook (ref. 22) has proposed a procedure for this case.

Although equation (23) can yield the mass during entry, neither the size nor the heat-transfer factor can be determined until the density of the meteoric body is known. Again if the body is a sphere of known density then (for $m_o \cong 0$) the radius can be found from

$$r^3 = \frac{3}{2\pi\tau_o\rho_m}\int_t^{t_o} \frac{I}{V^3}\,dt \tag{27}$$

and the heat-transfer factor from equations (10) and (23) as

$$\frac{C_H}{C_D\zeta} = \frac{4}{\pi r \rho_o \tau_o}\left(\frac{I}{\bar{\rho} r^2 V^6}\right) \tag{28}$$

The luminosity method as outlined above is applicable only to meteors in the free molecular flow regime. In continuum flow the total luminosity is composed of contributions from the excited air in the shock layer (resulting from air-to-air molecular collisions) as well as from the products of ablation (resulting from air-to-meteor vapor molecular collisions). Thus (ref. 23),

$$\frac{dm}{dt} = -\frac{2(I - I_g)}{\tau_o V^3} \tag{29}$$

where I_g is the gas-cap luminosity. For bodies at meteoric speeds, the gas-cap luminosity will generally be much less than the total gas-cap radiation would indicate since most of the air radiation is in the ultraviolet which is not received at the photographic plates (usually the cutoff occurs at wavelengths of 3500 Å or greater).

A second difficulty with the use of equation (29) is that for the case of continuum flow, τ_o has not been evaluated. The molecular collisions of air and vapor are generally less energetic so one expects the continuum τ_o to differ from that appropriate to free molecular flow but, at present, by unknown amounts.

A third difficulty is the following: In the dynamic method, the mass-loss rate dm/dt refers to the meteoric body, but in the photometrical method, this is not necessarily the case. The ablation luminosity, as noted earlier, results from the collisions of air and vapor molecules and hence does not appear until the material from the body is vaporized. If, as a result of excessively great aerodynamic forces or thermal stress, material is jettisoned from the body in the solid state or if it flows off the body in the liquid state, there will be a time lag until vaporization of the debris occurs in the wake. Hence the mass, m, in the photometrical method refers to the vaporizing mass in the system (body plus wake) and thus is not synonymous with the body mass itself.

The final difficulty is that the equation for mass obtained by integration of equation (29) has a constant of integration which cannot, in the general case, be evaluated. This was noted earlier to be a difficulty even in free molecular flow for which, in the usual case, the factor $C_H/C_D\zeta$ is larger than for continuum flow. Thus, as noted in the earlier discussion of equation (21), one cannot approach the limiting case of equation (25) until the entry speed is even greater in the continuum flow case than is required in the free molecular flow case.

In spite of the difficulties outlined above, the photometrical method has much promise. It is employed in the analysis of five of the meteors of this report. The procedures in these special cases are treated in appendix C.

In reviewing the variation with altitude of the heat-transfer factors for the several meteors considered herein, as obtained from either the dynamical or photometrical analysis, it is most valuable to compare the results with estimated values of the heat-transfer factors assuming either pure vapor or pure fluid ablation. Appendix D gives the details of the estimation procedure used in this report.

METEOR DATA

The tracking results obtained from the photographic records of six meteors have been used for analysis of size and heat-transfer history during entry to be given later. Pertinent details of the individual meteors are given in the following:

1. Meanook meteor 132

This meteor was photographed in Canada on October 20, 1952 at the Meanook and Newbrook Meteor Observatories. A description of the results is given in reference 24. Luminosity data as well as velocity and acceleration are available as a function of time and altitude. The luminosity data are not tabulated herein but are shown in figures introduced later. The velocity and acceleration data are given in table II. The listing is more complete than that given in the original report of reference 24 and contains a correction for one acceleration value which, as originally given, was in error. These complete values were communicated to the senior author by Dr. Peter Millman of the National Research Council of Canada.

2. Ondřejov meteor 15761

This meteor was photographed on the night of August 13, 1958 at the Ondřejov Observatory and Prcice Station in Czechoslovakia. The data on this meteor in complete form are obtained from reference 25. The data from table 4 of the reference are given in table III of this report. The luminosity data are given in a figure introduced later in the report.

3. Harvard meteor 1242

This meteor was photographed from the Harvard College Observatory and the Oak Ridge Station (now Agassiz Station) in Massachusetts on February 6, 1945. The reduced data are given in table IV as obtained from reference 26 with the exception of the probable error values which were communicated to the senior author by Mrs. Annette Posen of the Harvard College Observatory staff. The probable errors in acceleration were given in percent and converted to the tabular values shown. The probable errors in velocity were reported to be negligible so that the error of ±5 m/sec is appropriate to the original data (given to closest 10 m/sec).

4. Sacramento Peak meteor 19816

This meteor was photographed on December 8, 1958 with the Super-Schmidt meteor cameras at the Sacramento Peak and Organ Pass Meteor Stations in New Mexico. The reduced data are given in table V as obtained from reference 26. The value of probable errors in velocity and acceleration were communicated to the senior author by Mrs. Annette Posen of the Harvard College Observatory staff.

5. Ondřejov meteor 27471

This meteor was photographed on the night of October 26, 1960 at the Ondřejov Observatory and Prcice Station in Czechoslovakia. The data on this meteor are to be published (ref. 27). The data shown in table VI were those Dr. Ceplecha distributed at the International Symposium on the Astronomy and Physics of Meteors held in Cambridge, Massachusetts, August 28 - September 1, 1961.

6. Ondřejov meteor Příbram

This brilliant fireball (-19th absolute magnitude) fell on April 7, 1959 in Czechoslovakia (ref. 28) and was photographed at the Ondřejov Observatory and the second station at Prcice. At the Ondřejov Observatory, one camera with rotating shutters provided data from which velocity and acceleration could be deduced only over the initial portion of the trajectory (90 km > h > 40 km) wherein the large descending body was still intact. Structural collapse began at a slightly lower altitude and progressive separations followed. The resulting trajectories of the fragments were photographed but velocity data from the later flight records are not complete. The separation of the main body into 17 pieces was photographed well enough so that 4 of the resulting meteorites were found from the tracking data. Table VII gives the velocity and deceleration data for the beginning segment of the trajectory. The luminosity data from the reference have been plotted in figures introduced later in this report.

RESULTS

It is the purpose of this report to determine to what extent analysis of meteor tracking data can contribute to our knowledge of heat transfer to large entry bodies in continuum flow at entry speeds well in excess of earth parabolic speed. Results of the analyses of each of the six meteors introduced in the preceding sections will be given and discussed in order to attempt to answer the following questions, which are basically three:

1. Can the photographic record of the flight of a meteoric body through the atmosphere provide the measurement of velocity as a function of altitude with the degree of accuracy required for the meteor size and heat-transfer results to be meaningful when analyzed by the dynamical method?

2. Do the heat-transfer results appear reasonable? In particular, what do they infer regarding the structural integrity of meteoric bodies subjected to large aerothermodynamic loads?

3. Does the photometrical method of analysis yield results in agreement with the dynamical method? In particular, does it appear that the assumption of a constant value for the luminous efficiency factor, τ_o, independent of air density, size, or speed, is valid?

Meanook Meteor 132

The reduced[3] velocities and accelerations data are given by the circled points in figures 1 and 2. The solid lines on these figures show velocity and acceleration variation with altitude calculated by means of a sixth-degree, least-squares polynomial fit in which all velocity and acceleration data were used to evaluate the coefficients in the series. Not only do the reduced flight data show remarkably smooth variations with altitude but these data are self-consistent as indicated by the results obtained from the series.

In figure 3 the variations of meteor density-radius product with altitude as deduced from the point-to-point solution and the series representation of the data are seen to be in good agreement, except at the highest altitudes where small errors in acceleration can promote large errors in the meteor density-radius product. The results are certainly acceptable.[4]

The circled points of figure 4 give the measured luminous intensity as a function of altitude for this meteor. The solid curves show what is calculated as total luminous intensity for meteor densities of 800 and 900 kg/m^3 presuming that the luminous efficiency factor, τ_o, has the value suggested by Jacchia (see appendix E, eqs. (E12) and (E13)). The dashed curves represent the calculated contribution of the shock layer to the luminous intensity which, for this meteor, is a small part of the total. The inference, here, is that the meteor density is between 800 and 900 kg/m^3 - that is to say, less than the density of water (1000 kg/m^3). The fact that the variation of the calculated and observed intensities with altitude is roughly the same indicates that τ_o is apparently not importantly influenced by meteor velocity or air density but it should not be inferred from this figure that the proper value for τ_o could not be either larger or smaller than that used for these calculations. For example, had the value of τ_o used been zero the

[3]In this report "original data" is defined as the data deduced from each and every segment of the occulted meteor track on the meteor camera photographic plates while "reduced data" is that obtained from least-squares fits to groups of original data points; see appendix B.

[4]Note that the abscissa of figure 3 should properly be $(\rho_m r/C_D)$. Thus if C_D were to increase at the highest altitudes shown, one could account for the observed trend. Just such an increase would occur if this region were characterized by transition from continuum ($C_D \cong 1$) to free molecular ($C_D \cong 2$) flow. For the expected density the body size is so large relative to the mean free path that this explanation is not attractive here.

agreement between the shock layer luminous intensity alone would have agreed about as well with the observed intensities if the meteor density were assumed to be 240 kg/m^3. This is seen in figure 5. However, it must be noted that τ_o cannot be either zero or very small compared to Jacchia's value because the observed spectrum (ref. 24) shows such strong radiation in the wavelengths corresponding to the typical meteoric material (iron, calcium, etc.) that the air radiation wavelengths are not evident by comparison.

Figure 6 gives the variation of the heat-transfer factor, $C_H/C_D\zeta$, with altitude. The point-to-point values are shown as the circled values while the series values are shown by the solid line. The dotted curves represent the estimated values[5] for the heat-transfer factor when the meteor density is assumed to be 900 kg/m^3 for both vapor and fluid ablation. It is seen that even the estimated values for fluid ablation fall short of those deduced from the flight data by the dynamical method. Presumably this low-density meteoric body, supposedly porous, was subject to successive structural failures from the high aerodynamic and thermodynamic stresses induced so that a fair fraction of the surface material was ablated in the solid state. Thus the heat of ablation would be low so that the heat-transfer factor exceeds what would otherwise be expected.

Let us turn now to the results as predicted by the photometrical analysis. The best fit for velocity and acceleration was obtained with an assumed meteor density of 850 kg/m^3. Figures 7 and 8 give the results which are certainly satisfactory when compared to the flight data. Figure 9 shows a comparison of the meteor density-radius product as determined by the photometrical analysis with those deduced by point-to-point dynamical analysis (circled points) and the least-squares series dynamical analysis (dashed curve). Figure 10 shows a similar comparison of the results obtained from the photometrical and dynamical methods for the variations with altitude of the heat-transfer factor. These results are in rather remarkable agreement.

All in all, the results of this study of Meanook meteor 132 are most encouraging. The reduced velocity and acceleration data as well as the observed luminous intensity are of high quality and are mutually consistent. One cannot escape the conclusion that tracking of meteors by the photographic method can be precise.

Ondřejov Meteor 15761

It is of considerable interest to compare the results of the dynamical analysis of this meteor with that of Meanook meteor 132. Figures 11 and 12 give the reduced data for this meteor and compare it with the sixth-degree least-squares series results for which the series coefficients are based on all the velocity and acceleration data. As for the previous meteor, the

[5]The present estimates do not agree with those given in reference 23 which contained some serious errors in evaluation of radiation heat-transfer contributions.

velocity variation with altitude appears smooth and well defined. The accelerations are not so satisfactory, however, but the reduced values of mean error appear sufficiently large, in the main, to permit a reasonably smooth variation to be defined. The meteor density-radius product, as seen in figure 13, now appears ragged and ill defined. The serious weakness of the dynamical method is that in passing from velocity to acceleration (or to the density-radius product) to the heat-transfer factor, each function involves, in turn, differentiation of the last. Thus unless the velocity, for example, is unusually well defined, the heat-transfer results are apt to appear chaotic. Figure 14 demonstrates this well. On first view of these results they appear to be worthless. But, if instead of looking at the altitude distribution, one calculates by the dynamical method the mean value of the heat-transfer factor over the whole altitude range, one obtains

$$\frac{C_H}{C_D\zeta} \times 10^8 = 1.98 \pm 0.71 \text{ sec}^2/\text{m}^2 \tag{30}$$

by the point-to-point method which compares favorably with

$$\frac{C_H}{C_D\zeta} \times 10^8 = 2.13 \text{ sec}^2/\text{m}^2 \tag{31}$$

for the mean value obtained from the series method.

A question naturally arises as to why the quality of the data for this meteor appears to be so inferior to that for the Meanook meteor 132. One likely explanation is that on the night the Czechoslovakian meteor was photographed, the upper atmosphere was turbulent so that the light was diffracted in different directions at different positions along the trajectory leading to an apparent fluctuation in speed which, in fact, was not real. Such atmospheric turbulence causes jitter of a fixed star image seen through a telescope. Astronomers refer to such a situation as "a poor seeing condition."[6] Conversely, the Canadian meteor results were probably obtained under good seeing conditions.

Figure 15 gives the observed luminous intensity for the Ondřejov meteor 15761 as shown by the solid curve. The dashed curves show the calculated characteristics for an assumed meteor density of 1000 kg/m^2. The agreement between the calculated and observed trends are so inadequate as not to fix the probable value of density by examination of this figure. The photometric analysis does indicate that about the best fit of the meteor density-radius product with that calculated from the dynamical analysis gives a meteor density of 1100 kg/m^3, as shown on figure 16, which was accordingly the value used in estimating the heat-transfer characteristics. As for Meanook meteor 132 this meteor is apparently composed of some weak porous material.

---

[6]It would seem advisable at meteor photography stations to install a telescope to measure the jitter of the image of some fixed star (e.g., Polaris) so that the probable accuracy of the meteor tracking data could be assessed.

The results of the photometrical method appear far more satisfactory. Figures 16, 17, and 18 compare the meteor density-radius product, velocity, and acceleration from this method and from the dynamical method. Finally, figure 19 compares the heat-transfer results of the photometrical analysis with the series method of the dynamical analysis. The photometrical results are reasonable ones. As for Meanook meteor 132, a constant value for τ_o therefore seems appropriate.

Harvard Meteor 1242

Figures 20 and 21 give the velocity and acceleration data for this meteor and, for comparison, the results of a fourth-degree least-squares series. The comparison is not encouraging. Thus the curves of meteor density-radius product (fig. 22) and the heat-transfer factor obtained (fig. 23) are ragged. However, if one excludes the high-altitude point-to-point value for the heat-transfer factor, the point-to-point results would seem reasonable for stone (ρ_m = 3400 kg/m^3) when compared with the estimated values. However, a comparison of the calculated luminosity employing Jacchia's value for luminous efficiency (appendix E) favors some more dense material such as iron (ρ_m = 7800 kg/m^3) as the meteoroid composition (fig. 24).

It is the opinion of Cook, Jacchia, and McCrosky (ref. 26) that this meteoroid is a typical asteroidal stone, so that one perhaps can use the photometrical analysis to define a better value for the luminous efficiency factor, τ_o, than that used throughout this report. Accordingly, in these calculations a range of values were assumed for τ_o. Figures 25, 26, and 27 give the velocity, acceleration, and meteor density-radius ratio for the "best fit" case for which

$$\tau_o = 0.85 \times 10^{-20} \frac{\text{kw sec}^4}{\text{kg m}^5} \tag{32}$$

The heat-transfer factor from the photometrical analysis with this value of the luminous efficiency factor is shown in figure 28 wherein it is compared with the point-to-point values from the dynamical analysis and with the estimates for stone. These photometric values are less ragged in their altitude variations than are the dynamical values. One expects this behavior from such a small and slow-speed stone body because aerodynamic loads and thermal stress are low so that solid-state ablation should be minimized. The velocities are low so that the estimated values should be reasonably accurate, as essentially no extrapolation of our present knowledge is required. Nevertheless, the photometric values are well above the vapor estimates.

Sacramento Peak Meteor 19816

The reduced data for velocity and acceleration are compared with the fifth-degree least-squares series solution in figures 29 and 30, respectively. Figures 31 and 32 give the meteor density-radius product and the heat-transfer variations with altitude, respectively, for both the point-to-point and series solution of the dynamical analysis. The estimated heat-transfer characteristics assuming vaporizing stone (ρ_m = 3400 kg/m^3) are in reasonable agreement with the point-to-point values when the probable errors are taken into account. The assumption of stone density seems to give fair to poor agreement between the level of the calculated and observed luminous intensity[7] (fig. 33).

As in the case of the preceding meteor, this one is considered (ref. 26) to be typical asteroidal stone. Hence, again, the photometrical analysis might serve to give a better value for the luminous efficiency factor, τ_o, than that which has been used throughout this report. Figures 34, 35, and 36 give the velocity, acceleration, and meteor density-radius product for the "best fit" value which is

$$\tau_o = 0.95 \times 10^{-20} \frac{\text{kw sec}^4}{\text{kg m}^5} \tag{33}$$

Figure 37 gives the heat-transfer-factor variation with altitude from the photometrical analysis with the above value for the luminous efficiency factor. Point-to-point dynamical analysis results are given for comparison as well as the estimates for stone. The values are on the average somewhat above the estimates for vapor ablation.

Ondřejov Meteor 27471

For this meteor, velocity data only are given. Figure 38 compares the original data with a fit by a fourth-degree least-squares series. Figure 39 gives a similar comparison with the reduced data. If one uses the reduced velocity data to define a series in which the seven velocity values determine seven coefficients, the resulting accelerations are those shown by the circled points in figure 40. These values are, therein, compared with the fourth-degree least-squares series result and the agreement is excellent. Hence, as seen in figure 41, the agreement in the meteor density-radius products is also very good except at the highest altitudes where small differences in acceleration make large changes in the value of the product. The variation in heat-transfer factor with altitude (fig. 42) shows similar agreement. Luminosity data are not available for this meteor so no photometric analysis could be made. The estimated heat-transfer characteristics were

[7]It will be noted that more original data are given in the figure than in reference 26. These were provided by Dr. R. E. McCrosky in a private communication.

evaluated assuming that the meteoroid was either heavy stone or iron. For vapor ablation there is little difference in the estimate unlike the case for fluid ablation. Ceplecha, from examination of the spectrum, considered that this meteor could have been iron. The dynamical analysis values lie between the vapor and fluid estimates. They suggest that this meteoric body may well be iron which experienced sufficient ablation as vapor to reduce the heat-transfer coefficient from that estimated for iron with purely fluid ablation.

Ondřejov Meteor Příbram

Before examining the Příbram case in detail it is advisable to review the fundamental equation of motion used in the analysis. Equation (1), as it stands, is correct for a body which either does not ablate in the vapor phase, or, if it does, experiences no net reaction in the direction of motion from such ablation. For bodies in continuum flow which experience vapor ablation, such will not usually be the case since some jet reaction to increase the retarding force is to be expected. One may approximate the magnitude of this reaction in the following way:[8] As shown in sketch (a) ablation from the forward face of the body provides a two-gas flow field in the compression cap. If the efflux of vapor is not large, the pressure in the gas cap ahead of the interface will be essentially the same as it would have been in the absence of ablation. The average value for this pressure is therefore the drag per unit area

$$p = \frac{1}{2} C_D \rho V^2 \qquad (34)$$

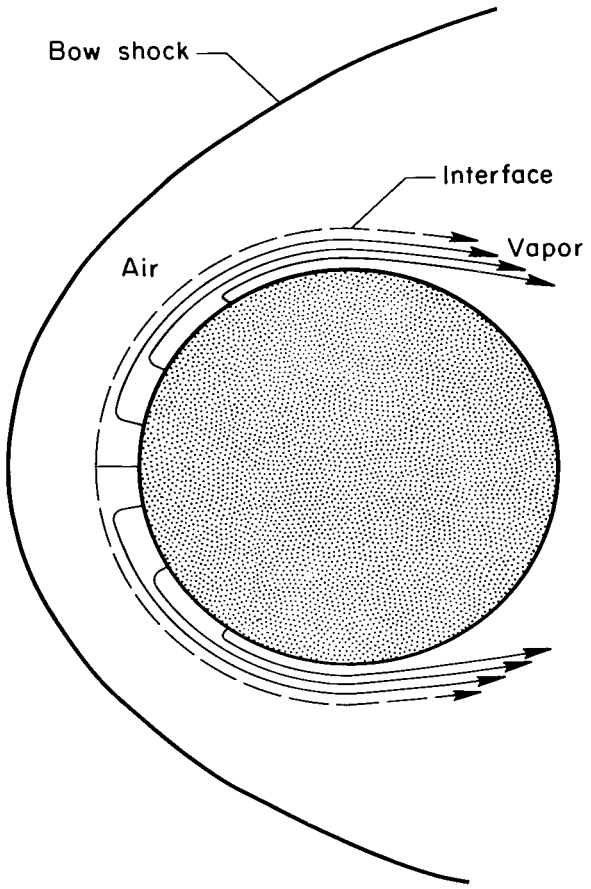

Sketch (a)

The equation of motion is then[9] - if V_v, the velocity of efflux of the vapor from the surface relative to the body, is arbitrarily assumed, for maximum retrothrust, to be counter to the direction of motion of the body

[8]This analysis was developed jointly by Barrett Baldwin, Vernon Rossow, E. Dale Martin, and the senior author of this report.

[9]See reference 29 for a discussion of the equation of motion of a body experiencing a change of mass with time.

$$m \frac{dV}{dt} = mg \sin \theta - \frac{1}{2} C_D \rho V^2 A + V_v \frac{dm}{dt} \tag{35}$$

and since

$$\frac{dm}{dt} = -\rho_v V_v A \tag{36}$$

then

$$m \frac{dV}{dt} = mg \sin \theta - \frac{1}{2} C_D \rho V^2 A - \rho_v V_v^2 A \tag{37}$$

The gas law with equation (34) gives

$$\rho_v = \frac{p}{RT_v} = \frac{1}{2} \frac{C_D \rho V^2}{RT_v} \tag{38}$$

so that equation (37) becomes

$$m \frac{dV}{dt} = mg \sin \theta - \frac{1}{2} C_D \rho V^2 A \left(1 + \frac{V_v^2}{RT_v}\right) \tag{39}$$

Now, in equation (10), the kinetic energy of the ablating vapor must be added to the intrinsic heat of ablation so

$$\left(\zeta_v + \frac{V_v^2}{2}\right) \frac{dm}{dt} = - \frac{1}{2} C_H \rho V^3 A \tag{40}$$

With equations (36) and (38) this becomes

$$V_v^3 + 2\zeta_v V_v - \frac{2RT_v C_H V}{C_D} = 0 \tag{41}$$

The solution for V_v is

where

$$\left.\begin{aligned} V_v &= 2\sqrt{\frac{2\zeta_v}{3}} \sinh \frac{\varphi}{3} \\ \sinh \varphi &= \frac{RT_v C_H V}{C_D (2\zeta_v/3)^{3/2}} \end{aligned}\right\} \tag{42}$$

Thus the motion equation can be written

$$m \frac{dV}{dt} = mg \sin \theta - \frac{1}{2} C_{D_{eff}} \rho V^2 A \tag{43a}$$

wherein the maximum possible value of $C_{D_{eff}}$ is

$$C_{D_{eff_{max}}} = C_D \left(1 + \frac{8\zeta_v}{3RT_v} \sinh^2 \frac{\varphi}{3}\right)$$

wherein

$$\sinh \varphi = \frac{RT_v C_H V}{C_D (2\zeta_v/3)^{3/2}} \qquad (43b)$$

For values of φ of interest in this report $\varphi \cong \sinh \varphi$

$$C_{D_{eff_{max}}} = C_D \left[1 + \frac{RT_v}{\zeta_v^2} \left(\frac{C_H V}{C_D}\right)^2\right] \qquad (43c)$$

where for a molecular weight of vapor of 50

$$R = 166 \text{ m}^2/\text{sec}^2 \text{ }^\circ\text{K} \qquad (44a)$$

and with

$$T_v = 3\times10^3 \text{ }^\circ\text{K}$$

$$\zeta_v = 9.2\times10^6 \text{ m}^2/\text{sec}^2$$

gives

$$C_{D_{eff_{max}}} = C_D \left[1 + 0.59 \left(\frac{C_H}{C_D}\right)^2 \left(\frac{V}{10^4}\right)^2\right] \qquad (44b)$$

For all of the meteors except Příbram, the estimated heat-transfer coefficient is sufficiently small compared to the drag coefficient or the speeds are so low that the effect of retrorocket thrust from ablated vapors is trivial, as can be seen in figure 43.

For Příbram the assumption of unity for the drag coefficient can be in considerable error at the lower altitudes. For several of the analyses of data for Příbram we have therefore considered the two extremes for the drag coefficient (see appendix D)

$$C_{D_{eff_{min}}} = C_D = 1 + C_H \qquad (45a)$$

and

$$C_{D_{eff_{max}}} = C_D \left[1 + 0.59 \left(\frac{C_H}{C_D}\right)^2 \left(\frac{V}{10^4}\right)^2\right]$$

or

$$C_{D_{eff_{max}}} = \left(1 + C_H\right) \left[1 + 0.59 \left(\frac{C_H}{1 + C_H}\right)^2 \left(\frac{V}{10^4}\right)^2\right] \qquad (45b)$$

It was noted earlier for the Příbram meteor that, although the rotating shutter tracking cameras provide flight data for about a 50-kilometer altitude change, the body was so large that the speed change over this interval was very small indeed (less than 500 m/sec in more than 20 km/sec total). Nevertheless, the quality of the data on velocity (fig. 44) and acceleration (fig. 45) at first glance appears excellent. A second-degree polynomial fit using all the reduced data to determine the series coefficients gives smoothly varying values which with few exceptions lie within the listed mean errors. However, when one examines the variation of meteoroid radius with altitude, assuming a drag coefficient of unity, one finds (fig. 46) that the indicated variation is unrealistic (i.e., over a range of altitude, radius increases with decreasing altitude). The series results suggest that the radius at entry might have been as large as, perhaps, 0.3 m but more likely less. It is interesting to note that Ceplecha (ref. 28) has estimated that the initial mass for a drag coefficient of unity ($\Gamma = 0.5$) was 700 kg which corresponds to a radius at entry of 0.37 m.

Another attempt was made to ascertain the probable size of this meteoric body using an analysis, employing a step-by-step integrational procedure, as follows: For an assumed body radius at an altitude of 100 km with assumed velocity of 20,867 km/sec, the estimated heat transfer and drag coefficient (appendix D) were found. These values were used over an interval of 1 km altitude to find the values of r and V at 99-km altitude. The procedure was repeated down to an altitude of 40 km. The calculations were made for a range of values of initial radius and for both the maximum effective drag coefficient (eq. (45b)) and the minimum (eq. (45a)). The results of these calculations are shown in figures 47 and 48. Figure 47 suggests that the radius must be much less than 0.1 m,[10] while 48 suggests that it might be between 0.1 and 0.2 m.

The photometrical analysis of Příbram followed the procedure outlined in appendix C. As noted therein the analysis assumed that the effective drag coefficient could be the minimum or maximum. Figure 49 shows the calculated radius variation with altitude for entry radii up to 1.6 meters. Clearly, the photometrical results are at variance with the dynamical results in that, as seen in figure 49, the initial radius must be of more than 1.3 meters if the body is not to vanish before it reaches an altitude of 40 km. The velocities and accelerations as obtained from the photometrical analysis are shown in figures 50 and 51. The results for the large radius are in complete disagreement with the data even for those results obtained with the maximum effective drag. With reference to the luminous intensity (fig. 52)[11] the photometrical analysis indicates that the calculated luminous intensity[12] from the shock layer accounts for all the luminosity at the highest altitudes

[10]Such small values are absurd. The total mass of the found meteorites is about 6 kg. The mass of a chrondrite having a radius of 0.1 m is only 14 kg.

[11]On this figure the gas-cap luminous intensity is shown only for the minimum effective drag case. The values for the maximum effective drag case are the same.

[12]The calculated shock-layer intensities are in error at the lower altitudes since no allowance for absorption within the layer was made.

when the entry radius is about 1.8 m. However, at peak intensity, even with a heat-transfer coefficient of unity and with all the released energy appearing as visible light, the radius must be a minimum of about 4 meters.

One partial explanation for this latter inconsistency is the following: In reference 30 it is noted that at very high speeds the radiation from the shock layers of a blunt body will be predominantly in the ultraviolet wavelengths. If the air density ahead of the shock is sufficient, this radiation will be absorbed in the region immediately ahead of and beside the shock layer. Presumably, at the lower altitudes this preheating could suffice to produce visible radiation from this region and so materially increase the apparent visible radiation from the gas cap. However, the calculated value of η for this meteor at the lower altitudes is about 0.1 and one would not expect the preheating to more than double or treble this value. This presumed phenomenon is thus alone incapable of explaining the large discrepancy which exists.

Another partial explanation is the following: It is readily appreciated that for this meteor at lower altitudes the heating rates are very high so that essentially an explosive efflux of ablated material in the solid as well as the gaseous state may have occurred.[13] Thus one conceivably may explain the large effective size. Moreover, the efflux of material should, in the main, be toward the direction of motion so that the deceleration of the main body would be enhanced. This may serve to explain, in part at least, the discrepancy between the measured velocity variation with altitude and that expected from photometric consideration.

This meteor record is, thus, enigmatic. The results of the photometrical analysis are not self-consistent nor are they consistent with the meager results obtained from the dynamical analysis.

DISCUSSION AND CONCLUDING REMARKS

With reference to the dynamical method of analysis of meteor tracking data obtained from the conventional photographic technique, it appears that with "good seeing" conditions, as for Meanook 132 the velocity-acceleration record can, in fact, be sufficiently precise to yield valuable heat-transfer data if the meteor density is known or can be inferred from a photometrical analysis.

It appears that the photometrical method of analysis is sound in principle. The Meanook meteor 132 and the Ondřejov meteor 15761 luminosity data suggest that the luminous efficiency factor τ_0 apparently is constant or

[13]Plate II of reference 1 is a remarkable photograph of the Pasamonte meteor for which such explosion occurred. This friable meteoric body, which must have been of great mass, was reduced to dust and a multitude of small meteorites during its entry to the atmosphere. Of the more than 100 meteorites found, the mass of the largest was but 292 gr.

nearly so (i.e., not a strong function of speed or air density) in continuum flow. However, for these meteors the density is an unknown - the photometric analysis was used, in fact, to estimate size - so the magnitude of τ_o cannot, of course, be inferred from these examples.

On the other hand, the Harvard meteor 1242 and the Sacramento Peak meteor 19816 are presumably asteroidal stone so that their density would be expected to be about 3400 kg/m^3. These two meteors, therefore, permit refined estimates of the luminous efficiency factor. Also since their speeds during entry are considerably different they may, perhaps, shed some light on the variation of τ_o with speed. For the unusually slow Harvard meteor 1242 the peak luminosity occurs in the range from 9 to 12 km/sec while for the Sacramento Peak meteor 19816, in the range 12 to 19.

In figure 53 the "best fit" values for τ_o for these two meteors are plotted as a function of speed and compared with the value used as a standard in this report. It is seen that but a trivial variation with speed is indicated and that the standard (Jacchia's value) used in the report is probably too high for stones in continuum flow. It is of interest to note that in reference 26 a smaller value of τ_o appeared appropriate (from analysis of these same two meteors). The suggested value for stones (from ref. 26), in the units of this report, is

$$\tau_o = 1.06 \times 10^{-20} \frac{kw\ sec^4}{kg\ m^5}$$

This value is in essential agreement with the results of the analysis of this report.

Had a lower value than Jacchia's been used in the photometric analysis of the Příbram meteor, an even larger value for the probable initial size for this body would have been obtained. Similarly, the Meanook 132 and Ondřejov 15761 would have been estimated to be of even lower density.

Not much can be inferred about the heat-transfer characteristics of the various meteors from the comparison of the flight values of the heat-transfer factor with the estimates. All of these meteors are large enough to have experienced continuum flow during the high-heating period of flight. For the meteor 1242 the results of the photometrical analysis and of the average for the dynamical analysis essentially agree with the estimates for fluid ablation. For a stone meteoroid with such a slow speed of entry this would not be surprising, as noted earlier. Sacramento Peak meteor 19816, for which the flight speeds are considerably higher, shows both from the photometrical and dynamical results to be in much closer agreement with the estimates for vapor ablation. This, again, is in keeping with expectation. For the other meteors the results are more inconclusive. Both Meanook meteor 132 and Ondřejov meteor 15761 are apparently composed of porous stone that is probably weak. The fact that the heat-transfer factors even exceed what was estimated for fluid ablation is therefore not surprising. For Ondřejov meteor 27471, which entered the atmosphere at a considerably higher speed than the others, the flight heat-transfer factors are reasonably consistent with the assumption

that this body is iron as suggested by Ceplecha. The Příbram meteor data are not self-consistent and so do not provide further heat-transfer information. This is most unfortunate for it is the only meteor considered for which the density is assuredly known.

The indication of all these comparisons is, however, that the estimated heat-transfer factors for vapor ablation are low. One reason for this discrepancy noted in reference 31 is that the estimated heat-transfer coefficients have not included one important contribution, namely the heating due to radiation from the ablated vapor. This contribution may be approximated in the following way: The total radiation rate resulting from ablation, $\dot{E}_a$, all of which is assumed to be luminous, must be the sum of that observed corresponding to I_a and that part received by the meteor, $k\dot{E}_a$. Then from the definition of luminous intensity, the total ablation radiation rate in units of kg m^2 sec^{-3} must be[14]

$$\dot{E}_a = 4\pi \left(\frac{1}{1 - k}\right) I_a \times 10^{13} \tag{46}$$

The ablation heat-transfer coefficient is thus

$$C_{H_a} = \frac{4\pi \left(\frac{k}{1 - k}\right) I_a \times 10^{13}}{\frac{1}{2} \rho V^3 A} = \frac{8 \left(\frac{k}{1 - k}\right) I_a \times 10^{13}}{\rho_o \bar{\rho} V^3 r^2} \tag{47}$$

which should be added to the original estimated C_H values. But from appendix E (eq. (E7)) with C_{H_a} included

$$I_a = \frac{\pi \tau_o \rho_o}{4} \left(\frac{C_H + C_{H_a}}{\zeta}\right) \bar{\rho} r^2 V^6 \tag{48}$$

so that

$$C_{H_a} = \left[\frac{\frac{2\pi\tau_o \left(\frac{k}{1 - k}\right) V^3 \times 10^{13}}{\zeta}}{1 - \frac{2\pi\tau_o \left(\frac{k}{1 - k}\right) V^3 \times 10^{13}}{\zeta}}\right] C_H \tag{49}$$

should be added to the original estimates.

[14]The blocked light, $k\dot{E}_a$, depends on the aspect from which the meteor is viewed, but since k is small, the error due to change in viewing aspect is ignored.

Low values of k are to be expected because the largest portion of the total ablative radiation emanates from the wake. This is evident in the photograph[15] of figure 54 of an ablating cone-cylinder body composed of "Lexan," a material that produces unusually intense radiation from its ablated vapor. In an unpublished work Jack Stephenson of Ames Research Center has calculated values of k from flight experiments at lower speeds than of interest here. He finds k to be a function of air density and velocity. Values of k for vapor ablation up to 0.05 were found (i.e., most of the radiation is in the wake) but there is no assurance that larger values might not be appropriate for meteor conditions. (Values for k with fluid ablation would be much less.) For the value of τ_o used herein (eq. (E13)) and for vaporizing stone (table I) equation (49) yields the values of C_{H_a}/C_H shown on figure 55. As speed increases, it is clear that ablation radiation can be an important contribution. This is particularly true if k for meteor conditions is much greater than Stephenson found at lower speeds. In fact, as noted by Craig and Davy, equation (49) becomes unstable at some velocity for which the denominator goes to zero. Of course, the heat-transfer coefficient then, in reality, approaches a limiting value as discussed earlier.

The NASA has recently supported a proposal by the Smithsonian Astrophysical Observatory to construct and operate a network of meteor observatories in the midwestern states for accurately tracking bright meteors by photographic methods with the intent of retrieving the meteorites. This "Prairie Network," it is hoped, will provide us with much new and needed meteor data from which we stand to learn a good deal about the aerodynamics and heating of large bodies at speeds well in excess of earth parabolic speed. Because the meteorites will hopefully be recovered, the meteor density will be known so that much of the uncertainty of results attendant with the analyses of the meteors of this paper will be absent. In particular; we should be able to learn much about the influence of velocity and air density on the luminous efficiency as well as to provide better estimates of heat-transfer factors for comparison with the results deduced from the flight data.

Ames Research Center
National Aeronautics and Space Administration
Moffett Field, Calif., Feb. 28, 1964

[15]This photograph was made with an "image-converter" camera by Mr. Max Wilkins in a ballistic range of the Ames Research Center. The body has a diameter of 1/2 inch and the flight speed is 7.2 km/sec.

APPENDIX A

SYMBOLS

The following symbols are used in this report. The symbols in parentheses are those used by meteor astronomers and are equal to the report symbols.

$a_1, a_2, \ldots, a_n$	coefficients of a power series in $\bar{\rho}$, $m^2 \cdot sec^{-2}$
A	cross-sectional area of meteoroid sphere, m^2 ($Am^{2/3}$)
A_{sh}	area of bow shock assumed equal to A, m^2
c	constant
C	constant
C_D	drag coefficient, dimensionless (2γ or 2Γ)
C_H	heat-transfer coefficient, dimensionless (λ or Λ)
$\frac{dV}{dt}$	acceleration, $m \cdot sec^{-2}$
$\dot{E}$	time rate of radiant energy release, $kg\ m^2\ sec^{-3}$
g	acceleration of gravity, $m\ sec^{-2}$
G_1, G_2, G_3, G_4	probable error functions, dimensionless
h	altitude, m
I	luminous intensity, $kw\ m^{-2}$
I(0 mag)	$10^{-0.4\ M_p}$
k	fraction of ablation vapor radiation received by body
K_n	Knudsen number, l/r, dimensionless
l	mean free path of air molecules at altitude h, m
l_o	mean free path of air molecules at sea level, m
m	mass, kg
M_{bs}	apparent bolometric magnitude of the sun

M_p	absolute photographic magnitude
M_v	absolute visual magnitude
$\dot{q}$	time rate of heating per unit area, kg sec^{-3}
r	radius of meteoroid sphere, m
s	solar constant, kw $\cdot$ m^{-2}
t	time, sec
T	temperature, ^{o}K
U	velocity normal to shock wave, m $\cdot$ sec^{-1}
v	shock-layer volume, m^3
V	meteoroid velocity at any altitude h, m $\cdot$ sec^{-1}
V_v	efflux velocity of ablating vapor, m sec^{-1}
α	ablation parameter, dimensionless
β	inverse of scale height, m^{-1}
δ	shock-layer thickness, m
Δ	probable error or mean error as case may be
ζ	heat of ablation per unit mass in energy units, m^2 sec^{-2} (Q or ζ)
η	fraction of shock-layer radiation in visible range of wavelengths, dimensionless
θ	trajectory angle measured from local horizontal, degrees of arc (cos Z_R = sin θ)
ρ	air density at altitude h, kg/m^3
ρ_o	sea-level air density, kg/m^3
$\overline{\rho}$	ratio of ρ to ρ_o
ρ_m	meteor density, kg/m^3
σ	ablation asymptote, dimensionless
τ	luminous efficiency, kw sec^3 kg^{-1} m^{-4}

τ_o	luminous efficiency factor, kw sec^4 kg^{-1} m^{-5}
ω	angle measured between radius to stagnation and radius to arbitrary point, radians

Subscripts

a	ablation
c	convective
e	equilibrium radiative
eff	effective
E	entry to the atmosphere
f	fluid ablation
g	gas cap
lim	limit
max	maximum
min	minimum
n	nonequilibrium radiative
s	stagnation point
u	uncorrected for approach to free molecular flow
uu	uncorrected for approach to free molecular flow and for approach to limiting permissible value of C_H/C_D
v	vapor ablation
o	sea level

Superscripts

p	power of density in equilibrium radiation equation
q	power of velocity in equilibrium radiation equation
s	power of velocity in nonequilibrium radiation equation

APPENDIX B

COMPUTATIONAL PROCEDURES FOR THE DYNAMICAL METHOD OF ANALYSIS OF METEOR TRACKING DATA

The photographic plate of a meteor camera with a rotating shutter of known rotation rate provides a time-distance record of the descent of a meteoric body in the atmosphere. From this plate and a streak photograph from a second observatory camera, located along a base line some distance from the first, one can determine the velocity, V, and the acceleration, dV/dt, of the body as a function of time, t. The records provide, in addition, the angle between the trajectory and the local horizontal θ (or vertical, Z_R). Hence, the velocity and accelerations can also be expressed as functions of altitude, h. A very large amount of "original data" is thus obtained but the accuracy of the individual values is relatively poor for many reasons (one of which is discussed in the report). To improve the accuracy of the values, meteor astronomers customarily analyze groupings of these data by the method of least squares. The results of such analyses provide a lesser amount of information of higher probable accuracy. These data are referred to, herein, as "reduced data."

The Czechoslovakians make a practice of publishing both the original and the reduced data and of including the mean error in these data as well. Their reports are thus very complete. In the United States and Canada the original data are not reported and generally the probable errors or mean errors are not given.

Two computational methods have been employed in this report for determining the size and heat-transfer characteristics from the meteor tracking data provided. The first, called the point-to-point method, employs the reduced data. It is simple and conveniently provides probable or mean errors in the final results if the probable or mean errors in velocity and acceleration are given. The second method, called the series method, can be used with either the original or the reduced data and is applicable whether or not acceleration information is provided.

THE POINT-TO-POINT METHOD

For any altitude, h, the product of the meteor density and radius may be found for the given velocity and acceleration from equation (14) as

$$\rho_m r = -\frac{3C_D\rho_o}{8}\left[\frac{\bar{\sigma}V^2}{(dV/dt) - g\sin\theta}\right] \tag{B1}$$

For mks units and with the 1959 ARDC Standard Atmosphere (ρ_o = 1.225 kg/m^3) and with C_D = 1, then the density-radius product (kg/m^2)

$$\rho_m r = -0.459 \left[\frac{\bar{\rho} V^2}{(dV/dt) - g \sin \theta} \right] \tag{B2}$$

The gravity term, as noted earlier, is generally trivial and, accordingly, ignored. The actual meteor size requires knowledge of the meteor density ρ_m. If the mean errors in velocity, ΔV, and in acceleration, $\Delta(dV/dt)$, are given, the mean error $\Delta(\rho_m r)$ can be found (treating the mean errors as probable errors - see ref. 32) as

$$\Delta(\rho_m r) = \pm \rho_m r \sqrt{\left(\frac{2\Delta V}{V}\right)^2 + \left[\frac{\Delta(dV/dt)}{(dV/dt) - g \sin \theta}\right]^2} \tag{B3}$$

Equations (13) and (7) give

$$\frac{dr}{r} = \frac{C_H}{6 C_D \zeta} d(V^2 + 2gh) \tag{B4}$$

and if we set $C_H/C_D\zeta$ constant over any altitude interval h_1 (upper) to h_2 (lower) then

$$\frac{C_H}{C_D \zeta} = \frac{6 \ln (r_1/r_2)}{V_1^2 - V_2^2 + 2g(h_1 - h_2)} \tag{B5}$$

so that from (B1) and (B5), if C_D is unity,

$$\frac{C_H}{C_D \zeta} = \frac{6 \ln \left\{ \frac{\bar{\rho}_1 V_1^2 [(dV/dt)_2 - g \sin \theta]}{\bar{\rho}_2 V_2 [(dV/dt)_1 - g \sin \theta]} \right\}}{V_1^2 - V_2^2 + 2g(h_1 - h_2)} \tag{B6}$$

The mean error $\Delta(C_H/C_D\zeta)$ can be found from (see ref. 32)

$$\Delta \left(\frac{C_H}{C_D \zeta} \right) = \pm \frac{6 \sqrt{G_1^2 + G_2^2 + G_3^2 + G_4^2}}{V_1^2 - V_2^2 + 2g(h_1 - h_2)} \tag{B7}$$

where

$$\left.\begin{aligned} G_1 &= \frac{2\Delta V_1}{V_1}\left(1 - \frac{C_H V_1^2}{6C_D\zeta}\right) \\ G_2 &= \frac{2\Delta V_2}{V_2}\left(1 - \frac{C_H V_2^2}{6C_D\zeta}\right) \\ G_3 &= \frac{\Delta(dV/dt)_1}{(dV/dt)_1 - g \sin\theta} \\ G_4 &= \frac{\Delta(dV/dt)_2}{(dV/dt)_2 - g \sin\theta} \end{aligned}\right\} \qquad (B8)$$

The values of $C_H/C_D\zeta$ and $\Delta(C_H/C_D\zeta)$ are assumed to apply at the mean of the altitudes h_1 and h_2.

THE SERIES METHOD

The method is based upon the assumption that since V and r are functions of h, they are also functions of $\bar{\rho}$. A power series in $\bar{\rho}$ is therefore used in the form

$$\ln(V^2 + 2gh) = a_0 + a_1\bar{\rho} + a_2\bar{\rho}^2 + a_3\bar{\rho}^3 + \ldots a_n\bar{\rho}^n \qquad (B9)$$

Differentiation gives

$$\frac{d}{d\bar{\rho}}(V^2 + 2gh) = 2V\frac{dV}{d\bar{\rho}} + 2g\frac{dh}{d\bar{\rho}} = (V^2 + 2gh)(a_1 + 2a_2\bar{\rho} + 3a_3\bar{\rho}^2 + \ldots na_n\bar{\rho}^{n-1}) \qquad (B10)$$

Now

$$\frac{dV}{dt} = \frac{dV}{d\bar{\rho}}\frac{d\bar{\rho}}{dh}\frac{dh}{dt} = -V\sin\theta\frac{d\bar{\rho}}{dh}\frac{dV}{d\bar{\rho}} = -\frac{\sin\theta}{2}\frac{d\bar{\rho}}{dh}\left(2V\frac{dV}{d\bar{\rho}}\right) \qquad (B11)$$

so that equations (B10) and (B11) give

$$\frac{dV}{dt} = g\sin\theta - \frac{1}{2}(V^2 + 2gh)(a_1 + 2a_2\bar{\rho} + 3a_3\bar{\rho}^2 + \ldots na_n\bar{\rho}^{n-1})\sin\theta\frac{d\bar{\rho}}{dh} \qquad (B12)$$

As is well known, air density varies nearly exponentially with altitude according to the formula

$$\bar{\rho} = e^{-\beta h} \qquad (B13)$$

where β is nearly constant. Thus differentiation of equation (B13) gives

$$\frac{d\bar{\rho}}{dh} = -e^{-\beta h}\left(\beta + h\,\frac{d\beta}{dh}\right) = -\bar{\rho}\left(\beta + h\,\frac{d\beta}{dh}\right) \tag{B14}$$

so that equation (B12) can be written

$$\frac{dV}{dt} = g \sin\theta + \frac{1}{2}(V^2 + 2gh)\left(\beta + h\,\frac{d\beta}{dh}\right)\sin\theta(a_1\bar{\rho} + 2a_2\bar{\rho}^2 + \ldots na_n\bar{\rho}^n) \tag{B15}$$

Table VIII gives the 1959 ARDC values of ρ (from ref. 19) and values of $\beta + h(d\beta/dh)$ for the altitude range of interest in this report. Equation (B15) in the form

$$\frac{(dV/dt) - g\sin\theta}{(1/2)(V^2 + 2gh)[\beta + h(d\beta/dh)]\sin\theta} = a_1\bar{\rho} + 2a_2\bar{\rho}^2 + 3a_3\bar{\rho}^3 + \ldots na_n\bar{\rho}^n \tag{B16}$$

is also useful.

Employing these series for analysis is useful in cases wherein:

(a) The data are incomplete.

(b) The data variations with altitude are erratic.

(c) The data are both incomplete and erratic.

An example of case (a) is one wherein nonerratic reduced data for V are given but dV/dt data are not. Then, if p values of V are given as a function of h, values of the series coefficients in equation (B9) can be found up to and including a_n where

$$n = p - 1 \tag{B17}$$

Then the acceleration can be found from equation (B15).

An example of case (b) is one wherein both V and dV/dt, which vary erratically with altitude, are given for p values of altitude. In this event one can find the a_n coefficients from equations (B9) and (B16) for

$$n < 2p - 1 \tag{B18}$$

by a standard least-squares method employing an electronic computer. In such cases, n can be as much less than $2p - 1$ as is necessary to smooth the data. (For such cases, a_0 must be found from the velocity data alone.)

An example of case (c) is one wherein V is given for p values of h but the data are erratic and no values of dV/dt are given. Then the a coefficients can be found by least-squares solution for

$$n < p - 1 \tag{B19}$$

where n is sufficient to smooth the data. This procedure is valuable where large numbers of original velocity data are given.

In this report, wherein the series method of analysis has been employed, after the series coefficients were found, the velocity and accelerations were computed (using eqs. (B9) and (B15)) at intervals of 1000 m altitude. Then the density-radius product was calculated for each altitude by equation (14) and then the heat-transfer factor was calculated for each altitude h (see eq. (13)) by (drag coefficient assumed constant)

$$\frac{C_H}{C_D\zeta} = \frac{8 \sin \theta}{2000\rho_o}\left[\frac{(\rho_m r)_{h+1000} - (\rho_m r)_{h-1000}}{\bar{\rho}V^2}\right] \tag{B20}$$

No hard and fast rules were employed to fix the choice of the degree of the least-squares polynomial fit for the individual analysis of meteors. Generally, for any particular case, the largest degree polynomial was used that would provide reasonably smooth variations of the dependent variables with altitude.

APPENDIX C

COMPUTATIONAL PROCEDURES FOR THE PHOTOMETRICAL METHOD OF ANALYSIS OF METEOR TRACKING DATA

In this report, the photometrical method of analysis is applied to all the meteors discussed except Ondřejov meteor 27471 for which luminosity data are not available. The computational procedures are the following:

I MEANOOK METEOR 132 AND ONDŘEJOV METEOR 15761

It is assumed that at some one altitude, h_1, the velocity and the meteor density-radius product are as given by the dynamical method. Then the heat-transfer factor, $C_H/C_D\zeta$, at that altitude can be found. To this end we note that in the same manner in which for free molecular flow equation (28) (for the heat-transfer factor) can be derived from equation (23), so from equation (29) one derives for continuum flow the expression

$$\frac{C_H}{C_D\zeta} = \frac{4}{\pi C_D \rho_o \tau_o}\left(\frac{I - I_g}{\bar{\rho} r^2 V^6}\right) = \frac{4}{\pi C_D \rho_o \tau_o}\left(\frac{I_a}{\bar{\rho} r^2 V^6}\right) \tag{C1}$$

wherein I_a is the ablation luminous intensity.

The acceleration can then be evaluated from the dynamics as equation (5)

$$\frac{dV}{dt} = g \sin\theta - \frac{3C_D\rho_o}{8\rho_m}\left(\frac{\bar{\rho}V^2}{r}\right) \tag{C2}$$

so that

$$\frac{dV}{dh} = -\frac{dV/dt}{V \sin\theta} \tag{C3}$$

and, in turn, from equation (13)

$$\frac{dr}{dh} = \frac{\rho_o C_D}{8\rho_m \sin\theta}\left(\frac{C_H}{C_D\zeta}\right)\bar{\rho}V^2 \tag{C4}$$

Using (see eq. (E13))

$$\left.\begin{aligned} \tau_o &= 1.612\times10^{-20}\ \frac{\text{kw sec}^4}{\text{kg m}^5} \\ \rho_o &= 1.225\ \text{kg/m}^3 \\ C_D &= 1 \\ g_{mean} &= 9.6\ \text{m/sec}^2 \end{aligned}\right\} \tag{C5}$$

Equations (C1), (C2), (C3), and (C4) become (for $I - I_g$ units of kw m^{-2})

$$\frac{C_H}{C_D\zeta} = 0.64\times10^{20}\ \frac{I - I_g}{\bar{\rho} r^2 V^6} \tag{C6}$$

$$\frac{dV}{dt} = 9.6 \sin\theta - \frac{0.46}{\rho_m}\left(\frac{\bar{\rho}V^2}{r}\right) \tag{C7}$$

$$\frac{dV}{dh} = -\frac{dV/dt}{V \sin\theta} \tag{C8}$$

$$\frac{dr}{dh} = \frac{0.153}{\rho_m \sin\theta}\left(\frac{C_H}{C_D\zeta}\right)\bar{\rho}V^2 \tag{C9}$$

and I_g is calculated by the procedure given in appendix E.

At an altitude increment Δh from the altitude h_1 the velocity and radius can be found from

$$\left.\begin{aligned} V &= V_1 + \frac{dV}{dh}\Delta h \\ r &= r_1 + \frac{dr}{dh}\Delta h \end{aligned}\right\} \tag{C10}$$

and this computational process can then be repeated to find V, dV/dt, r, $C_H/C_D\zeta$ at a next altitude and so forth. Thus, from the single initial values of V_1 and r_1, the measured value of $\sin\theta$, and the known values of the total luminous intensity, I, as a function of altitude, a whole flight history can be calculated.

This procedure was employed for Meanook meteor 132. The total luminous intensity variation with altitude was that given in figure 4; the starting values were

$$\left.\begin{aligned} h_1 &= 68{,}000 \text{ m} \\ V_1 &= 17{,}422 \text{ m/sec} \\ \sin\theta &= 0.868 \\ \rho_m r_1 &= 54 \text{ kg/m}^2 \end{aligned}\right\} \qquad \text{(C11)}$$

and the altitude increment

$$\Delta h = -1000 \text{ m}$$

For the Ondřejov meteor 15761 the same procedure was used with the total luminous intensity variation with altitude given in figure 15, the starting values

$$\left.\begin{aligned} h_1 &= 77{,}000 \text{ m} \\ V_1 &= 22{,}000 \text{ m/sec} \\ \sin\theta &= 0.4631 \\ \rho_m r_1 &= 50 \text{ kg/m}^2 \end{aligned}\right\} \qquad \text{(C12)}$$

and the altitude increment

$$\Delta h = -1000 \text{ m}$$

For both meteors the calculations were carried through for a range of values of ρ_m. The results presented in the report are only for that value of ρ_m which appears to give best agreement between the reduced data with the calculated values of velocity as a function of altitude.

II ONDŘEJOV METEOR PŘÍBRAM

The reduced data for this meteor are only given over an altitude range for which the velocity is very nearly constant. As a result, the dynamical method of analysis yields self-conflicting results. In fact, one cannot even find the body size, but the result would suggest that the radius was perhaps between about 0.1 and 0.4 m at the highest altitude for which data are given (about 90 km). Accordingly, the photometrical method was used to determine the initial size. The calculation procedure was the same as outlined for Meanook 132 except that the meteor density was known

$$\left.\begin{aligned} \rho_m &= 3500 \text{ kg/m}^3 \\ \text{and the assumed starting conditions were} & \\ h_1 &= 100{,}000 \text{ m} \\ V_1 &= 20{,}867 \text{ m/sec} \\ \sin\theta &= 0.683 \end{aligned}\right\} \quad \text{(C13)}$$

while the initial radius was assumed to have a series of arbitrary values. Both maximum and minimum effective drag coefficients were assumed to apply in equation (C2). The results of these calculations are discussed in the report.

III HARVARD METEOR 1242 AND SACRAMENTO PEAK METEOR 19816

In the opinion of Cook, Jacchia, and McCrosky (ref. 26) both of these meteors are asteroidal stone, so that it has been assumed that the density is (ref. 7)

$$\rho_m = 3400 \text{ kg/m}^3$$

The photometrical analysis is used in these cases to find values of τ_o which will bring the results of the photometrical analysis in essential agreement with the flight velocity and acceleration data. Thus the calculative procedure is that given in section I of this appendix but a range of values of τ_o is used to find what mean value of τ_o will give a best fit of the velocities and accelerations so calculated with those obtained from flight.

The starting conditions for the analysis of Harvard meteor 1242 are

$$h_1 = 64{,}000 \text{ m}$$

$$V_1 = 11{,}960 \text{ m/sec}$$

$$\sin\theta = 0.632$$

$$r_1 = 0.0200 \text{ m}$$

corresponding to the value

$$\rho_m r_1 = 68 \text{ kg/m}^2$$

For the Sacramento Peak meteor 19816 they are

$$h_1 = 80{,}000 \text{ m}$$

$$V_1 = 20{,}640 \text{ m/sec}$$

$$\sin \theta = 0.716$$

$$r_1 = 0.0057 \text{ m}$$

corresponding to the value

$$\rho_m r_1 = 19.4 \text{ kg/m}^2$$

APPENDIX D

ESTIMATION OF THE HEAT-TRANSFER PARAMETER, $C_H/C_D\zeta$

At the outset it should be emphasized that any estimation of C_H for meteors usually involves extensive extrapolation of our present experimental data since speeds available in laboratory tests are generally well below meteor speeds, and the physical dimensions of the models employed in these tests are generally much below the dimensions of the meteoric bodies of interest here. Moreover, the actual shapes of these meteoric bodies are unknown as are the changes in shape along the entry trajectories. In addition, the actual processes of ablation are unknown (e.g., as noted in the text, irons will ablate freely in the liquid state while stones will vaporize as well as ablate in the solid state as a result of spalling due to thermal stress). However, vapor ablation provides an upper limit for the heat of ablation. As a result of these numerous uncertainties, we can expect that our estimates may only agree in order of magnitude with the flight results.

In accordance with the assumption used in the analysis of the flight record, we assume here that the body essentially acts as a sphere and that the size of the sphere is determined from the flight test results. We will determine the estimates of $C_H/C_D\zeta$, first, on the premise that ablation occurs only by vaporization and, second, only by liquid runoff.

Although this report is concerned only with continuum flow, it will be necessary to fair our continuum estimates in such a way that at the higher altitudes they will agree with those obtained from free-molecule flow theory ($C_H/C_D = 1/2$). Moreover, we must also provide for the fact that even in continuum flow C_H/C_D is limited in any real flow. This fraction can never exceed 1/2 since for purely convective heating, only about half of the energy dissipated as heat can be given to the body; the remainder must be left in the wake (Reynolds analogy, see, e.g., ref. 33). On the other hand, for purely gas-cap radiative heating only half of the radiant energy emitted can be received by the body; the other half must be radiated to space. The calculative procedure is, therefore, the following: The heat-transfer coefficient in continuum flow is calculated as the sum of the convective contribution plus the gas-cap radiative contribution from the air which is in thermodynamic and chemical equilibrium and that which is not in equilibrium. The convective contribution so calculated is uncorrected for the approach to free molecular flow, except that when the effect of vapor ablation to reduce the convective component is evaluated an allowance is made for the approach to free molecular flow. The radiative components (equilibrium and nonequilibrium) are uncorrected for limiting but are forced to zero as free molecular flow is approached. Finally, the sum of the uncorrected continuum components is, together, corrected for approach to limiting. The result applies for the energy limit and for free molecular flow since these values of $(C_H/C_D)_{lim}$ are the same (0.5).

It is well at this point to discuss the conditions for continuum flow as opposed to free molecular flow. The Knudsen number is defined as the ratio of the mean free path in the atmosphere, l, to the body radius at the altitude at which this mean free path applies. Approximately, the mean free path is related to the density ratio, $\bar{\rho}$, by

$$l = \frac{l_o}{\bar{\rho}} \tag{D1}$$

where the constant l_o is about 7.2×10^{-8} m. Thus the Knudsen number is

$$K_n = \frac{l}{r} = \frac{l_o}{\bar{\rho}r} = \frac{7.2\times10^{-8}}{\bar{\rho}r} \tag{D2}$$

When K_n exceeds, say, 4 or 5 (see ref. 34), the flow is, in essence, the free molecular type. When K_n is less than, say, 1/4 or 1/5, the flow is, in essence, continuum. Between these two regimes lies the so-called slip flow regime. Although practically no theory for the slip flow regime is available, experiment has shown (e.g., ref. 35) that the transition from continuum to free molecular flow is smooth. Thus a function which appropriately expresses such a transition may be of the type

$$e^{-K_n} = e^{-7.2\times10^{-8}/\bar{\rho}r} \tag{D3}$$

since for small K_n ($\ll 1$) this function approaches unity while for large K_n ($\gg 1$) it approaches zero.

In the following sections, the continuum heat-transfer coefficients are evaluated and corrected for approach to either the energy limit or the free molecular flow regime.

CONVECTIVE HEAT TRANSFER

To evaluate the convective component for a sphere in laminar[1] continuum flow we employ the procedure used by Chapman (ref. 36) to find the stagnation-point heating rate and then employ the analysis of Lees (ref. 37) to find the rate for an average surface element. Chapman's analysis which applies if no vapor ablation occurs gives the stagnation-point convective heat rate as

$$\dot{q}_{cfs_u} = \frac{1.755\times10^{-4}}{\sqrt{\bar{\rho}r}}\rho V^3 \tag{D4}$$

[1]For most of the cases considered in this report, the meteoric bodies are sufficiently small that experience indicates turbulent boundary-layer flow will not occur.

Lee's analysis, with Newtonian flow assumptions, gives for the forward face of the sphere an arbitrary surface element at high Mach number

$$\frac{\dot{q}_{cf_u}}{\dot{q}_{cf_{s_u}}} = \frac{2\omega \sin \omega \cos^2 \omega}{\sqrt{\omega^2 - \frac{\omega \sin 4\omega}{2} + \frac{1 - \cos 4\omega}{8}}} \quad ; \qquad 0 \leqq \omega \leqq \frac{\pi}{2} \tag{D5}$$

where ω is the angle between the radii measured from the stagnation point to the arbitrary surface element, and for the rear face

$$\frac{\dot{q}_{cf_u}}{\dot{q}_{cf_{s_u}}} = 0 \quad ; \qquad \frac{\pi}{2} \leqq \omega \leqq \pi \tag{D6}$$

Hence, the total heat input rate by convection is

$$\dot{Q}_{cf_u} = \int_S \dot{q}_{cf_u} \, dS = 4\pi r^2 \dot{q}_{cf_{s_u}} \int_0^{\pi/2} \frac{\omega \sin^2 \omega \cos^2 \omega \, d\omega}{\sqrt{\omega^2 - \frac{\omega \sin 4\omega}{2} + \frac{1 - \cos 4\omega}{8}}} = 0.735\pi r^2 \dot{q}_{cf_{s_u}} \tag{D7}$$

and

$$C_{H_{cf_u}} = \frac{\dot{Q}_{cf_u}}{(\pi/2)\rho V^3 r^2} = \frac{2.58 \times 10^{-4}}{\sqrt{\rho r}} \tag{D8}$$

When vapor ablation occurs, the issuing vapors fend off the air from the surface and so reduce the surface shear and the convective heat transfer. Theory (see ref. 38) gives the ratio of heat transfer with vapor ablation to that without ablation (or with fluid ablation) as

$$\frac{C_{H_{cv_u}}}{C_{H_{cf_u}}} = \frac{1}{1 + (\alpha/\zeta_v)V^2} \tag{D9}$$

where α depends upon the molecular weight of the issuing vapor. But this formulation does not properly consider the heat conduction in the sublayer. Thus while equation (D9) indicates that the ratio approaches zero as $(\alpha/\zeta_v)V^2$ becomes very large, experiments indicate (see ref. 39) that the ratio actually approaches an asymptotic value. Let this asymptotic value be σ. Then the formulation (ref. 40)

$$\frac{C_{H_{cv_u}}}{C_{H_{cf_u}}} = \frac{1 - \sigma}{1 + (\alpha/\zeta_v)V^2} + \sigma \tag{D10}$$

will more properly provide for the effects of vapor ablation. For stone or iron reference 38 indicates

$$\alpha \cong 0.3 \tag{D11}$$

The value of σ will depend not only on the heat conductivity of the ablating vapor but also upon the ratio of the convective to the radiative heat rates. For the calculations of this paper it is arbitrarily assumed that

$$\sigma = 0.2 \tag{D12}$$

At this point we shall partially correct for approach to free molecular flow by altering equations (D10), (D11), and (D12) to read (see eq. (D3))

$$\frac{C_{H_{cv_u}}}{C_{H_{cf_u}}} = \frac{0.8}{1 + (0.3V^2/\zeta_v)e^{-7.2\times10^{-8}/\bar{\rho}r}} + 0.2 \tag{D13}$$

Then the convective contribution for vapor ablation (the counterpart to eq. (D8)) is

$$C_{H_{cv_u}} = \frac{2.06\times10^{-4}}{\sqrt{\bar{\rho}r}} \left[\frac{1}{1 + (3\times10^7/\zeta_v)(V/10^4)^2 e^{-7.2\times10^{-8}/\bar{\rho}r}} + 0.25 \right] \tag{D14}$$

RADIATIVE HEAT TRANSFER - GENERAL REMARKS

The level of radiation from a unit volume of excited gas depends upon the density and enthalpy of the gas. For a spherical body the radiation from an element of the gas cap would vary within the cap, depending upon the position of the elementary volume, since the level of radiation depends upon the speed of the air normal to the surface of the shock (see sketch (b)). The elements directly ahead of the stagnation point radiate the most and the radiation level falls as we proceed around the body. To calculate the net radiation from the whole cap is tedious. Note, however, that the heat transfer is highest from both convection and radiation at the stagnation point. Thus the stagnation region as indicated in sketch (c) will ablate rapidly so that

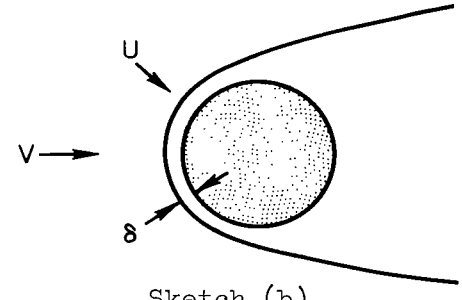

Sketch (b)

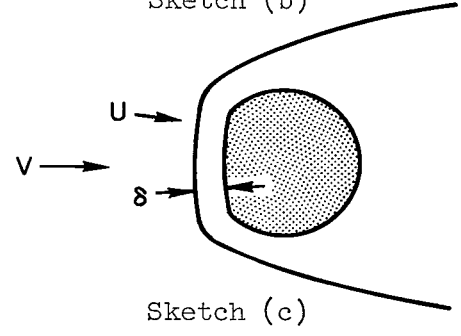

Sketch (c)

with time the body becomes blunted (provided it is not tumbling). The face of a body for which radiation predominates is flattened. Equilibrium radiative heating will thus be greatly increased with time not only because the average component velocity U now closely approaches the flight velocity V, but also because the gas-cap volume is increased since the shock standoff distance will be triple or more than that for a sphere. In order to avoid the complexity of calculating the radiative heating for a body of changing shape it is assumed that the gas-cap radiation corresponds to that for a "disk" shape (i.e., U = V) but with the shock standoff distance corresponding to that for a sphere. In this way, it is hoped that the integrated average value will be duplicated.

EQUILIBRIUM RADIATIVE HEAT TRANSFER

The time rate of energy radiation from an excited gas in thermodynamic and chemical equilibrium per unit volume can be expressed as

$$\frac{d\dot{E}_e}{dv} = C_e \bar{\rho}^p U^q \tag{D15}$$

Seiff (ref. 40) found from examining our present knowledge of gas radiation that essentially two regimes exist. For velocity $U < 13{,}700$ m/sec

$$\left.\begin{aligned} C_{e_1} &= 6.14\times10^{-49}\ \frac{kg}{m\ sec^3}\left(\frac{sec}{m}\right)^{15.45} \\ p_1 &= p = 1.8 \\ q_1 &= 15.45 \end{aligned}\right\} \tag{D16}$$

and for $U > 13{,}700$ m/sec

$$\left.\begin{aligned} C_{e_2} &= 6.44\times10^{-6}\ \frac{kg}{m\ sec^3}\left(\frac{sec}{m}\right)^{5.05} \\ p_2 &= p = 1.8 \\ q_2 &= 5.05 \end{aligned}\right\} \tag{D17}$$

In accordance with the assumptions given earlier then, the total radiation rate from the gas cap in equilibrium is then

$$\dot{E}_e = C_e \pi r^3 \left(\frac{\delta}{r}\right) \bar{\rho}^p V^q \tag{D18}$$

where δ/r is shock standoff distance ratio for a sphere, which is about 0.05 (see ref. 40). Now since for a thin gas cap only half of this radiation is received by the body, the other half being radiated to space, then

$$C_{H_{e_{uu}}} = \frac{(1/2)\dot{E}_e}{(1/2)\rho_o \bar{\rho} V^3 \pi r^2} \tag{D19}$$

or

$$C_{H_{e_{uu}}} = \left(\frac{C_e}{\rho_o}\right)\left(\frac{\delta}{r}\right) \bar{\rho}^{p-1} V^{q-3} r \tag{D20}$$

To correct for the approach to free molecular flow (where $C_{H_e} = 0$) then

$$C_{H_{e_u}} = \frac{C_e}{\rho_o}\left(\frac{\delta}{r}\right) \bar{\rho}^{p-1} V^{q-3} r \; e^{-7.2\times10^{-8}/\bar{\rho}r} \tag{D21}$$

With the constants from equations (D16) and (D17) and with $\delta/r = 0.05$, then

$$C_{H_{e_u}} = 41.6\bar{\rho}^{0.8}\left(\frac{V}{10^4}\right)^{2.05} r \; e^{-7.2\times10^{-8}/\bar{\rho}r} \; ; \qquad V > 13{,}700 \text{ m/sec} \tag{D22}$$

and

$$C_{H_{e_u}} = 1.58\bar{\rho}^{0.8}\left(\frac{V}{10^4}\right)^{12.45} r \; e^{-7.2\times10^{-8}/\bar{\rho}r} \; ; \qquad V < 13{,}700 \text{ m/sec} \tag{D23}$$

NONEQUILIBRIUM RADIATIVE HEAT TRANSFER

The region for which the gas-cap air is out of equilibrium is generally confined so near the shock wave that we may, for practical purposes, consider the nonequilibrium radiation to be proportional to the shock-wave area. If the density is high, the time rate of energy radiation from this thin lamina of gas, which is out of equilibrium, per unit of shock area can be expressed as

$$\frac{d\dot{E}_n}{dA_{sh}} = C_n V^s \tag{D24}$$

where the values for the constants as known at present are (see ref. 40)

$$\left.\begin{aligned} C_n &= 0.74\times10^{-22} \; \frac{\text{kg}}{\text{sec}^3} \left(\frac{\text{sec}}{\text{m}}\right)^7 \\ s &= 7 \end{aligned}\right\} \tag{D25}$$

Equation (D24) holds until the so-called collision limiting begins (see discussion in appendix C of ref. 40), corresponding to $\bar{\rho}_{CL} = 10^{-3}$, after which it is assumed that

$$\frac{d\dot{E}_n}{dA_{sh}} = C_n \times 10^3 V^s \bar{\rho} \tag{D26}$$

Now, if we correct for the approach to free molecular flow (see eq. (D3)) but not for energy limiting, remembering that only half of the radiation is received by the body (see eq. (D19)),

$$C_{H_{n_u}} = \frac{(1/2)(d\dot{E}_n/dA_{sh})\pi r^2 \; e^{-7.2\times10^{-8}/\bar{\rho}r}}{(1/2)\rho_o \bar{\rho} V^3 \pi r^2} \tag{D27}$$

Thus when the constants are inserted the nonequilibrium equations become

$$C_{H_{n_u}} = 0.6\times10^{-6}\bar{\rho}^{-1}\left(\frac{V}{10^4}\right)^4 e^{-7.2\times10^{-8}/\bar{\rho}r}; \qquad \bar{\rho} > 10^{-3} \tag{D28}$$

and, when corrected for collision limiting by equation (D26)

$$C_{H_{n_u}} = 0.6\times10^{-3}\left(\frac{V}{10^4}\right)^4 e^{-7.2\times10^{-8}/\bar{\rho}r}; \qquad \bar{\rho} < 10^{-3} \tag{D29}$$

TOTAL HEAT TRANSFER

The total heat transfer formed when the components are added (see eqs. (D8) or (D14) along with eqs. (D22) or (D23) and (D28) or (D29)) is unrealistic in that it is not limited as reality requires. In the limit C_H/C_D cannot exceed 1/2. The corresponding drag coefficient becomes the free-molecule value $C_D = 2$ (as opposed to unity for low-heat-transfer continuum flow). Thus to enforce the correct limit, the following procedure is employed: The corrected total heat-transfer coefficient is formed from

$$C_H = C_{H_u} e^{-2C_{H_u}} + \left(1 - e^{-C_{H_u}}\right)^2 \tag{D30}$$

and the corrected drag coefficient from

$$C_D = 1 + C_H \tag{D31}$$

These formulations satisfy the requirement since when

$$C_{H_u} = C_{H_{c_u}} + C_{H_{e_u}} + C_{H_{n_u}} \rightarrow 0 \tag{D32}$$

$$\left.\begin{aligned} C_H &\rightarrow C_{H_u} \\ C_D &\rightarrow 1 \end{aligned}\right\} \tag{D33}$$

and when

$$C_{H_u} = C_{H_{c_u}} + C_{H_{e_u}} + C_{H_{n_u}} \rightarrow \infty \tag{D34}$$

$$\left.\begin{aligned} C_H &\rightarrow 1 \\ C_D &\rightarrow 2 \end{aligned}\right\} \tag{D35}$$

The following table shows that equation (D30) produces the desired behavior. Certainly these results are reasonable for approach to the free molecular regime. For the approach to energy limiting in the continuum range it is correct in direction but probably too high. However, this limit is not closely approached for most of the meteors considered in this report.

C_{H_u}	C_H	C_D	C_H/C_D
0	0	1.00000	0
.05	.04762	1.04762	.04545
.1	.09093	1.09093	.08335
.2	.16693	1.16693	.14305
.3	.23182	1.23182	.18816
.5	.33879	1.33879	.25305
1.0	.53485	1.53485	.34847
1.5	.67827	1.67827	.40414
2.0	.78431	1.78431	.43956
3.0	.91038	1.91038	.37654
∞	1.00000	2.00000	.50000

For calculations of gas-cap luminous intensity discussed in appendix E it is necessary to find

$$C_{H_g} = C_{H_e} + C_{H_n} \tag{D36}$$

This quantity is then approximated as

$$C_{H_g} = \left(C_{H_{e_u}} + C_{H_{n_u}}\right)\left(\frac{C_H}{C_{H_u}}\right) \tag{D37}$$

where C_H and C_{H_u} correspond to vapor ablation of the meteoric surface.

In the preceding portions of this appendix it has been tacitly assumed that the radius of the meteoric body is known as a function of altitude from

the flight data. Actually for all of the meteors discussed in the report, with the exception of the Ondřejov meteor Příbram, the flight data only provide the meteor density-radius product, $\rho_m r$, as a function of altitude. Even for Příbram, as will be shown, though ρ_m is known $\rho_m r$ is so poorly determined that r must be considered an unknown.

For all of the meteors except Příbram, the following procedure is employed: For an assumed series of values of ρ_m, the radius variation with altitude is calculated. The calculation procedures of appendix E, part I, are used to find the gas-cap luminosity. The flight values of the heat-transfer factor $C_H/C_D\zeta$ are used to calculate the ablation luminosity by the method of appendix E, part II. The total luminous intensity is then determined (sum of the gas-cap and ablation luminosities) for each assumed meteor density and compared with the observed luminous intensity. The approximate meteor density is then chosen to be that which gives the closest agreement of these calculated and observed luminosities. This evaluation needs only to be approximate since the calculated values of the heat-transfer factors for either the assumed vapor or fluid ablation is not strongly influenced by small changes in the assumed meteor density.

For the Příbram meteor the calculation procedure is that given in appendix C, section II, and in appendix E.

There are several theoretical analyses of meteor heat transfer. The estimates of references 18 and 41 are too approximate for the needs of this report. The estimates of reference 42 are given for a wider range of speeds than considered herein and in ample detail. However, the latter reference assumes unrealistically that σ in equation (D10) is zero.

APPENDIX E

CALCULATION OF LUMINOUS INTENSITY

I GAS-CAP LUMINOSITY

The time rate of energy radiated from the shock layer to space is equal to the time rate of energy radiated to the body so that (in units of kg m^2/sec^3)

$$\frac{1}{2}\dot{E} = \frac{1}{2} C_{H_g} \rho_o \pi r^2 \bar{\rho} V^3 \tag{E1}$$

where C_{H_g} is the total radiative contribution to the heat-transfer coefficient (see appendix D). Only a fraction of this energy, η, is in the visible wavelength range (> 3500 Å). This fraction is

$$\eta\dot{E} = \frac{1}{2} \eta C_{H_g} \rho_o \pi r^2 \bar{\rho} V^3 \tag{E2}$$

To find the corresponding luminous intensity, defined as the luminous energy received on a 1 m^2 area at 100 km distance, one can calculate this quantity as if $2\eta\dot{E}$ were radiating to a sphere of 100 km radius so that the gas-cap luminous intensity in kw/m^2 ($\dot{E}$ in kg m^2 sec^{-3}) is

$$I_g = \frac{2\eta\dot{E}\times 10^{-13}}{4\pi} = 0.306\eta C_{H_g} r^2 \bar{\rho} V^3 \times 10^{-13} \tag{E3}$$

This is the gas-cap luminous energy which would be observed at a point directly ahead of the meteor.[1]

The fraction η is a function of the gas-cap temperature. The fraction is assumed to be essentially that part of the total radiation from a gray body which occurs for visible wavelengths longer than 3500 Å as given in table IX. (These values are altered at the lower temperatures for the known radiation from air which differs somewhat from that for a gray body.) The temperature of the gas cap is greater than the equilibrium gas-cap temperature as a result of the nonequilibrium contribution. The approximation is made that it is

---

[1]Note that I_g is sensitive to the aspect from which the meteor is seen. From the side only about half the radiating gas cap can be seen, for example. We have arbitrarily assumed that the full face can be seen for the purposes of this report.

$$T_g = T_e \left(\frac{C_{H_{e_u}} + C_{H_{n_u}}}{C_{H_{e_u}}} \right)^{1/4} \tag{E4}$$

where $C_{H_{e_u}}$ and $C_{H_{n_u}}$ are the heat-transfer coefficients given in appendix D and T_e is the temperature of the gas cap if equilibrium prevailed. Approximate values of T_e (from ref. 23) are plotted as a function of altitude and speed in figure 56.

II ABLATION LUMINOSITY

As noted in appendix B to find the meteor size when meteor density is unknown one must find the total luminous intensity. Hence it is necessary to find the approximate variation of the luminous intensity from the ablated vapor. To this end it is assumed that the luminous efficiency factor, τ_o, is that proposed by Jacchia (ref. 21) for free molecular flow.

From equation (29)

$$\frac{dm}{dt} = - \frac{2(I - I_g)}{\tau_o V^3} = - \frac{2I_a}{\tau_o V^3} \tag{E5}$$

but from equation (10)

$$\frac{dm}{dt} = - \frac{C_H \rho_o}{2\zeta} \bar{\rho} V^3 A \tag{E6}$$

so that from equations (E5) and (E6)

$$I_a = \frac{\pi C_D \rho_o \tau_o}{4} \left(\frac{C_H}{C_D \zeta} \right) \bar{\rho} r^2 V^6 \tag{E7}$$

III LUMINOUS EFFICIENCY

Meteor astronomers define luminous intensity as

$$I(0 \text{ mag}) = 10^{-0.4 M_p} \tag{E8}$$

where M_p, termed the absolute photographic magnitude, is the apparent photometric magnitude of the meteor that would be indicated by the photographic plate of a camera located 100 km from the meteor. The Harvard Observatory group after considering the spectra of meteors and the response of photographic plates to them have calculated that the absolute photographic magnitude can be related to the corresponding absolute visible magnitude by

$$M_p = M_v - 1.8 \tag{E9}$$

The luminous intensity defined as in equation (E8) is not meaningful to aerodynamicists. Accordingly, in this report luminous intensity is defined as the amount of luminous energy per unit area, in kilowatts per square meter, received on a photographic plate 100 km from a source. To relate the luminous intensity so defined with magnitude, it is noted the apparent bolometric magnitude of the sun, M_{bs}, corresponds to the solar constant s (the amount of energy received at the orbit of the earth outside the atmosphere), so that the absolute photographic magnitude of a meteor, M_p, can be related to the luminous intensity I by

$$\log_{10} \frac{s}{I} = -0.4M_{bs} + 0.4M_p \tag{E10}$$

Now $M_{bs} = -26.85$ while the solar constant lies in the range

$$1.35 \text{ kw/m}^2 \leqq s \leqq 1.39 \text{ kw/m}^2 .$$

Choosing $s = 1.37$ kw/m^2 then we obtain the conversion formulas

$$\left.\begin{aligned} \log_{10} I(\text{kw/m}^2) &= -9.882 - 0.4M_v \\ \log_{10} I(\text{kw/m}^2) &= -10.602 - 0.4M_p \\ \log_{10} I(\text{kw/m}^2) &= -10.602 + \log_{10} I(0 \text{ mag}) \end{aligned}\right\} \tag{E11}$$

Jacchia's value of the luminous efficiency factor[2]

$$\tau_o = 6.45\times10^{-19} \frac{0 \text{ mag sec}^4}{\text{g cm}^3} \tag{E12}$$

then becomes in our units

$$\tau_o = 1.61\times10^{-20} \frac{\text{kw sec}^4}{\text{kg m}^5} \tag{E13}$$

---

[2]Recently, Cook, Jacchia, and McCrosky (ref. 26) have recommended for meteoric stone

$$\tau_o = 4.26\times10^{-19} \frac{0 \text{ mag sec}^4}{\text{g cm}^3}$$

and for meteoric iron

$$\tau_o = 27.6\times10^{-19} \frac{0 \text{ mag sec}^4}{\text{g cm}^3}$$

IV FRACTION OF TOTAL LUMINOSITY DUE TO GAS CAP

Equation (E5) gives mass loss as proportional to the difference between the total luminous intensity less that due to the gas cap. The question then arises: What fraction of the total luminosity can the gas cap contribute?

From equations (E3) and (E2) for luminous intensity in kw m^{-2}

$$I_g = \frac{1}{4} \eta C_{H_g} \rho_o r^2 \bar{\rho} V^3 \times 10^{-13} \tag{E14}$$

and from equation (C1)

$$I - I_g = \frac{1}{4} \pi \tau_o C_H \rho_o \left(\frac{\bar{\rho} r^2 V^6}{\zeta} \right) \tag{E15}$$

so that

$$\frac{I_g}{I} = \frac{1}{1 + (\pi \tau_o C_H V^3 / \eta \zeta C_{H_g}) \times 10^{13}} \tag{E16}$$

As indicated in the report for continuum flow it appears that $\tau_o \cong 10^{-20}$ kw sec^4 kg^{-1} m^{-5} while I_g/I is largest for $C_{H_g} = C_H$ which is approximately true only for large bodies. Then for stones (eq. (E16)) the maximum value of the ratio is

$$\left(\frac{I_g}{I} \right)_{max} = \frac{1}{1 + (0.035/\eta)(V/10^4)^3} \tag{E17}$$

Since η is a function of air density as well as velocity for equilibrium radiation, the ratio depends on altitude as well as velocity. This fraction is shown in figure 57. Note that at very high speeds the gas-cap luminosity cannot be a large fraction of the total once vaporization begins, so that ignoring I_g in mass-loss-rate calculations by the photometrical method may not lead to large error for such cases.

REFERENCES

1. Nininger, H. H.: Out of the Sky. An Introduction to Meteoritics. Dover Pub., N. Y., 1959.

2. Öpik, E.: A Statistical Method of Counting Shooting Stars and Its Application to the Perseid Shower of 1920. Acta Commentat Universitat Tartuensis (Univ. Dorpat), 3, 5, 1922. (Also Tartu Observatory Pub. 25, no. 1, 1922)

3. Lindemann, F. A., and Dobson, G. M. B.: A Theory of Meteors and the Density and Temperature of the Outer Atmosphere to Which It Leads. Proc. Roy. Soc., London, A 102, Jan. 1, 1923, pp. 411-437.

4. Sparrow, C. M.: Physical Theory of Meteors. Astrophys. Jour., 1926, pp. 90-110.

5. Öpik, Ernst: Atomic Collision and Radiation of Meteors. Acta Commentat. Universitat Tartuensis, Acta and Comm. 26, 2, (USSR), 1933. (Harvard Univ. Reprint 100, 1933)

6. Hoppe, J.: Die Physikalischen Vorgänge bein Eindringen Meteorische Körper in die Erdatmosphare. Astron. Nach. 262, 1937, pp. 169-198.

7. Öpik, Ernst J.: Physics of Meteor Flight in the Atmosphere. Interscience Tracts on Physics and Astronomy No. 6. Interscience Pub., N. Y., 1958.

8. Elkin, William L.: Photographic Observations of the Leonids at the Yale Observatory. Astrophys. Jour., vol. 9, 1899, pp. 20-22.

9. Elkin, William L.: Results of the Photographic Observations of the Leonids, November 14-15, 1898, at the Yale Observatory. Astrophys. Jour., vol. 10, 1899, pp. 25-28.

10. Millman, Peter M., and Hoffleit, Dorret: Meteor Photographs Taken Through a Rotating Shutter. Harvard College Observatory Tercentenary Paper 31, Harvard Univ. Obs. Annals, vol. 105, 1937, pp. 601-21.

11. Fisher, W. J.: Newton-Denning Method of Computing Meteor Paths With Celestial Globe. Proc. Natl. Acad. Sci., vol. 19, Feb. 1933, pp. 209-12.

12. Chapman, Dean R.: On the Unity and Origin of the Australasian Tektites. Geochimica et Cosmochimica Acta, vol. 28, no. 6, June 1964, p. 841.

13. Whipple, F. L.: A Comet Model. II. Physical Relations for Comets and Meteors. Astrophys. Jour., 113, May 1951, pp. 464-74.

14. Whipple, F. L.: Photographing Meteor Orbits and Their Distribution in Space. Astronom. Jour., 59, 1954, pp. 201-17.

15. Jacchia, L. G.: The Physical Theory of Meteors. VIII. Fragmentation as Cause of the Faint-Meteor Anomaly. Astrophys. Jour., 121, March 1955, pp. 521-7.

16. Verniani, F.: On the Density of Meteoroids. I.- The Density of Bright Photographic Meteors. Bologna Topographica Compositori, 1962. (Also: Nuovo Cimento, vol. 26, no. 2, Oct. 16, 1962, pp. 209-30)

17. Allen, H. Julian, and Eggers, A. J., Jr.: A Study of the Motion and Aerodynamic Heating of Ballistic Missiles Entering the Earth's Atmosphere at High Supersonic Speeds. NACA Rep. 1381, 1958. (Supersedes NACA TN 4047)

18. Allen, H. J.: The Motion and Ablation of Meteoric Bodies. Aeronautics and Astronautics - Proc. Durand Centennial Conf., Nicholas Hoff and W. G. Vincenti, eds., Pergamon Press, 1960, pp. 378-416.

19. Minzner, Raymond A., Champion K. S. W., and Pond, H. L.: The ARDC Model Atmosphere, 1959. Air Force Surveys in Geophysics No. 115, (AFCRC-TR-59-267), Air Force Cambridge Res. Center, Aug. 1959.

20. Chapman, Dean R., and Larson, Howard K.: The Lunar Origin of Tektites. NASA TN D-1556, 1963.

21. Jacchia, Luigi G.: Ballistics of the Upper Atmosphere-Air Density Profile and Variations From the Study of Meteor Trajectories. Harvard College Obs. and MIT Center of Analysis Tech. Rep. 2, 1948, pp. 1-30.

22. Cook, A. F.: The Physical Theory of Meteors. VI. The Light Curve. Astrophys. Jour. 120, 1954, pp. 572-7.

23. Allen, H. Julian, and Yoshikawa, Kenneth K.: Luminosity From Large Meteoric Bodies. Smithsonian Contributions to Astrophysics. Proc. Symposium on the Astronomy and Physics of Meteors, vol. 7, 1963, pp. 181-194.

24. Millman, Peter M., and Cook, Allan F.: Photometric Analysis of a Spectrogram of a Very Slow Meteor. Astrophys. Jour., vol. 130, no. 2, Sept. 1959, pp. 648-662.

25. Ceplecha, Zd., Rajchl, F., and Sehnal, L.: Complete Data on Bright Meteor 1576l. Bulletin Astro. Inst. Czechoslovakia, vol. 10, no. 6, 1959, pp. 204-12.

26. Cook, A. F., Jacchia, L. G., and McCrosky, R. E.: Luminous Efficiency of Iron and Stone Asteroidal Meteors. Smithsonian Contributions to Astrophysics. Proc. Symposium on the Astronomy and Physics of Meteors, vol. 7, 1963, pp. 209-20.

27. Ceplecha, Zd., and Davies, J. G.: On the Change of the Heat Transfer Coefficient of Bright Meteors. Bulletin Astro. Inst. Czechoslovakia, 1963.

28. Ceplecha, Zd.: Multiple Fall of Příbram Meteorites Photographed. Bulletin Astro. Inst. Czechoslovakia, vol. 12, no. 2, 1960, pp. 21-47.

29. Timoshenko, S., and Young, D. H.: Advanced Dynamics. McGraw-Hill, N. Y., 1948, pp. 113-114.

30. Allen, H. Julian: Gas Dynamic Problems of Space Vehicles. Proc. NASA - Univ. Conf. on the Science and Technology of Space Exploration. Chicago, Ill., vol. 2, no. 54, Nov. 1-3, 1962, pp. 251-267.

31. Craig, Roger A., and Davy, William C.: Thermal Radiation From Ablation Products Injected Into a Hypersonic Shock Layer. NASA TN D-1978, 1963.

32. Scarborough, James B.: Numerical Mathematical Analysis. Fourth ed., Johns Hopkins Press, Baltimore, 1958, pp. 443-446.

33. McAdams, William H.: Heat Transmission. McGraw-Hill, N. Y., and London, 1942, pp. 162-164.

34. Stalder, Jackson R., Goodwin, Glen, and Creager, Marcus O.: Heat Transfer to Bodies in a High-Speed Rarefied Gas Stream. NACA Rep. 1093, 1952. (Supersedes NACA TN 2438)

35. Bloxsom, D. E., and Rhodes, B. V.: Experimental Effect of Bluntness and Gas Rarefaction on Drag Coefficients and Stagnation Heat Transfer on Axisymmetric Shapes in Hypersonic Flow. Jour. Aerospace Sci., vol. 29, no. 12, Dec. 1962, pp. 1429-42.

36. Chapman, Dean R.: An Approximate Analytical Method for Studying Entry Into Planetary Atmospheres. NASA TR R-11, 1959.

37. Lees, Lester: Recent Developments in Hypersonic Flow. Jet Propulsion, vol. 27, no. 11, Nov. 1957, pp. 1162-1178.

38. Adams, Mac C.: Recent Advances in Ablation. ARS Jour., vol. 29, no. 9, Sept. 1959, pp. 625-632.

39. Lundell, John H., Winovich, Warren, and Wakefield, Roy M.: Simulation of Convective and Radiative Entry Heating Advances in Hypersonic Techniques. Proc. Second Symposium on Hypervelocity Techniques. Plenum Press, N. Y., 1962, pp. 729-48.

40. Allen, H. Julian, Seiff, Alvin, and Winovich, Warren: Aerodynamic Heating of Conical Entry Vehicles at Speeds in Excess of Earth Parabolic Speed. NASA TR R-185, 1963.

41. Riddell, Frederick R., and Winkler, Howard B.: Meteorites and Re-entry of Space Vehicles at Meteor Velocities. ARS Jour., vol. 32, 1962, pp. 1523-1530.

42. Fay, James A., Moffett, W. Craig, and Probstein, Ronald F.: An Analytical Study of Meteor Entry. AIAA 63-451, 1963.

TABLE I.- ABLATION ENERGY PER UNIT MASS FOR METEORIC MATERIALS

Material	Ablation energy per unit mass, ζ, m^2/sec^2	
	Vapor ablation	Fluid ablation
Stone	9.2×10^6	1.9×10^6
Iron	9.1×10^6	1.5×10^6

TABLE II.- FLIGHT DATA FOR MEANOOK METEOR 132

($\sin \theta = 0.868$)

t, sec	h, km	V, km/sec	dV/dt, km/sec^2
0	67.59	17.42	-0.31
.1		17.39	-.36
.2	64.56	17.35	-.42
.3		17.30	-.50
.4	61.55	17.25	-.60
.5		17.18	-.73
.6	58.57	17.10	-.88
.7		17.00	-1.06
.8	55.58	16.89	-1.28
.9		16.75	-1.55
1.0	52.71	16.58	-1.88
1.1		16.37	-2.28
1.2	49.87	16.12	-2.76
1.3		15.82	-3.34
1.4	47.12	15.45	-4.02
1.5		15.01	-4.77
1.6	44.51	14.49	-5.67
1.7		13.86	-6.97
1.8	42.11	13.10	-8.18
1.9		12.24	-9.08
2.0	39.98	11.28	-9.97
2.1		10.25	-10.58
2.2	38.21	9.16	-11.21
2.3	37.46	(8.00)	

TABLE III.- FLIGHT DATA FOR ONDŘEJOV METEOR 15761

($\sin \theta = 0.4631$)

t, sec	h, km	V, km/sec	ΔV, km/sec	dV/dt, km/sec^2	$\Delta dV/dt$, km/sec^2
0.42443	68.696	21.750	±0.036	-0.56	±0.16
.82186	64.585	21.431	±.033	-.87	±.14
1.13871	61.479	21.122	±.042	-1.02	±.23
1.34575	59.437	20.895	±.052	-1.22	±.43
1.55279	57.422	20.552	±.069	-1.83	±.58
1.73461	55.687	20.122	±.077	-2.76	±.85
1.86468	54.478	19.750	±.055	-3.09	±.92
1.96820	53.532	19.421	±.035	-4.01	±.59
2.07172	52.605	19.054	±.040	-4.14	±.67
2.17523	51.694	18.697	±.039	-3.80	±.65
2.27875	50.801	18.267	±.036	-4.67	±.60
2.38227	49.933	17.799	±.030	-4.30	±.50
2.48579	49.087	17.258	±.035	-6.19	±.60
2.58931	48.273	16.673	±.032	-5.17	±.54
2.69283	47.482	16.094	±.019	-6.31	±.31
2.78699	46.792	15.509	±.033	-6.18	±.60
2.88244	46.114	14.881	±.047	-7.72	±.77
3.00207	45.311	13.983	±.080	-8.09	±1.34
3.10558	44.657	13.176	±.096	-8.16	±1.61
3.17805	44.223	12.544	±.100	-9.87	±2.42

TABLE IV.- FLIGHT DATA FOR HARVARD METEOR 1242

($\sin \theta = 0.632$)

t, sec	h, km	V, km/sec	ΔV, km/sec	dV/dt, km/sec^2	$\Delta dV/dt$, km/sec^2
1.0526	62.56	11.93	±0.005	-0.185	±0.013
1.6842	57.78	11.81	±.005	-.389	±.008
2.3158	53.10	11.48	±.005	-.660	±.007
2.9474	48.61	10.94	±.005	-1.024	±.010
3.5790	44.38	10.13	±.005	-1.505	±.030
4.2105	40.57	8.87	±.005	-2.23	±.067

TABLE V.- FLIGHT DATA FOR SACRAMENTO PEAK METEOR 19816

($\sin \theta = 0.716$)

t, sec	h, km	V, km/sec	ΔV, km/sec	dV/dt, km/sec^2	$\Delta dV/dt$, km/sec^2
0.764	80.13	20.67	±0.01	-0.158	±0.009
1.135	74.02	20.57	±.02	-.416	±.018
1.860	64.16	19.87	±.05	-2.02	±.05
2.038	61.06	19.27	±.09	-2.75	±.10
2.425	56.49	17.85	±.11	-5.92	±.11
2.623	53.75	16.36	±.18	-8.45	±.18
2.824	51.87	14.63	±.19	-9.67	±.19
3.124	48.92	10.77	±.30	-8.90	±.29

TABLE VI.- FLIGHT DATA FOR ONDŘEJOV METEOR 27471

($\sin \theta = 0.7575$)

h, km	V, km/sec
56.01	24.95
54.25	24.72
50.41	23.88
47.81	22.97
43.89	19.54
42.86	17.65
42.19	15.97

TABLE VII.- FLIGHT DATA FOR ONDŘEJOV METEOR PŘÍBRAM

($\sin \theta = 0.6853$; $\rho_m = 3500$ kg/m^3)

t, sec	h, km	V, km/sec	ΔV, km/sec	dV/dt, km/sec^2	$\Delta dV/dt$, km/sec^2
0.00000	88.594	20.887	±0.009	-0.031	±0.035
.85602	76.318	20.860	±.007	-.113	±.031
.85806	76.289	20.864	±.010	-.000	±.039
1.73230	63.837	20.838	±.013	-.100	±.049
2.49383	52.970	20.773	±.013	-.207	±.071
2.69203	50.164	20.717	±.013	-.370	±.068
3.06758	44.858	20.459	±.024	-1.080	±.160

TABLE VIII.- ALTITUDE FUNCTIONS

(Code: 0.434 -2 = 0.434×10^{-2})

h, m	$\bar{\rho}$	$\beta + h\frac{d\beta}{dh}$	h, m	$\bar{\rho}$	$\beta + h\frac{d\beta}{dh}$
38,000	0.434 -2	1.44 -4	64,000	0.179 -3	1.23 -4
39,000	.376 -2	1.42 -4	65,000	.158 -3	1.26 -4
40,000	.327 -2	1.41 -4	66,000	.139 -3	1.28 -4
41,000	.284 -2	1.39 -4	67,000	.122 -3	1.30 -4
42,000	.247 -2	1.38 -4	68,000	.107 -3	1.33 -4
43,000	.216 -2	1.36 -4	69,000	.937 -4	1.36 -4
44,000	.189 -2	1.34 -4	70,000	.817 -4	1.39 -4
45,000	.164 -2	1.32 -4	71,000	.710 -4	1.41 -4
46,000	.145 -2	1.30 -4	72,000	.616 -4	1.45 -4
47,000	.127 -2	1.28 -4	73,000	.532 -4	1.48 -4
48,000	.112 -2	1.26 -4	74,000	.458 -4	1.51 -4
49,000	.996 -3	1.24 -4	75,000	.393 -4	1.55 -4
50,000	.884 -3	1.21 -4	76,000	.336 -4	1.58 -4
51,000	.785 -3	1.18 -4	77,000	.287 -4	1.62 -4
52,000	.697 -3	1.15 -4	78,000	.243 -4	1.66 -4
53,000	.619 -3	1.12 -4	79,000	.206 -4	1.73 -4
54,000	.554 -3	1.09 -4	80,000	.173 -4	1.86 -4
55,000	.499 -3	1.07 -4	81,000	.142 -4	1.96 -4
56,000	.448 -3	1.07 -4	82,000	.116 -4	2.00 -4
57,000	.402 -3	1.09 -4	83,000	.947 -5	2.01 -4
58,000	.361 -3	1.11 -4	84,000	.775 -5	2.01 -4
59,000	.322 -3	1.13 -4	85,000	.634 -5	2.01 -4
60,000	.288 -3	1.15 -4	86,000	.518 -5	2.01 -4
61,000	.256 -3	1.17 -4	87,000	.424 -5	2.01 -4
62,000	.228 -3	1.19 -4	88,000	.347 -5	2.01 -4
63,000	.202 -3	1.21 -4	90,000	.284 -5	2.01 -4

TABLE IX.- THE GAS TEMPERATURE FUNCTION

$T_G(^{\circ}K \times 10^{-3})$	η	$T_G(^{\circ}K \times 10^{-3})$	η	$T_G(^{\circ}K \times 10^{-3})$	η
1	1.0000	21	0.173	41	0.035
2	1.0000	22	.156	42	.033
3	1.0000	23	.141	43	.031
4	.995	24	.128	44	.029
5	.972	25	.117	45	.028
6	.928	26	.108	46	.026
7	.856	27	.100	47	.024
8	.772	28	.091	48	.023
9	.692	29	.083	49	.022
10	.611	30	.076	50	.021
11	.544	31	.070	51	.020
12	.480	32	.065	52	.019
13	.425	33	.060	53	.018
14	.381	34	.056	54	.017
15	.338	35	.052	55	.016
16	.302	36	.049	56	.015
17	.269	37	.045	57	.014
18	.240	38	.043	58	.014
19	.215	39	.040	59	.013
20	.192	40	.038	60	.013

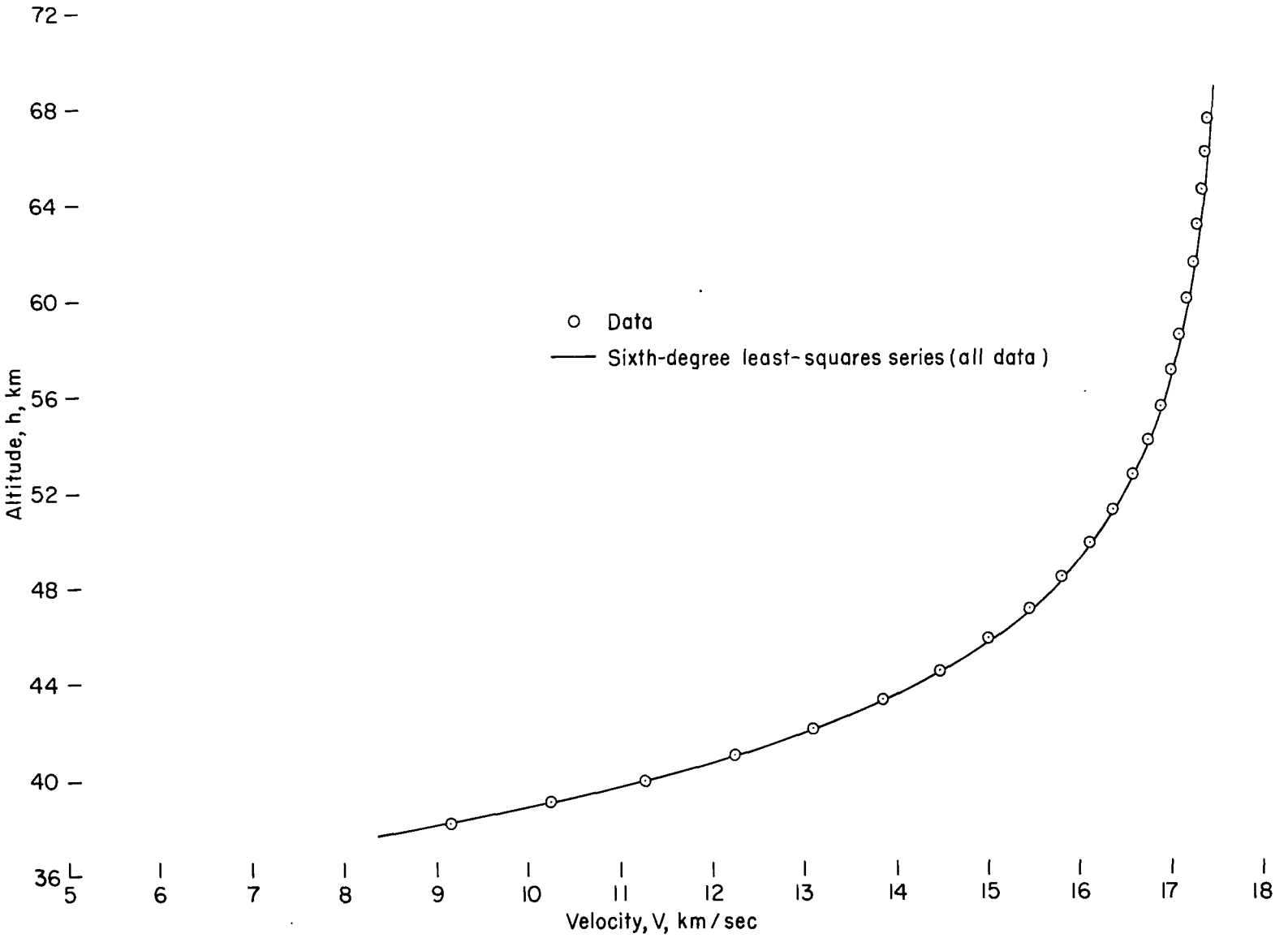

Figure 1.- Comparison of polynomial fit of velocity with data for Meanook meteor 132.

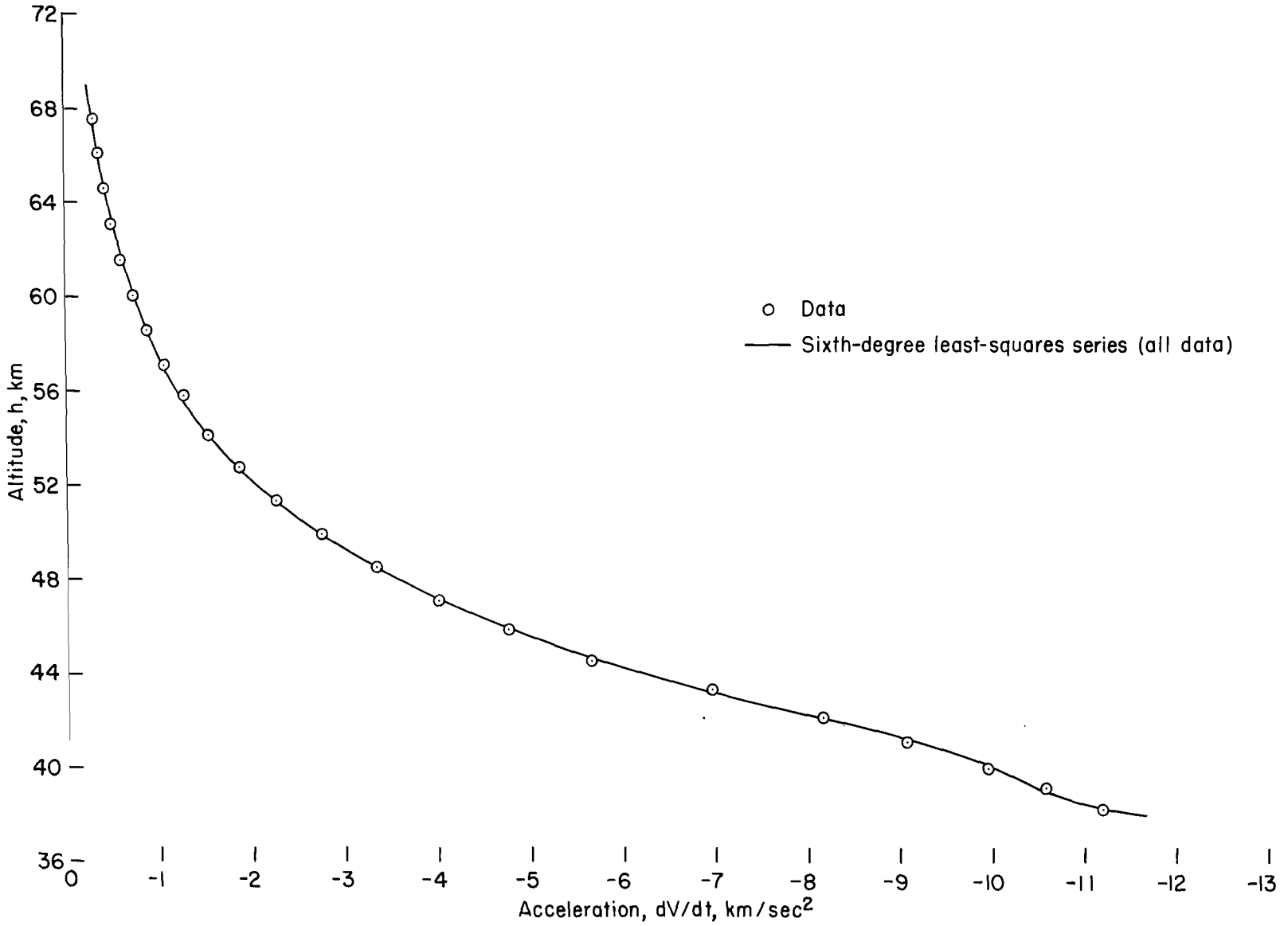

Figure 2.- Comparison of polynomial fit of acceleration with data for Meanook meteor 132.

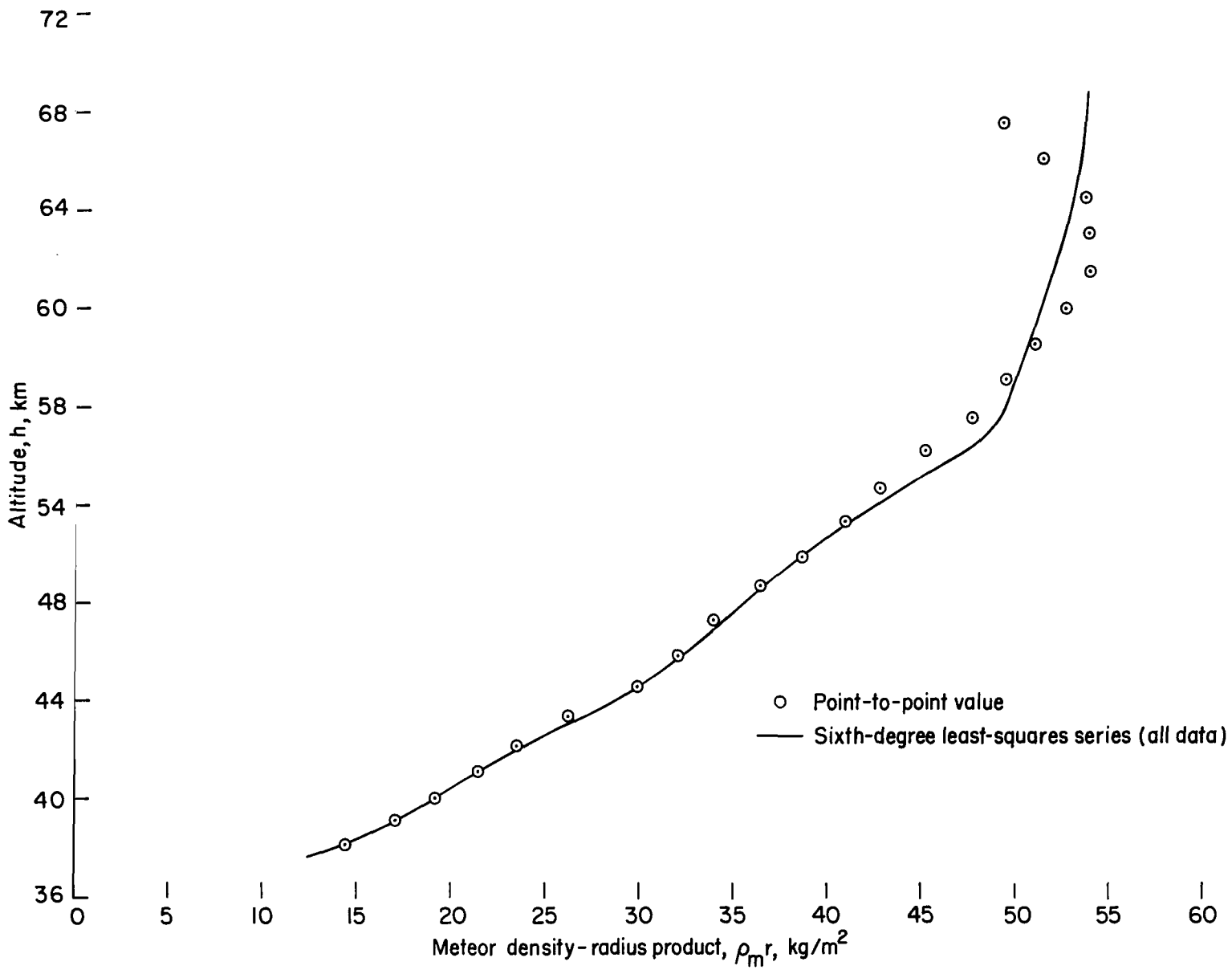

Figure 3.- Results of dynamical analyses of meteor density-radius product for Meanook meteor 132.

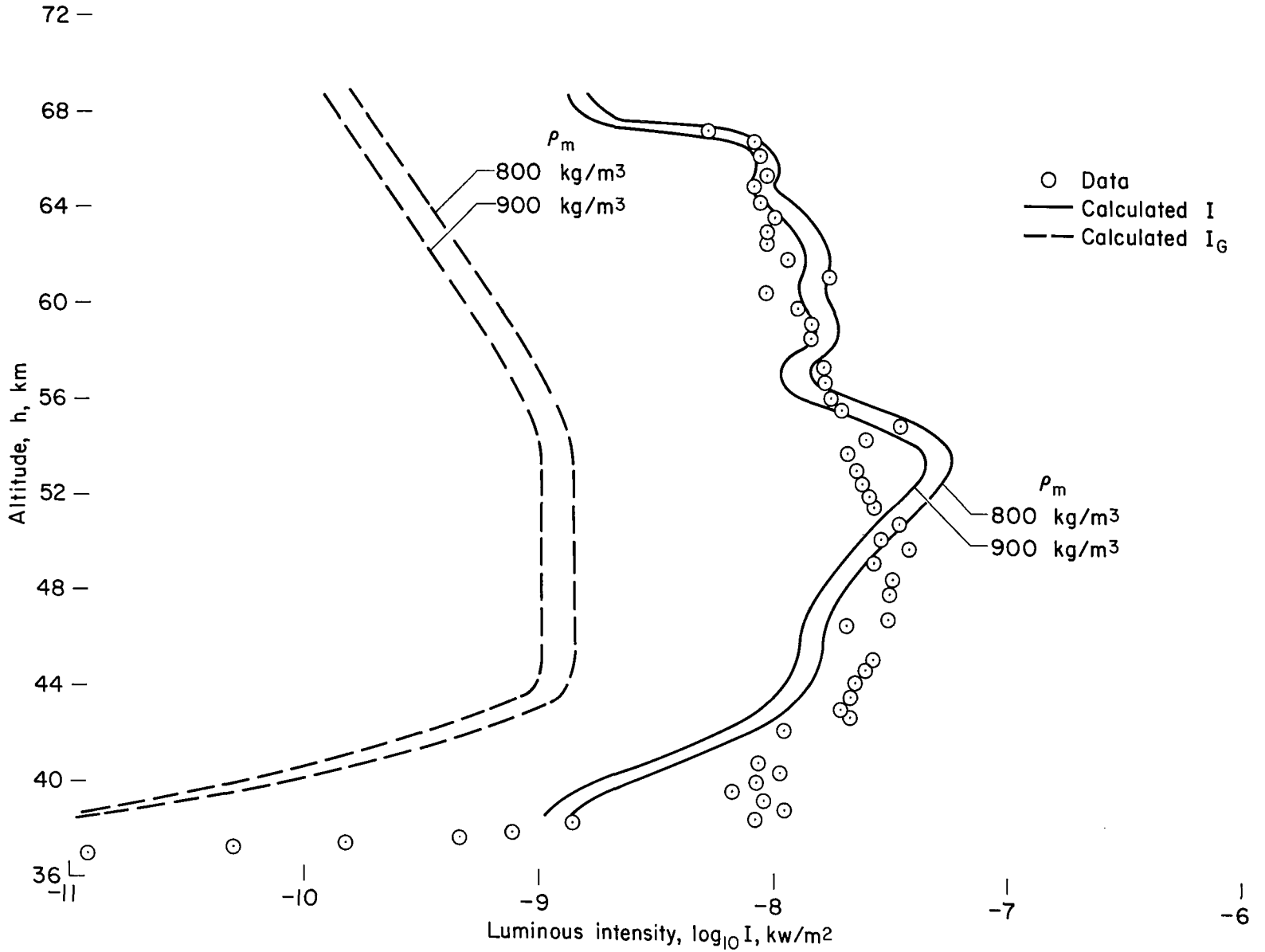

Figure 4.- Comparison of measured luminous intensity with that calculated for best fit using the standard value of τ_0 for Meanook meteor 132.

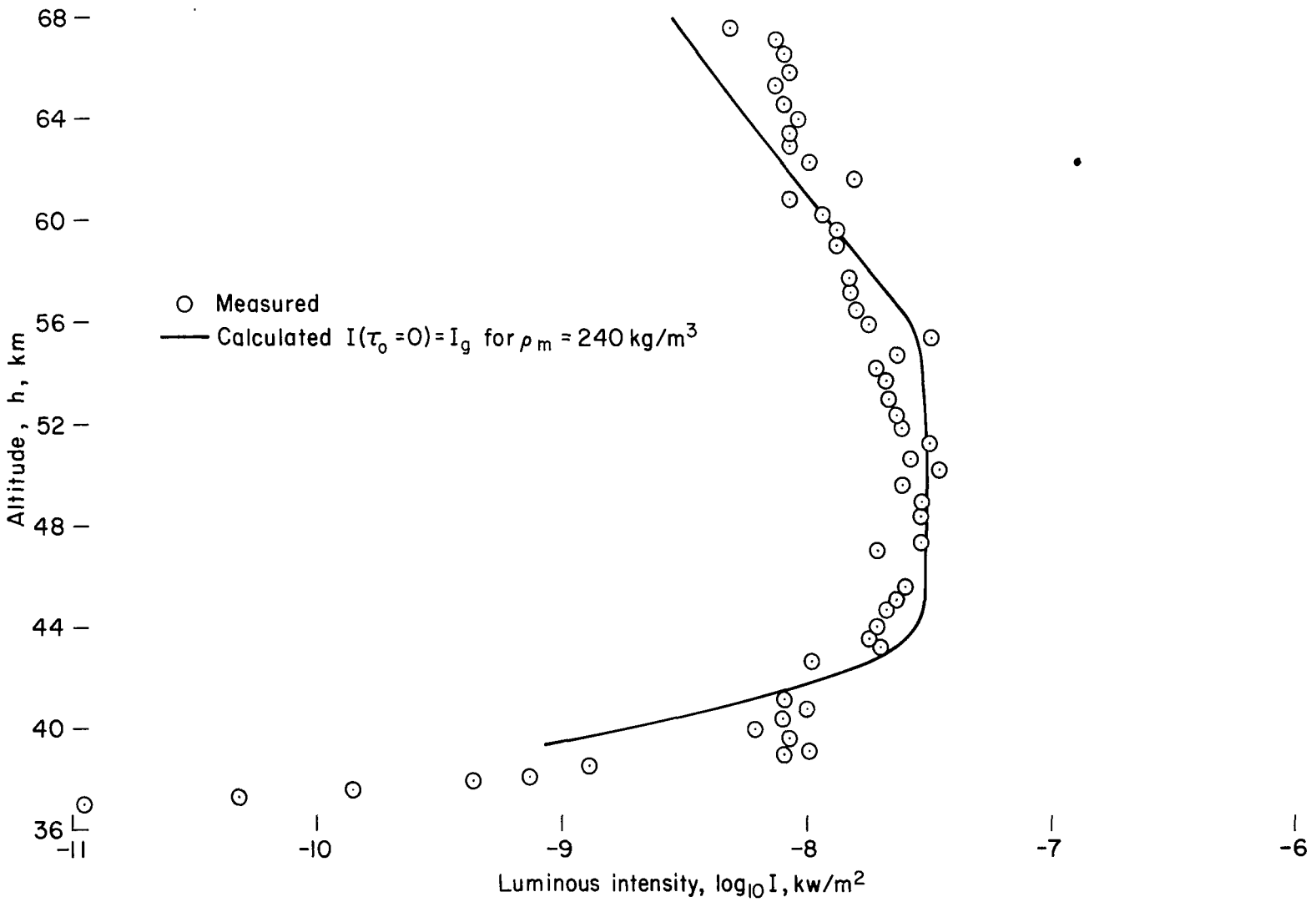

Figure 5.- Comparison of measured luminous intensity with that calculated for best fit using a zero value for τ_0 for Meanook meteor 132.

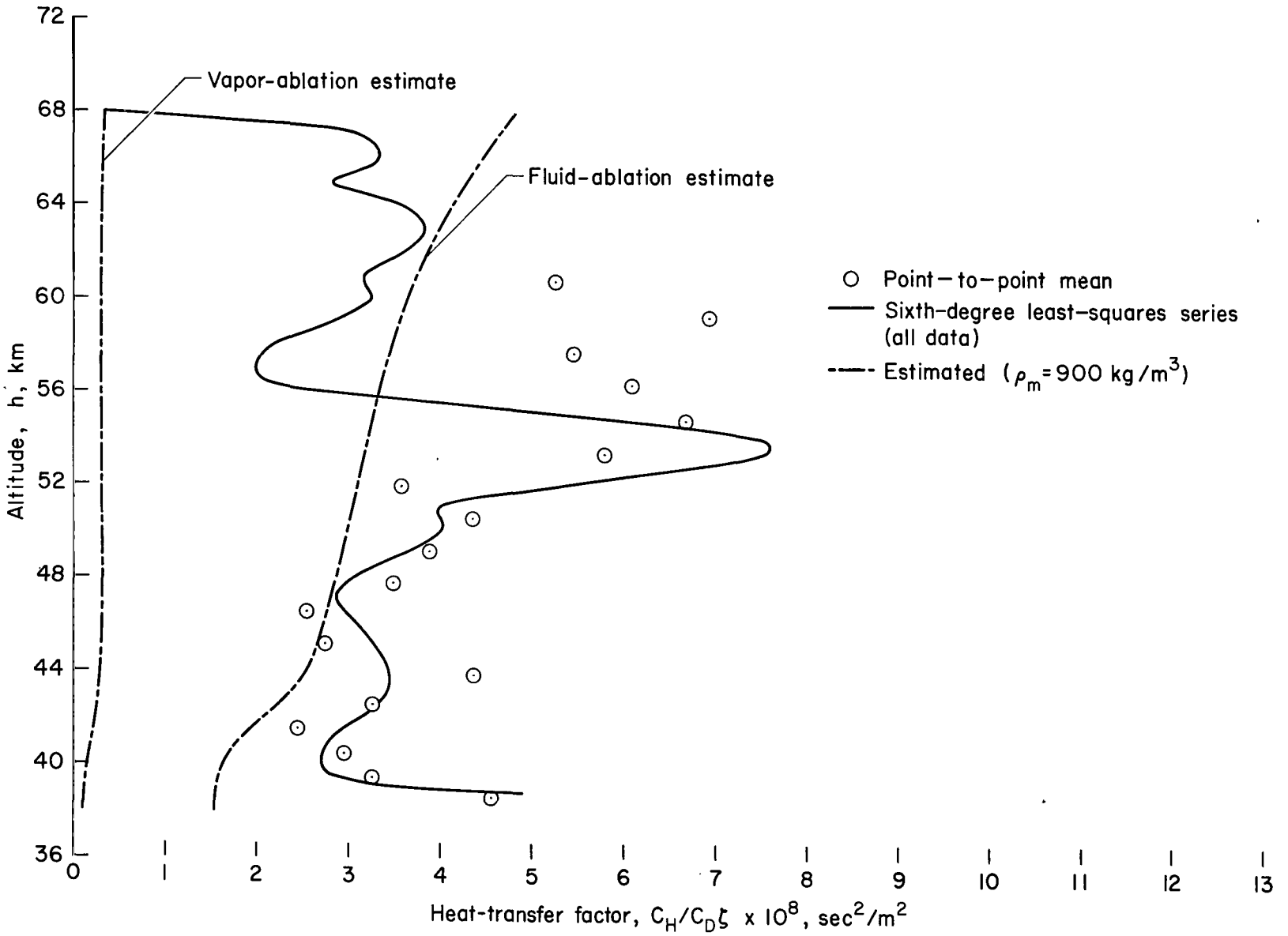

Figure 6.- Comparison of calculated heat-transfer factors obtained from dynamical analyses with fluid- and vapor-ablation estimates for Meanook meteor 132.

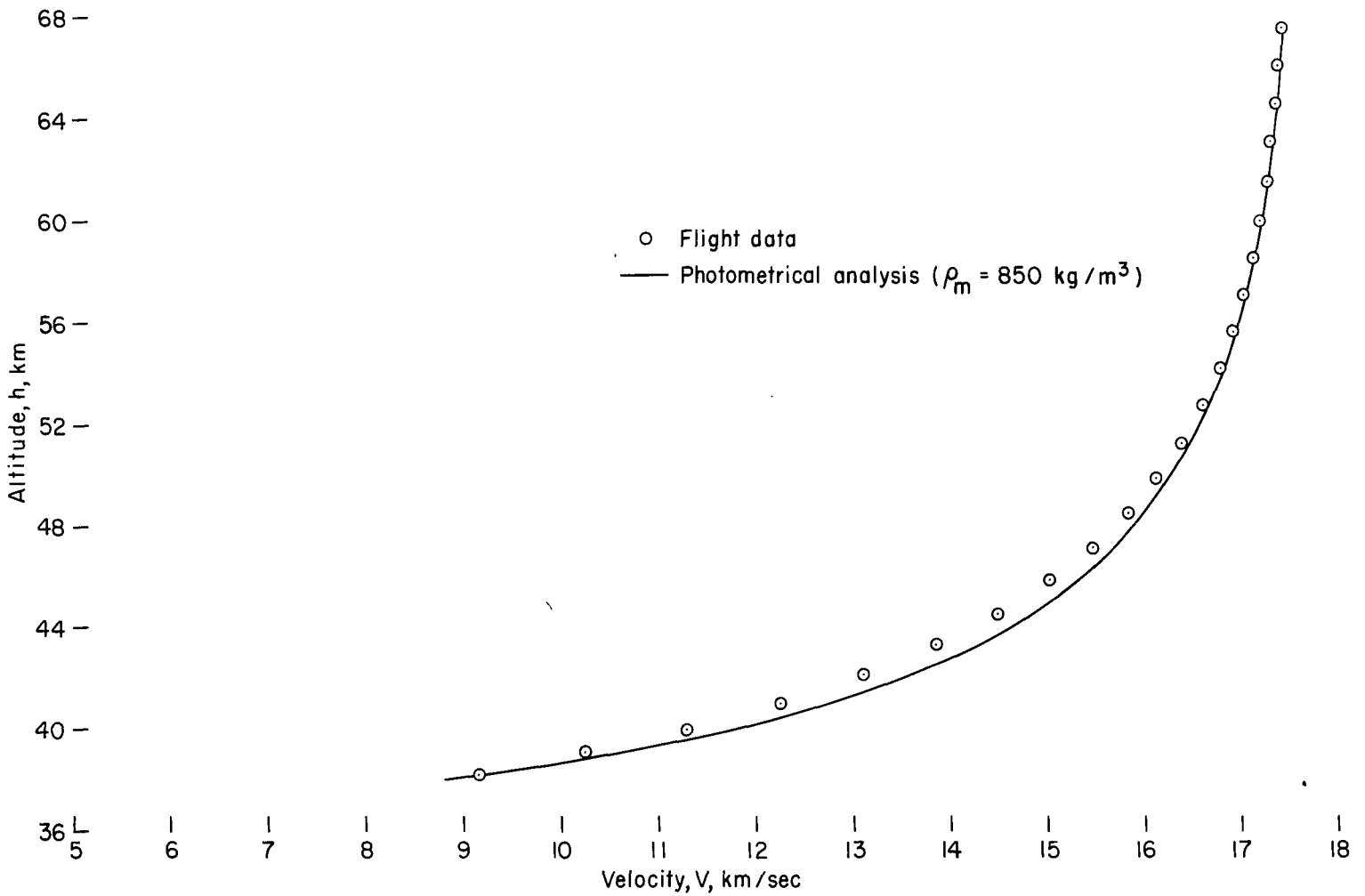

Figure 7.- Comparison of calculated best-fit photometrical results of velocity with data for Meanook meteor 132.

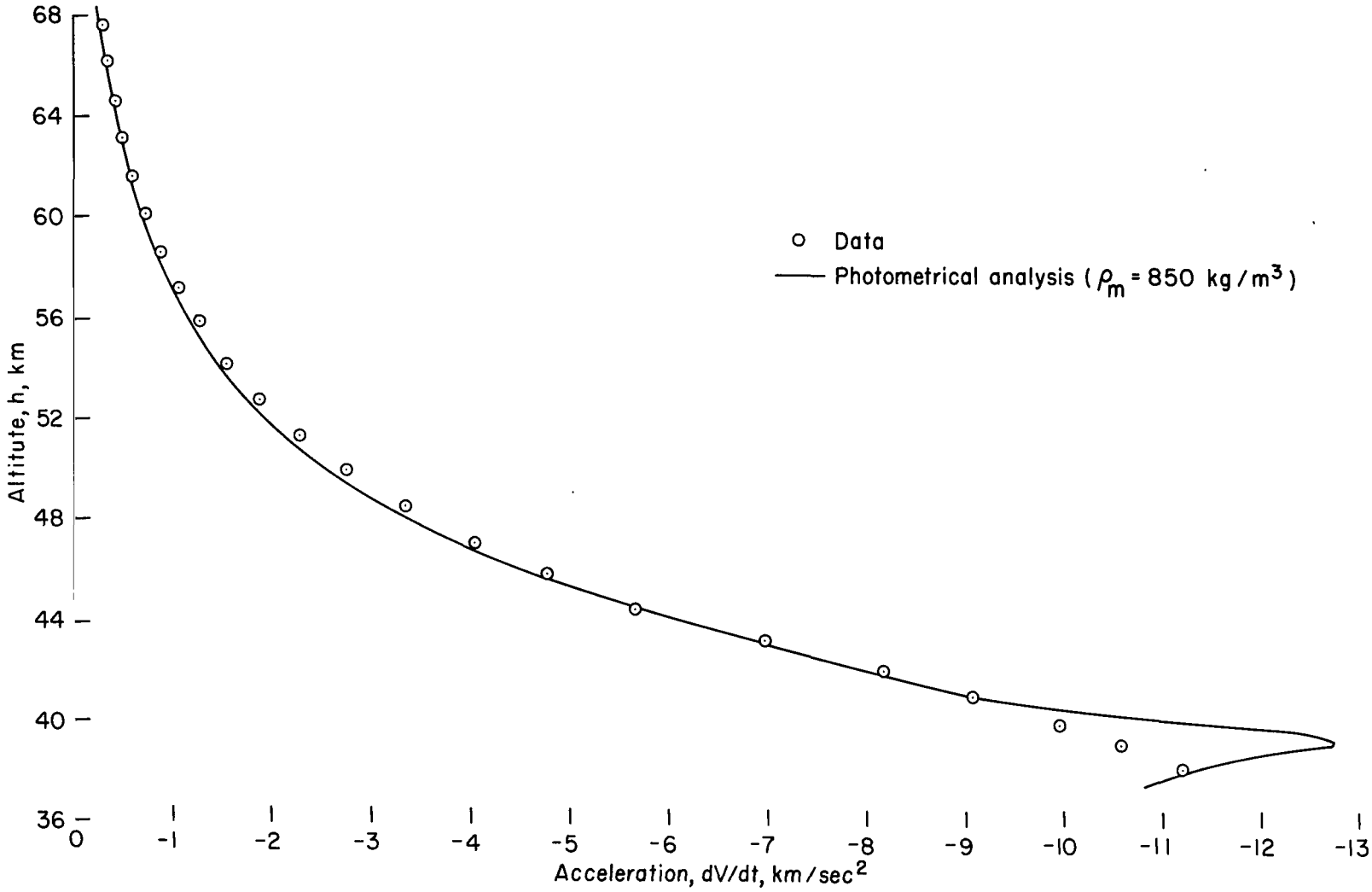

Figure 8.- Comparison of calculated best-fit photometrical results of acceleration with data for Meanook meteor 132.

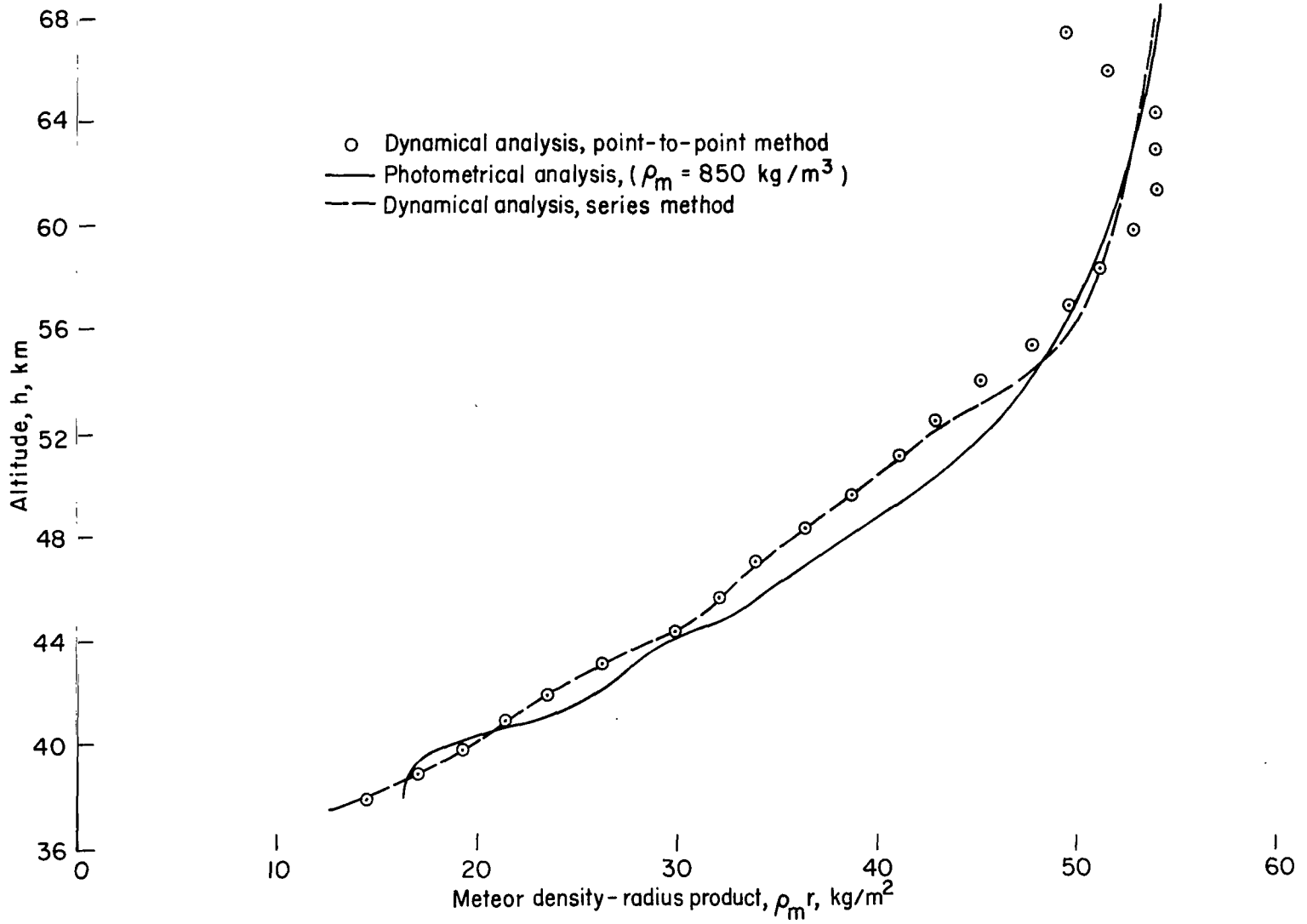

Figure 9.- Comparison of calculated meteor density-radius product as obtained from the dynamical and photometrical analyses for Meanook meteor 132.

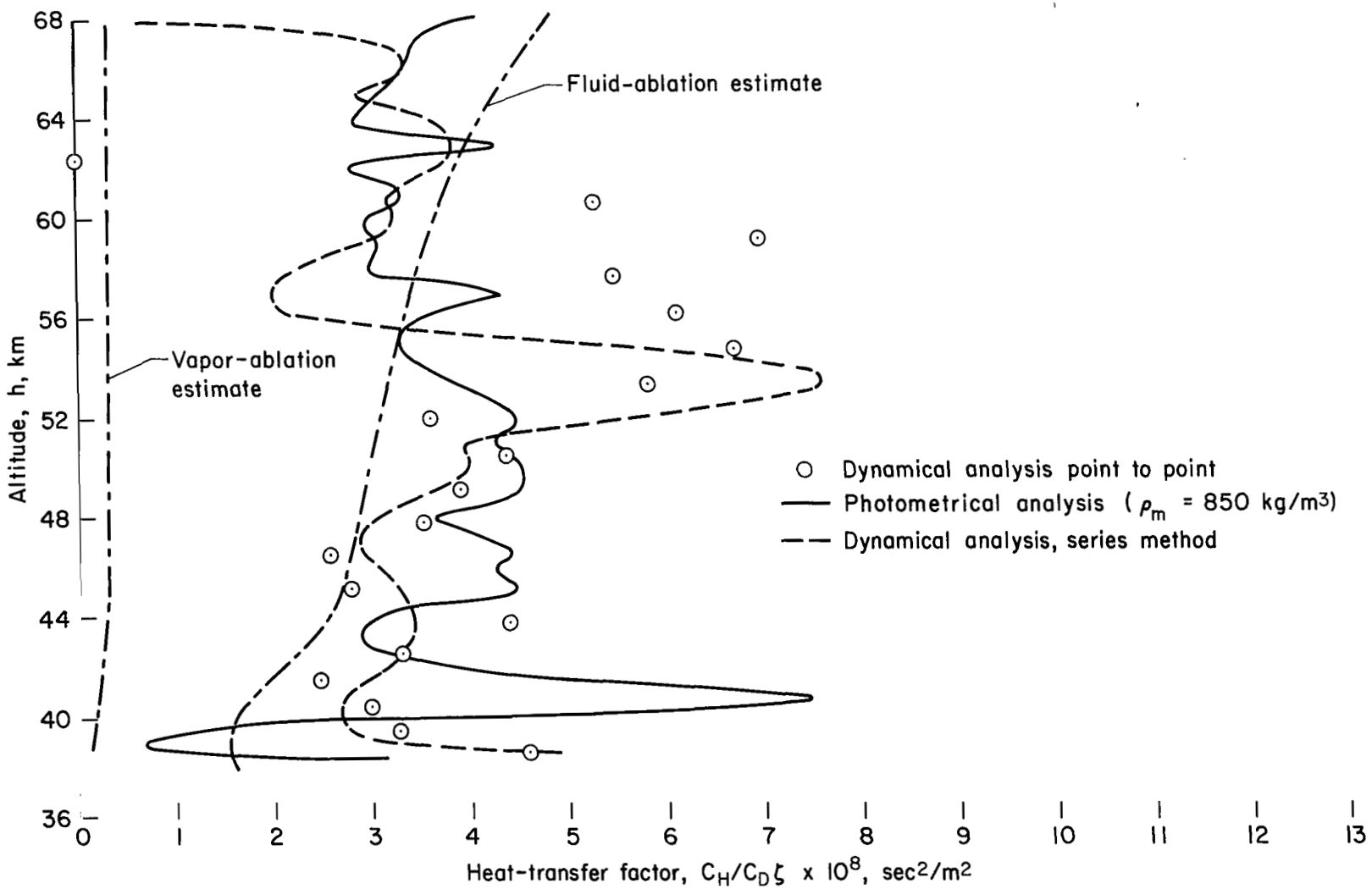

Figure 10.- Comparison of calculated heat-transfer factors as obtained from the dynamical and photometrical analyses with fluid- and vapor-ablation estimates for Meanook meteor 132.

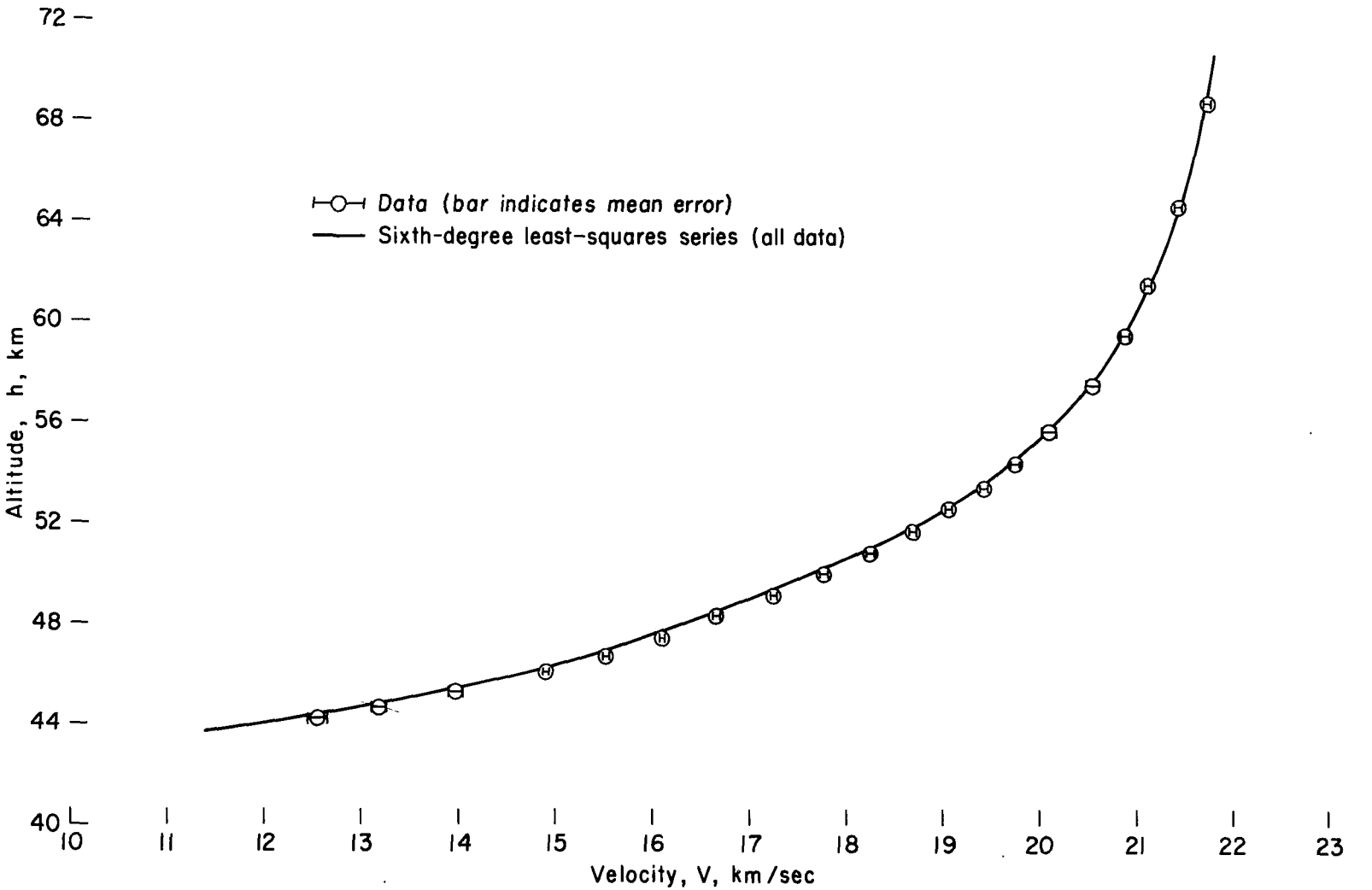

Figure 11.- Comparison of polynomial fit of velocity with data for Ondřejov meteor 15761.

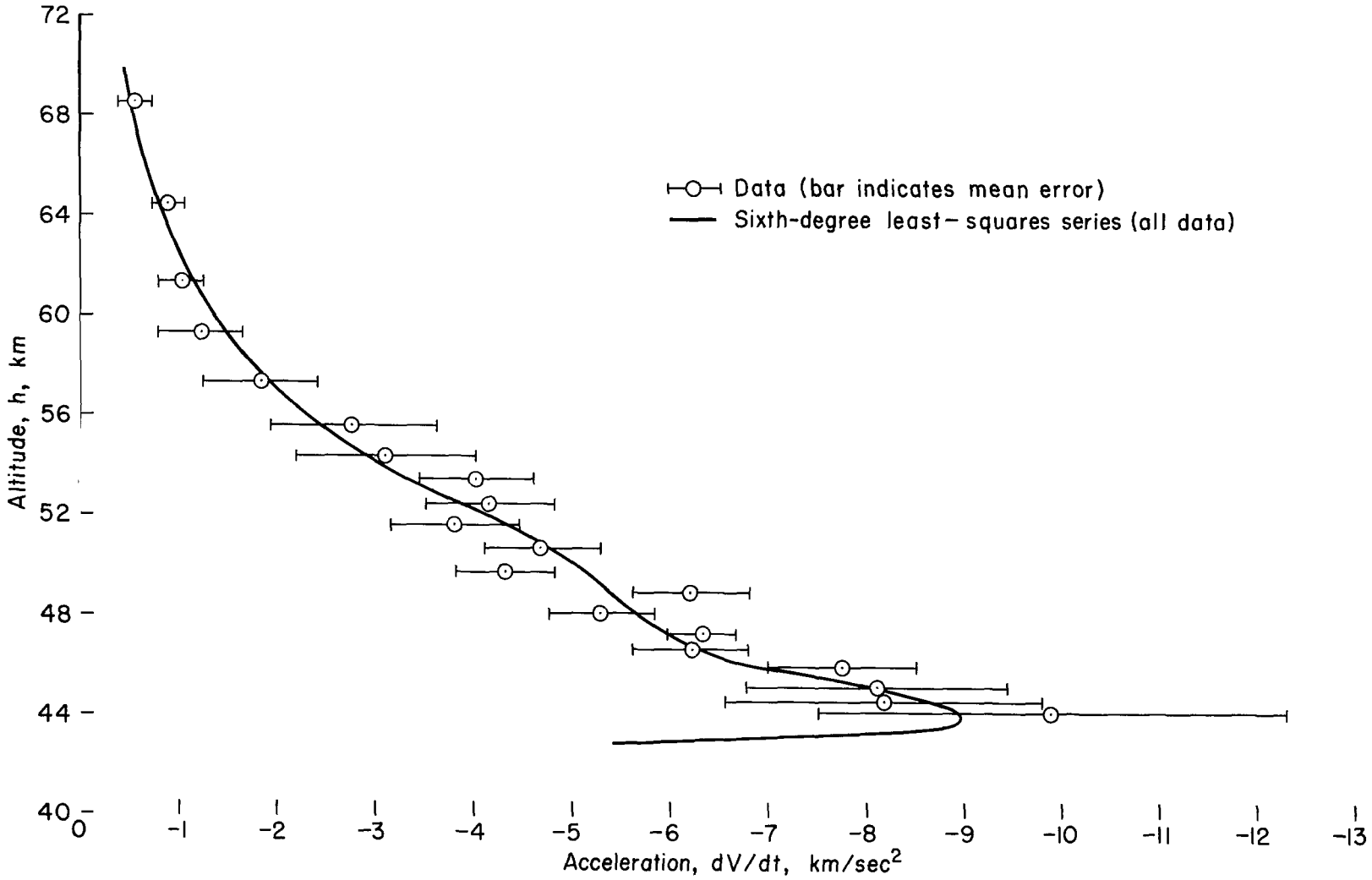

Figure 12.- Comparison of polynomial fit of acceleration with data for Ondřejov meteor 15761.

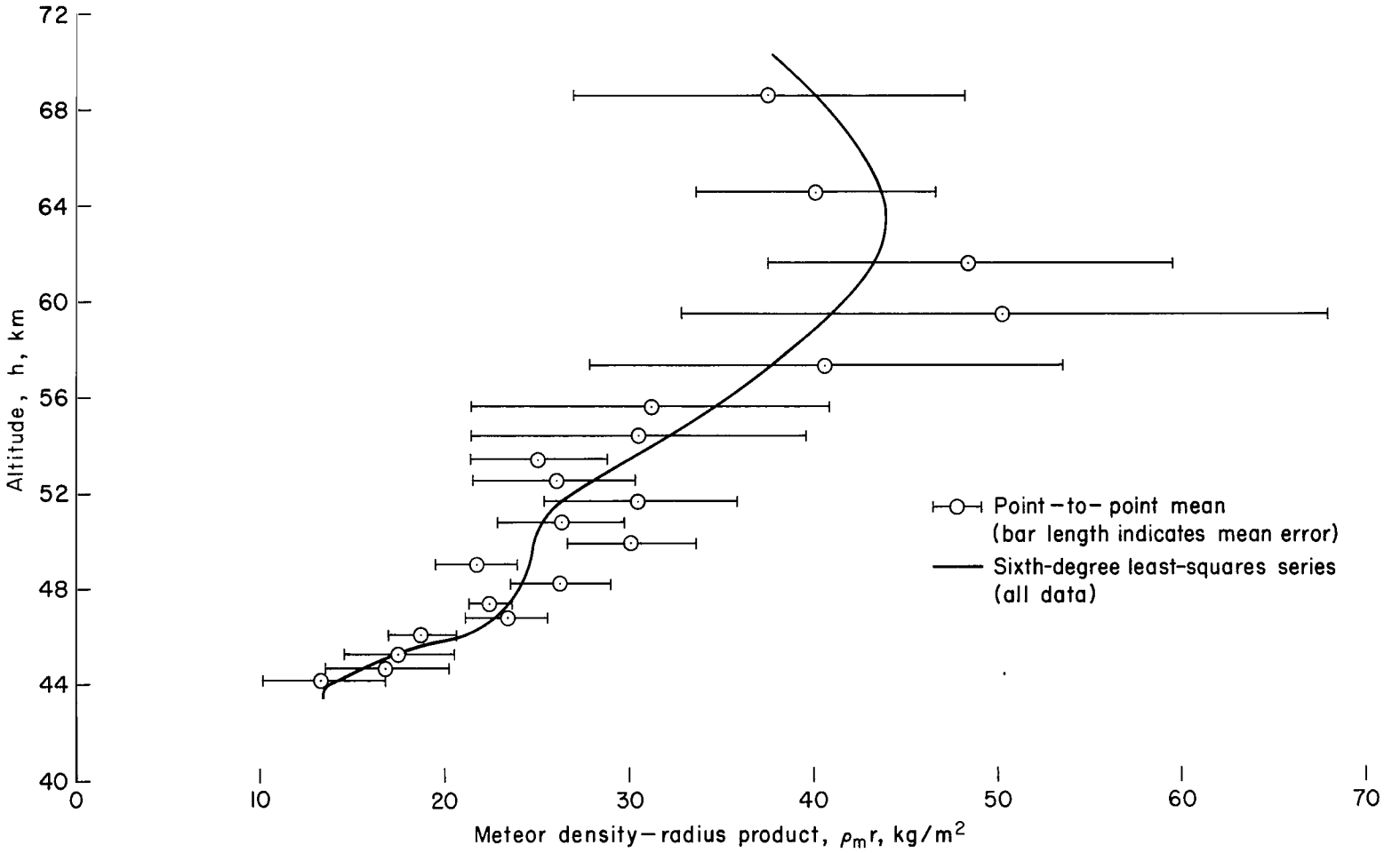

Figure 13.- Results of dynamical analyses of meteor density-radius product for Ondřejov meteor 15761.

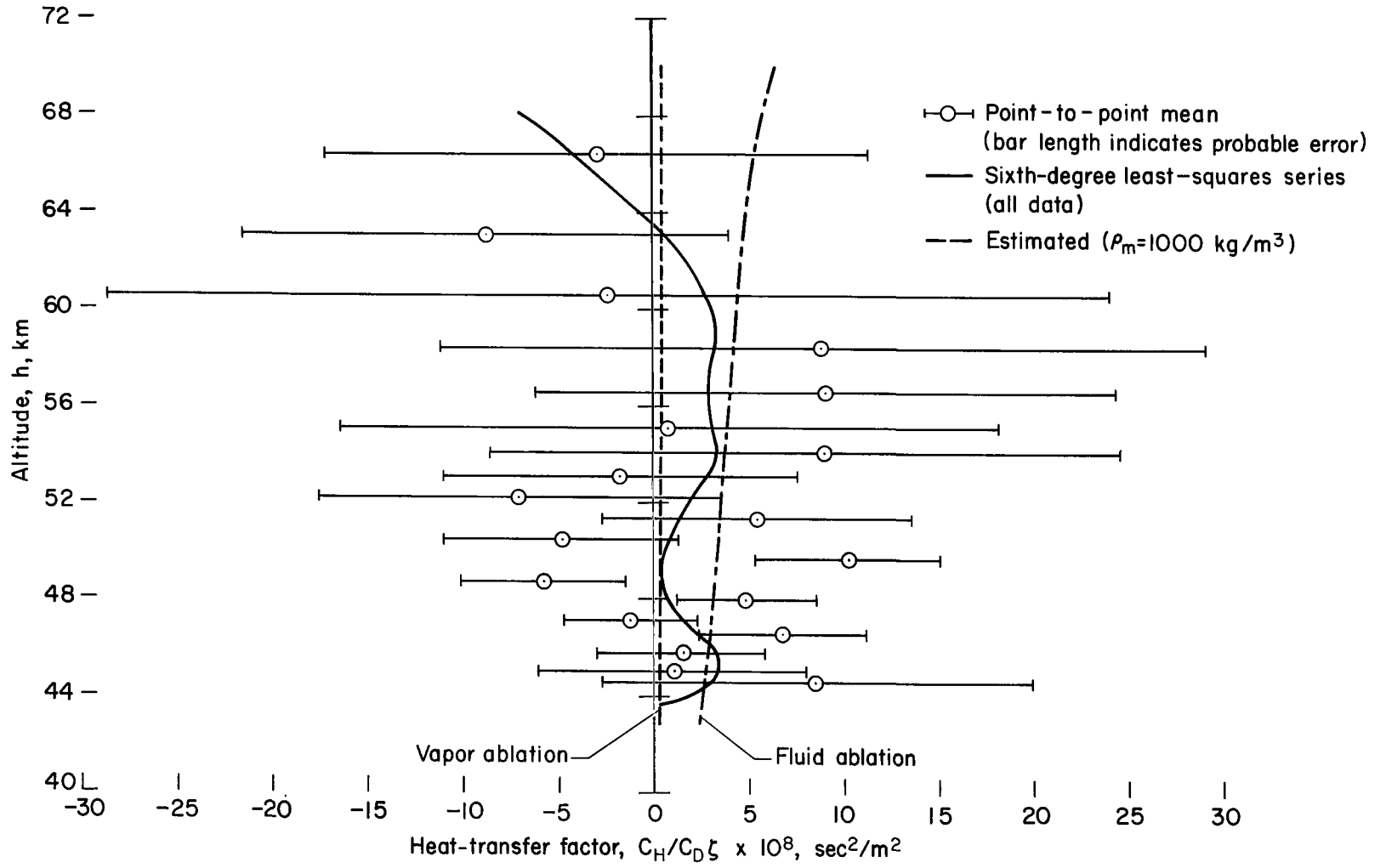

Figure 14.- Comparison of calculated heat-transfer factors obtained from dynamical analyses with fluid- and vapor-ablation estimates for Ondřejov meteor 15761.

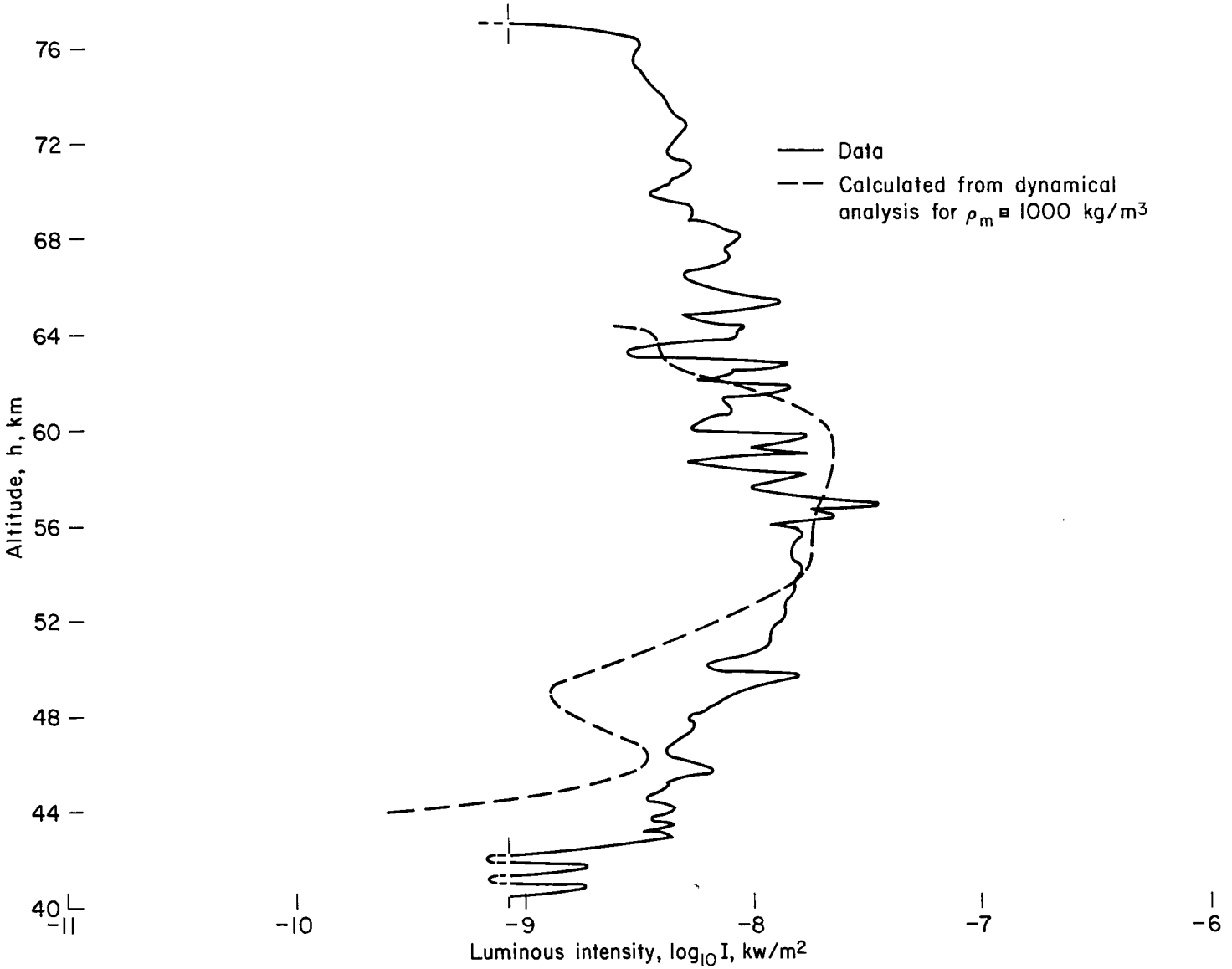

Figure 15.- Comparison of measured luminous intensity with that calculated for near best fit using the standard value of τ_0 for Ondřejov meteor 15761.

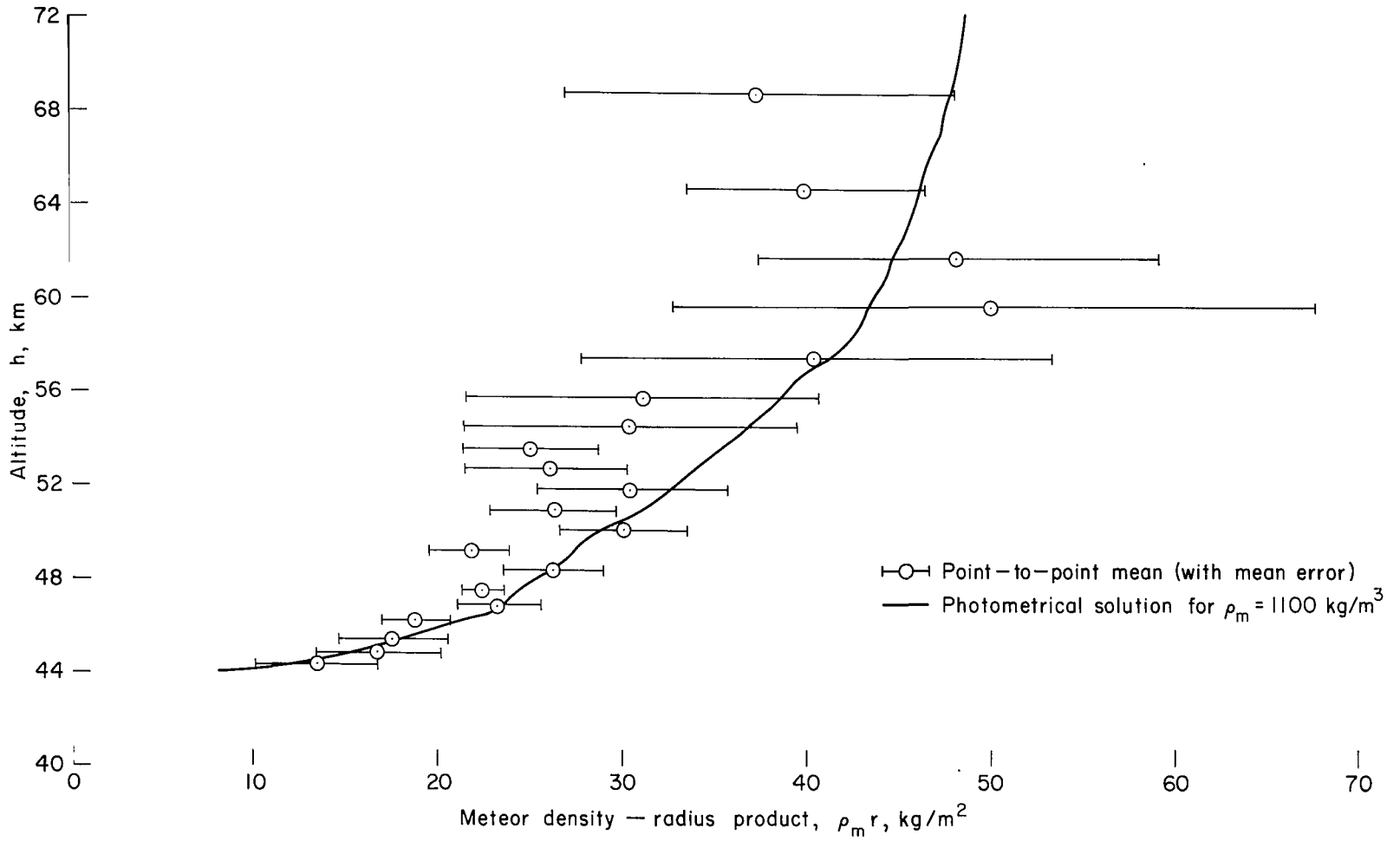

Figure 16.- Comparison of calculated meteor density-radius product as obtained from dynamical and best-fit photometrical analyses for Ondřejov meteor 15761.

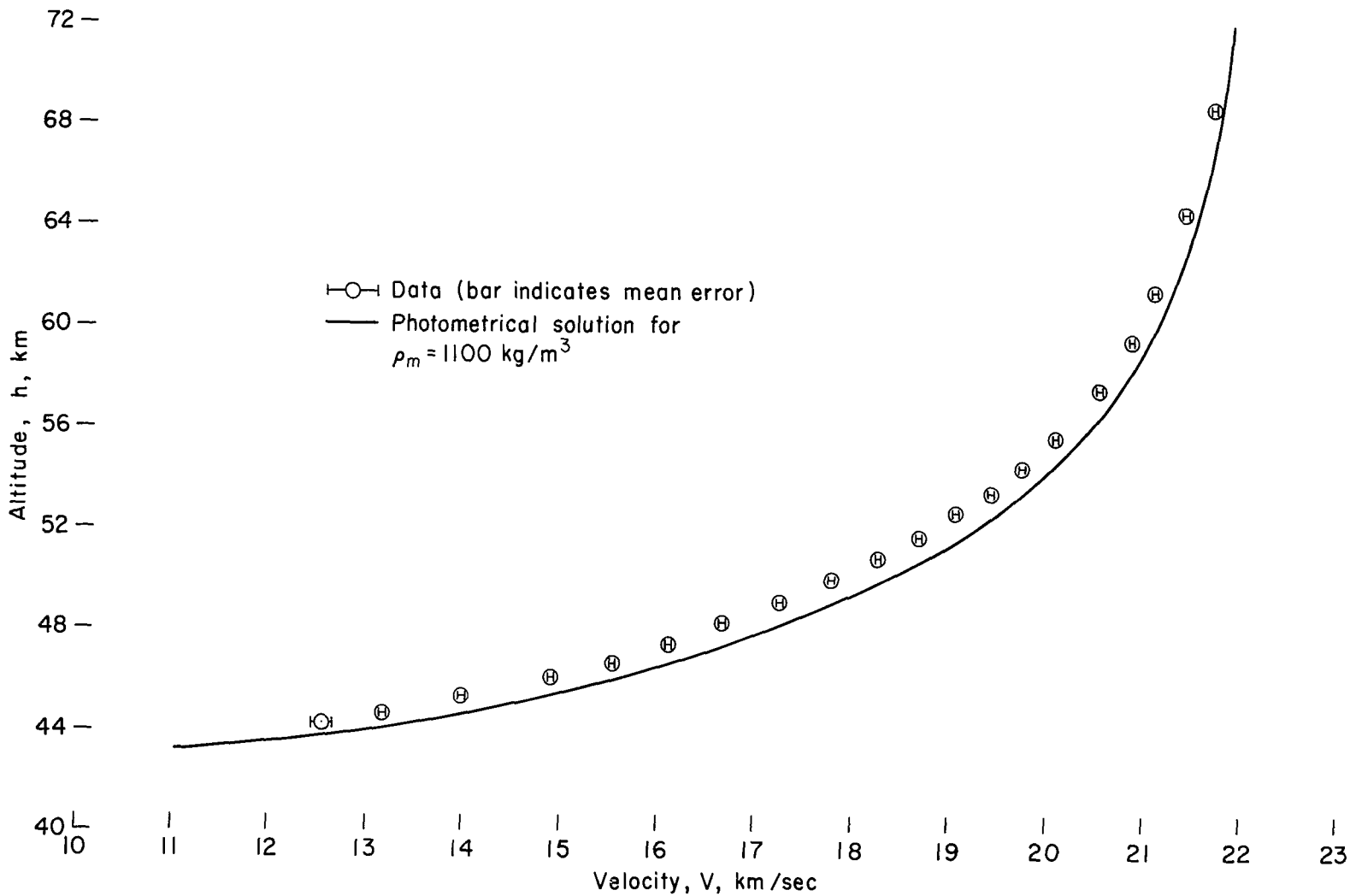

Figure 17.- Comparison of calculated best-fit photometrical results of velocity with data for Ondřejov meteor 15761.

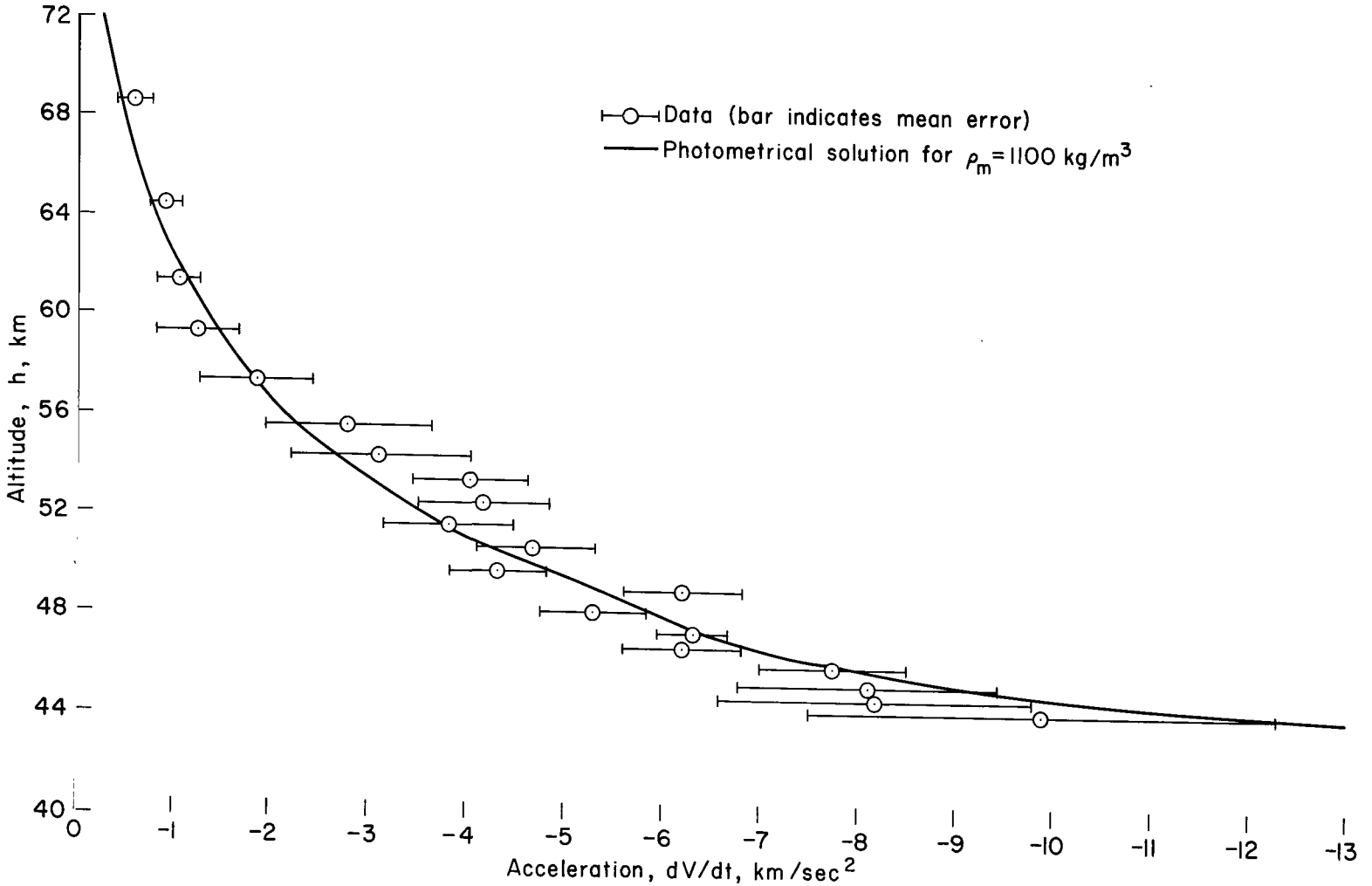

Figure 18.- Comparison of calculated best-fit photometrical results of accelerations with data for Ondřejov meteor 15761.

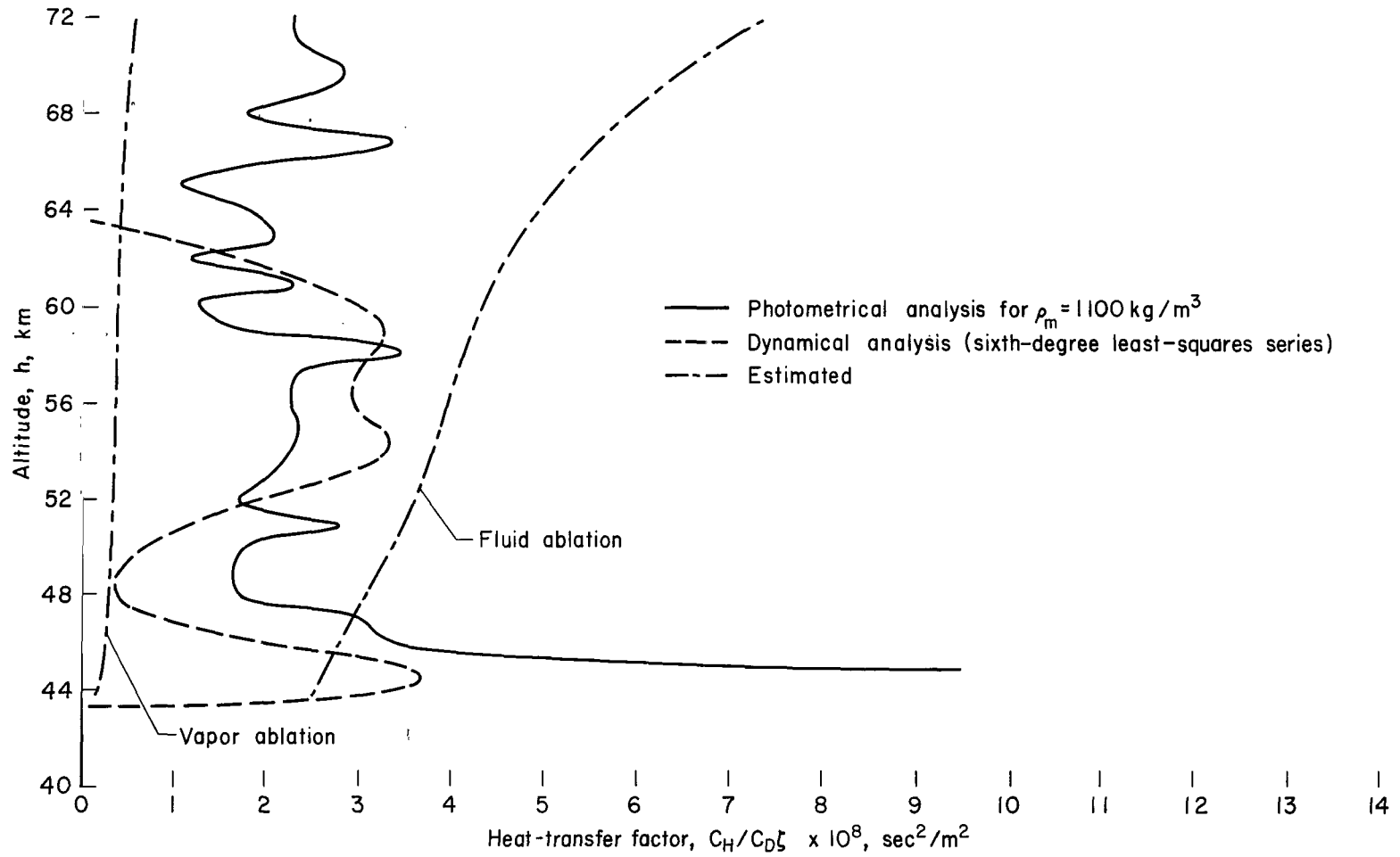

Figure 19.- Comparison of calculated heat-transfer factors as obtained from the dynamical and photometrical analyses with fluid- and vapor-ablation estimates for Ondřejov meteor 15761.

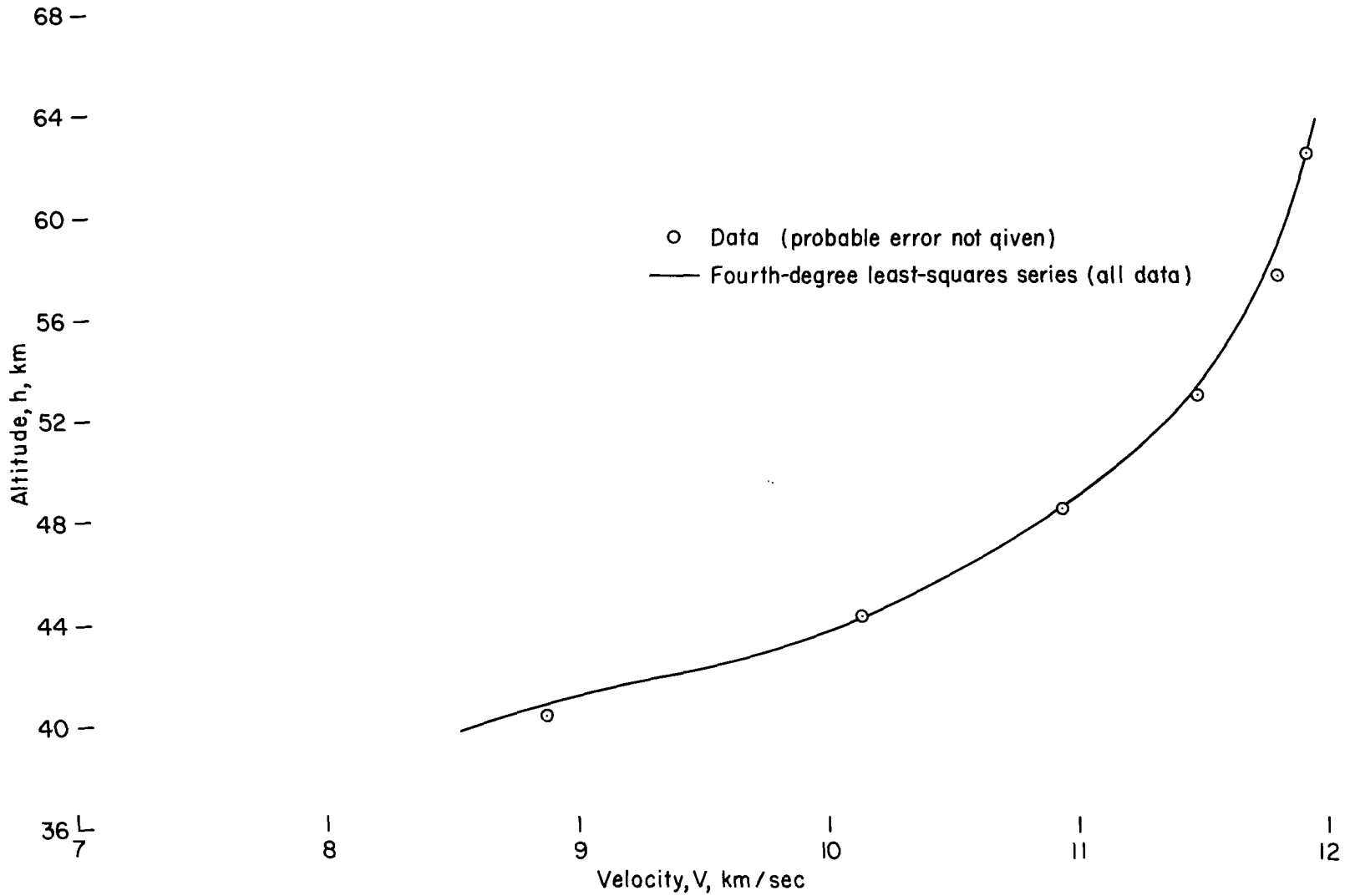

Figure 20.- Comparison of polynomial fit of velocity with data for Harvard meteor 1242.

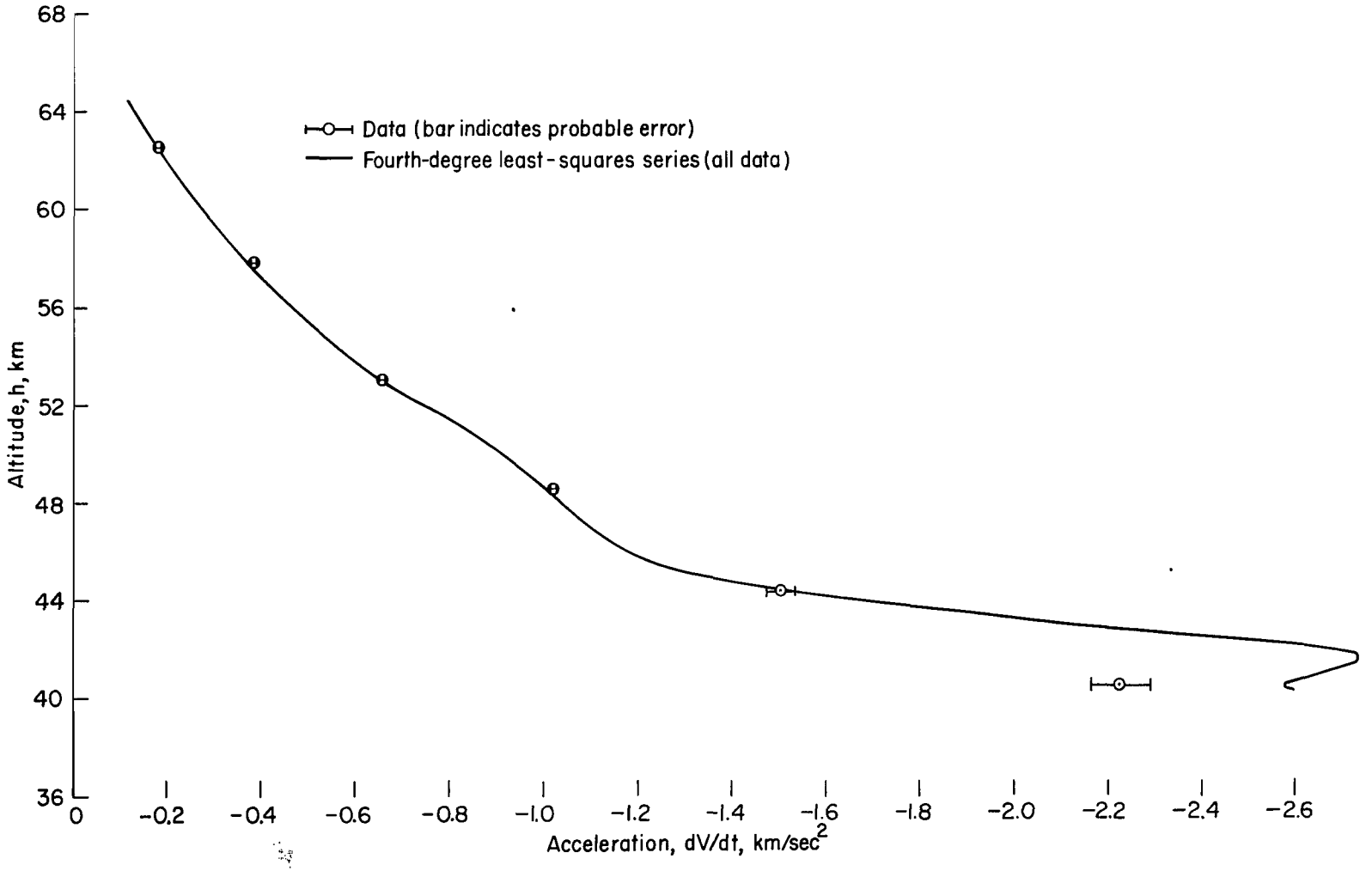

Figure 21.- Comparison of polynomial fit of acceleration with data for Harvard meteor 1242.

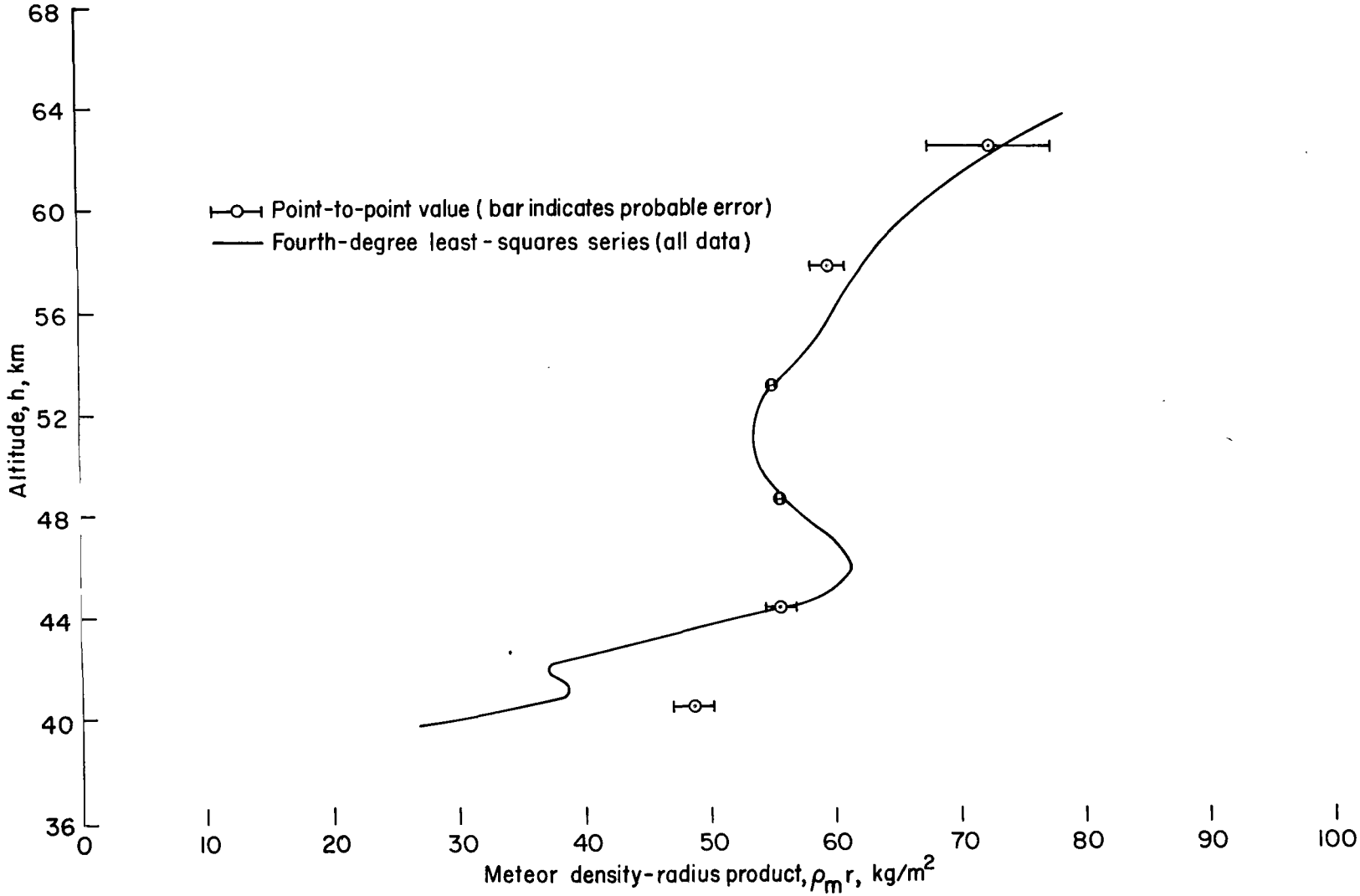

Figure 22.- Results of dynamical analyses of meteor density-radius product for Harvard meteor 1242.

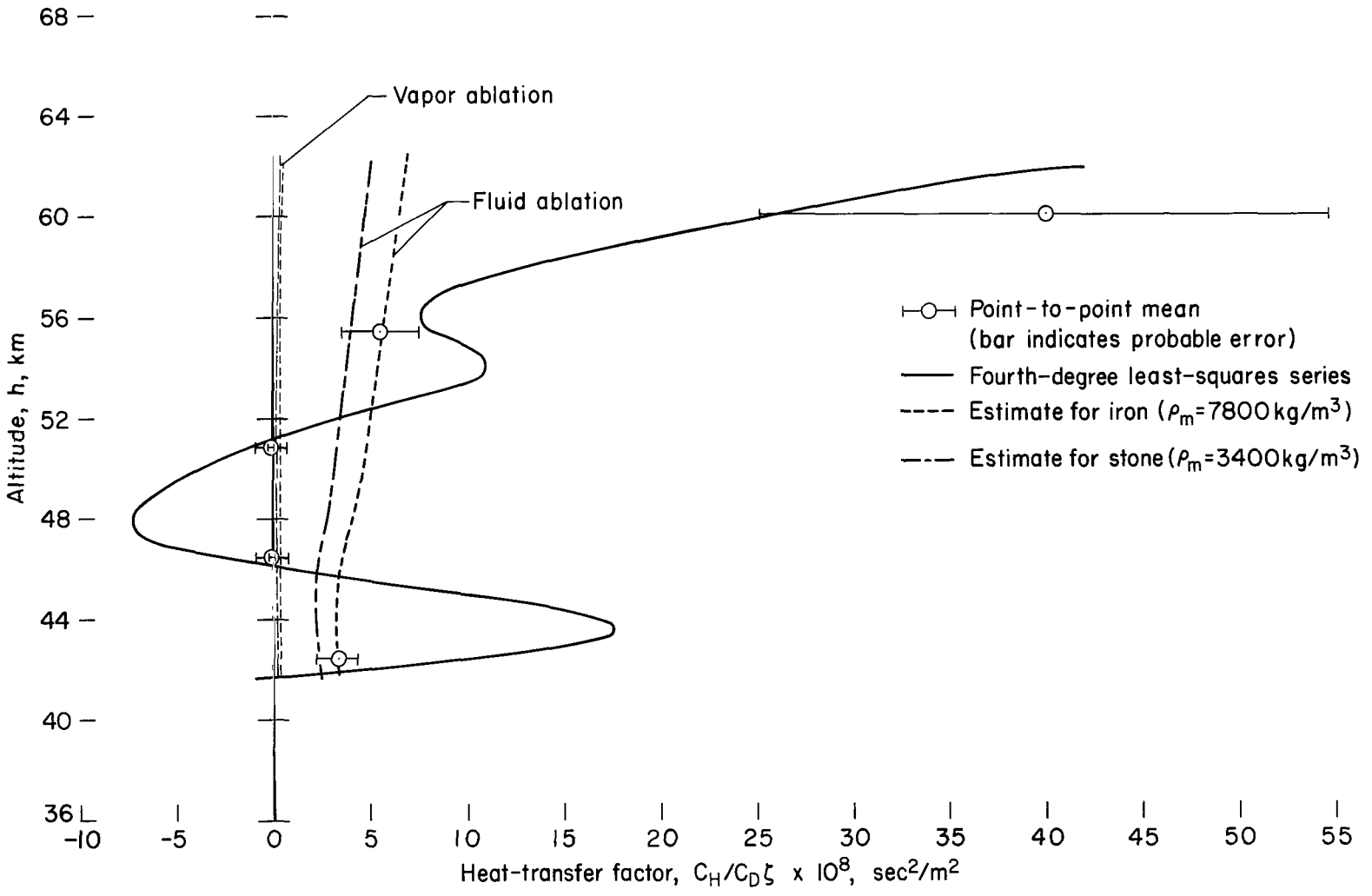

Figure 23.- Comparison of calculated heat-transfer factors obtained from dynamical analyses with fluid- and vapor-ablation estimates for Harvard meteor 1242.

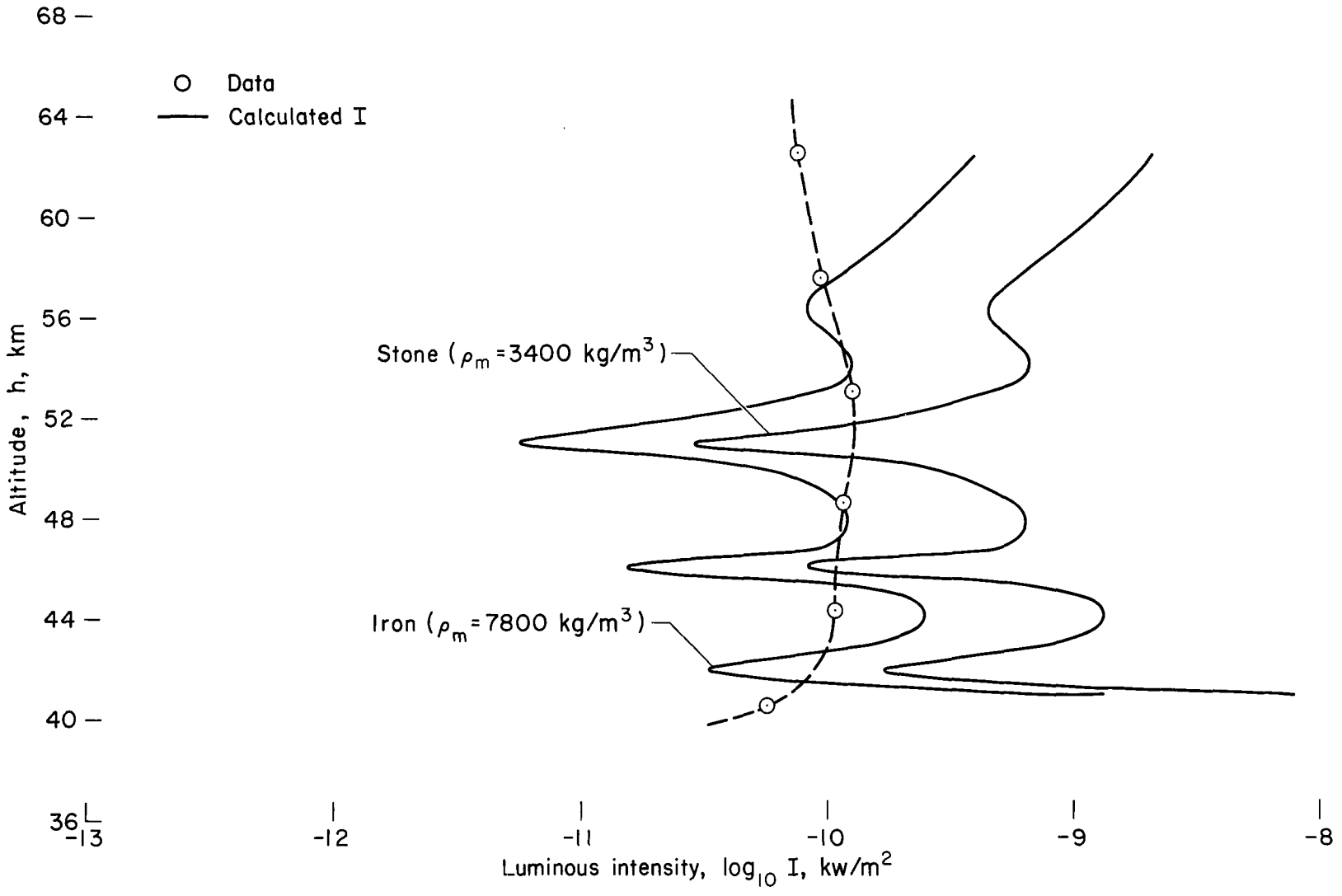

Figure 24.- Comparison of measured luminous intensity with that calculated using the standard value of τ_0 for Harvard meteor 1242.

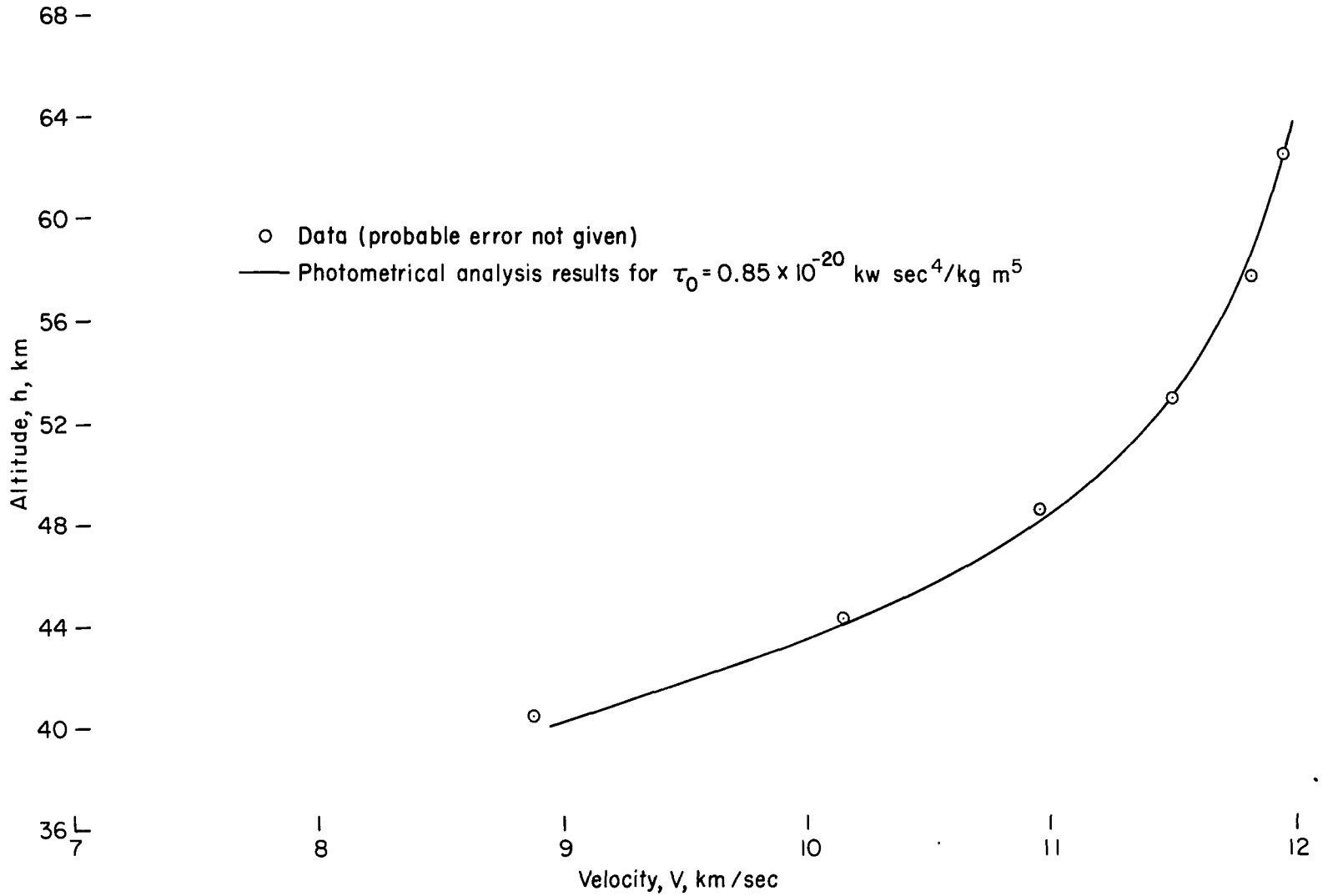

Figure 25.- Comparison of calculated velocity with data using asteroidal stone density and best-fit value of τ_0 for Harvard meteor 1242.

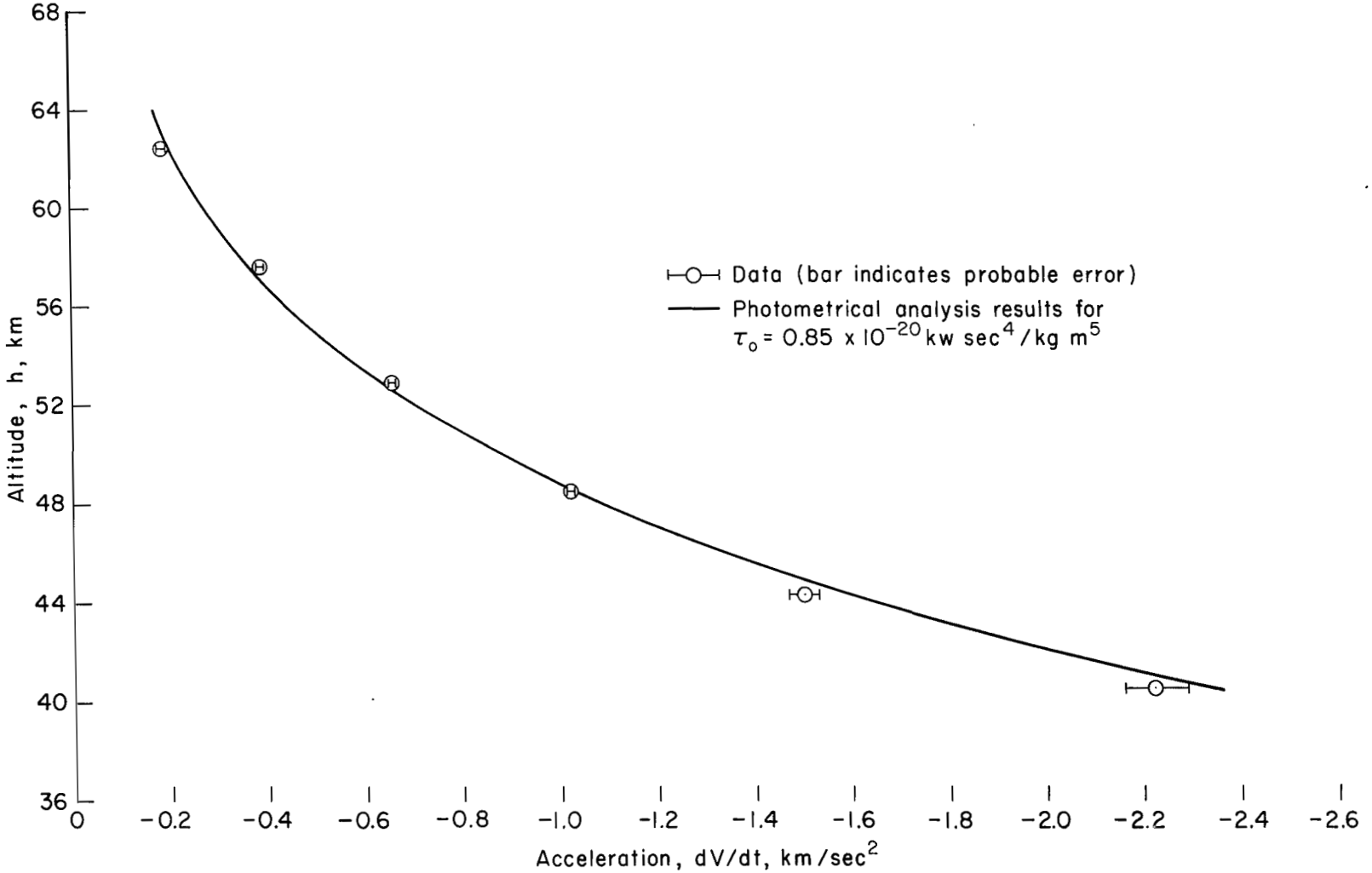

Figure 26.- Comparison of calculated acceleration with data using asteroidal stone density and best-fit value of τ_o for Harvard meteor 1242.

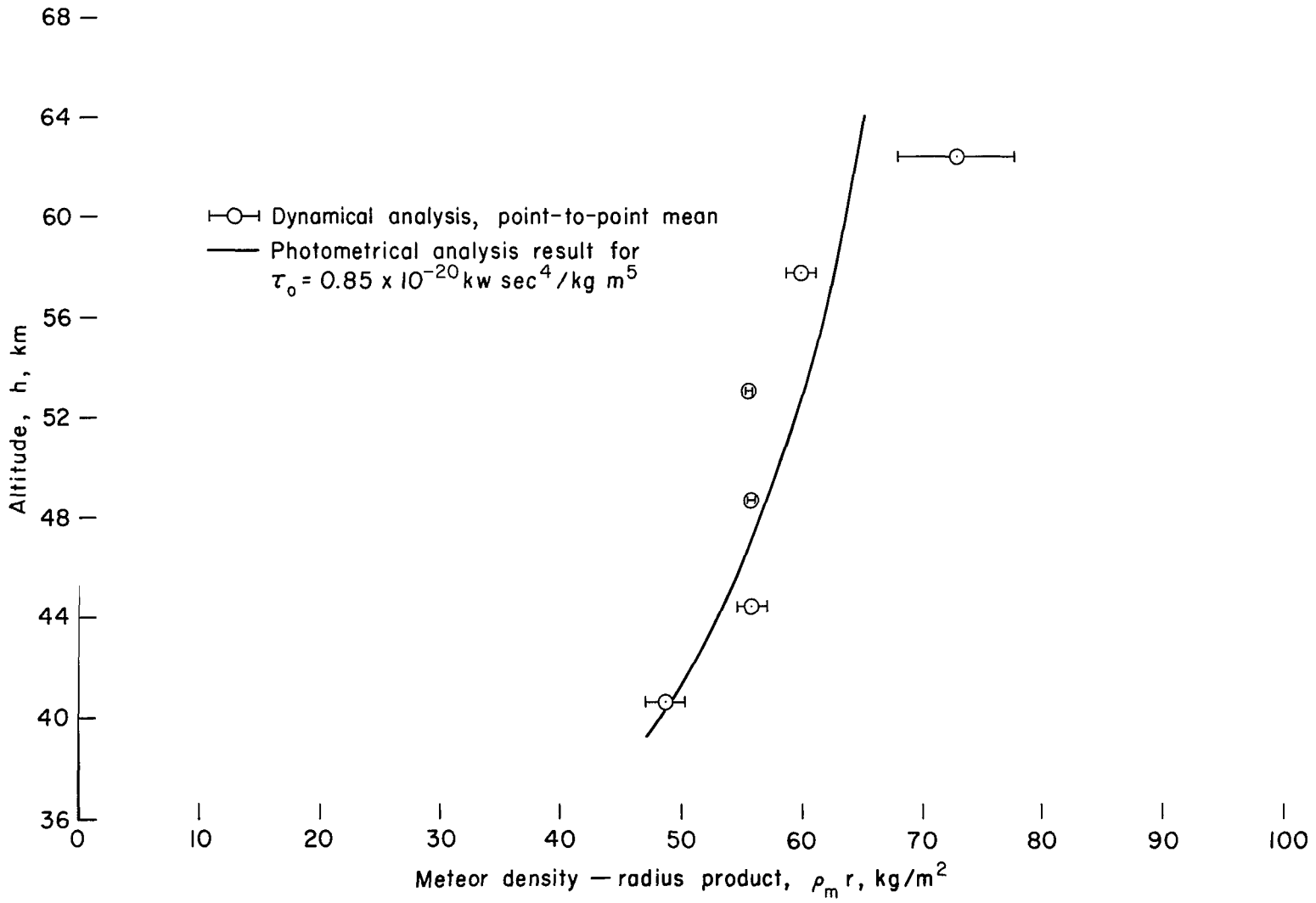

Figure 27.- Comparison of meteor density-radius product calculated from dynamical analysis and photometrical analysis using asteroidal stone density and best-fit value of τ_0 for Harvard meteor 1242.

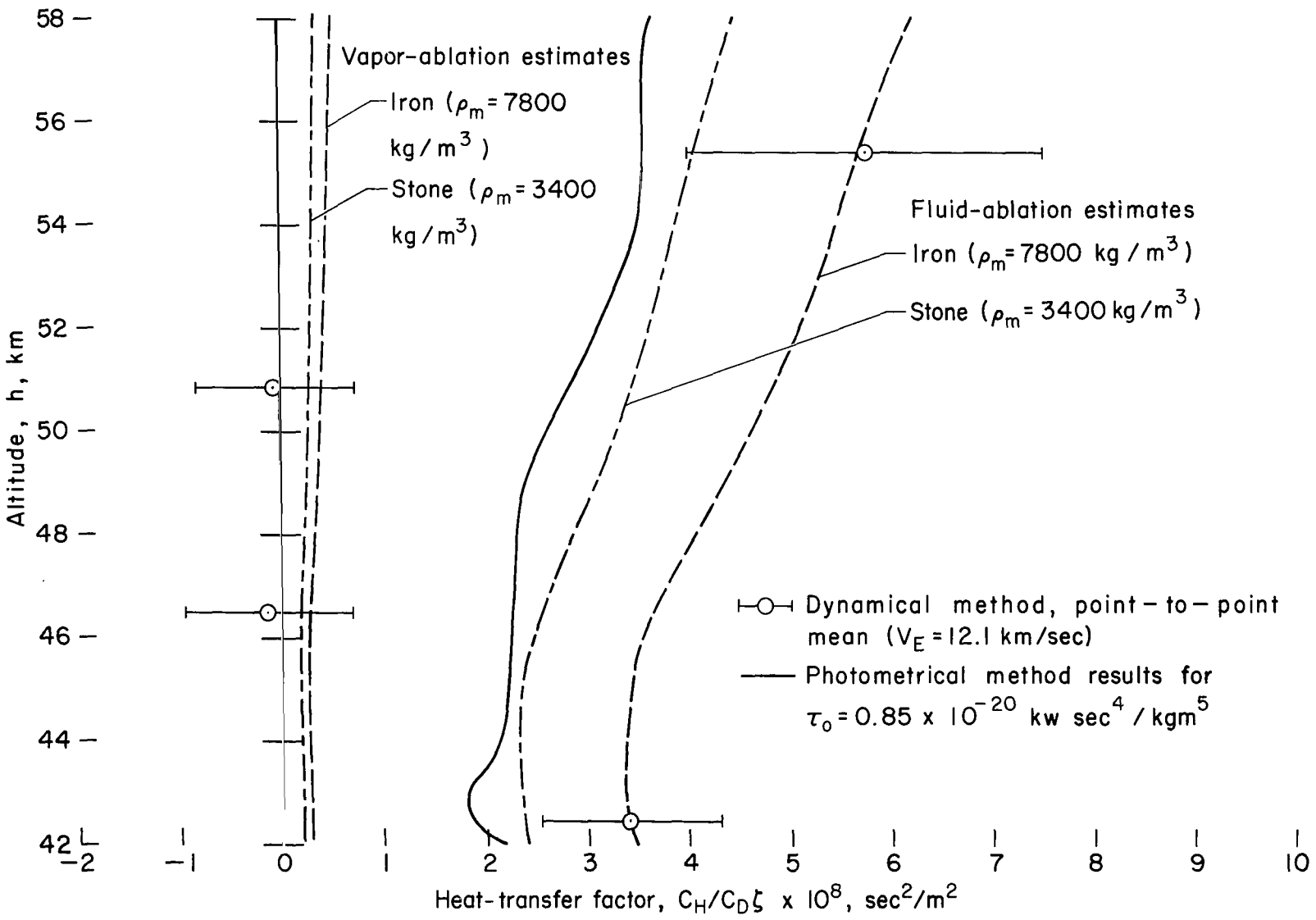

Figure 28.- Comparison of calculated heat-transfer factors obtained from dynamical and photometrical (best-fit τ_0) analyses with fluid and vapor estimates for Harvard meteor 1242.

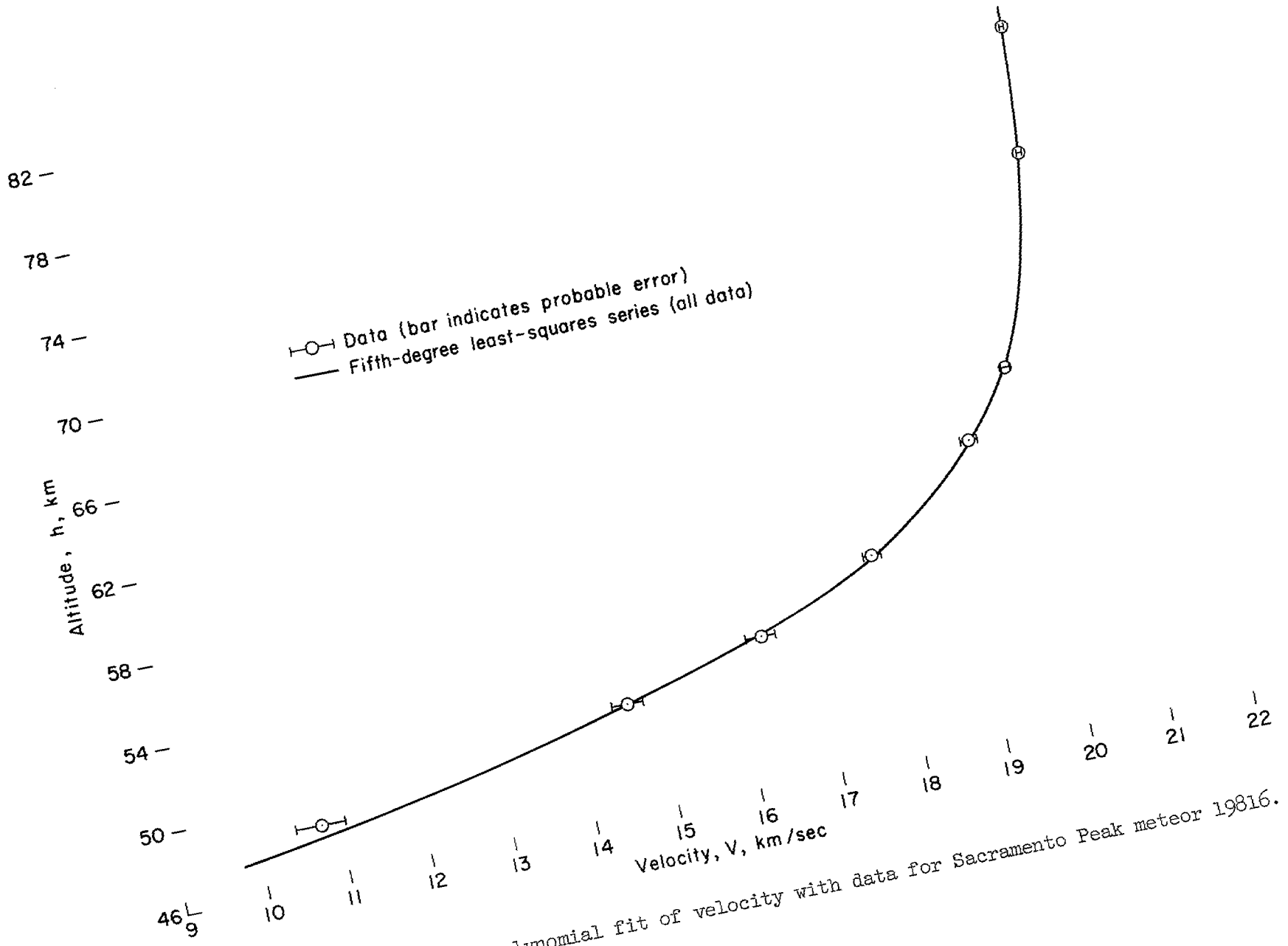

Figure 29.- Comparison of polynomial fit of velocity with data for Sacramento Peak meteor 19816.

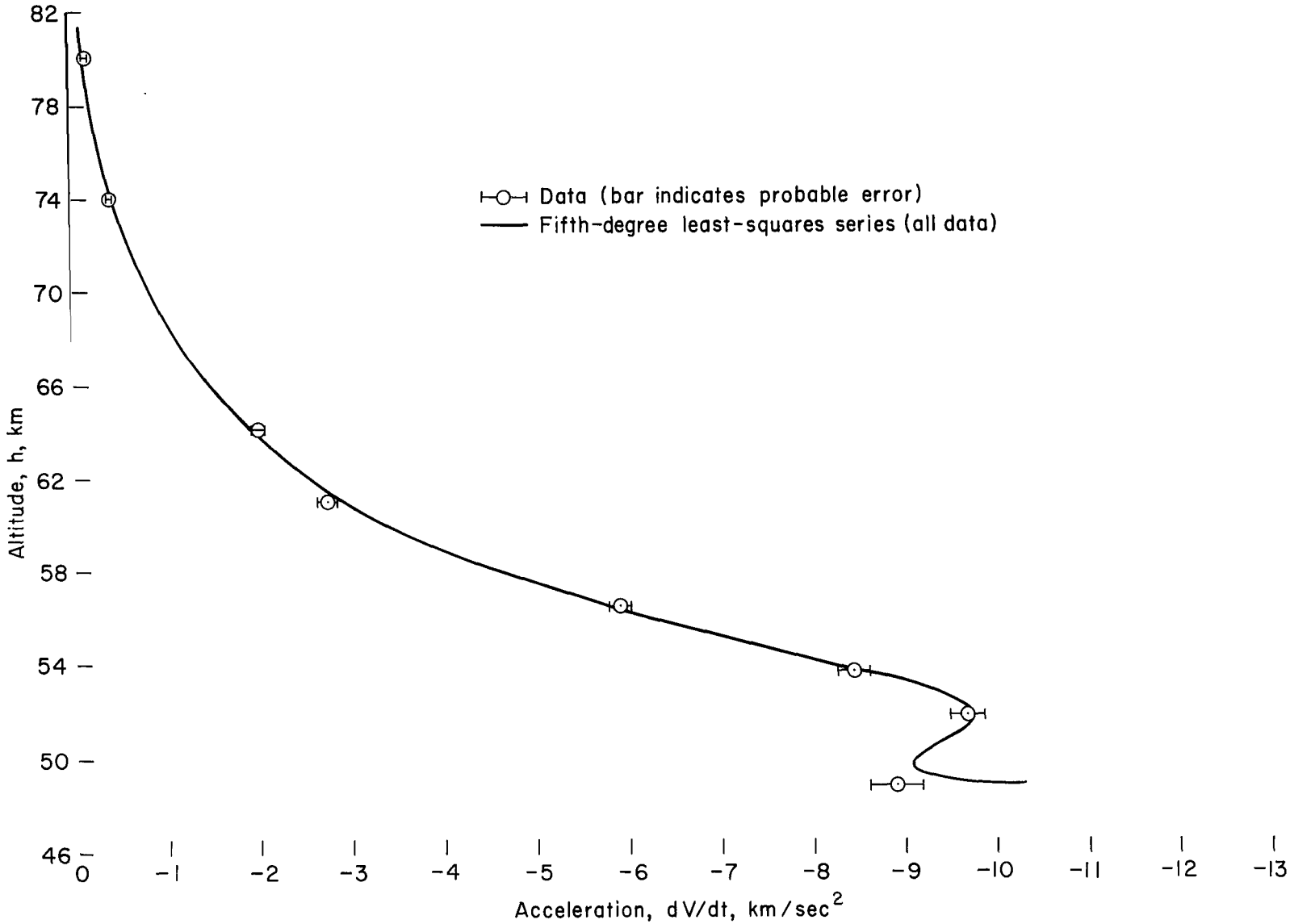

Figure 30.- Comparison of polynomial fit of acceleration with data for Sacramento Peak meteor 19816.

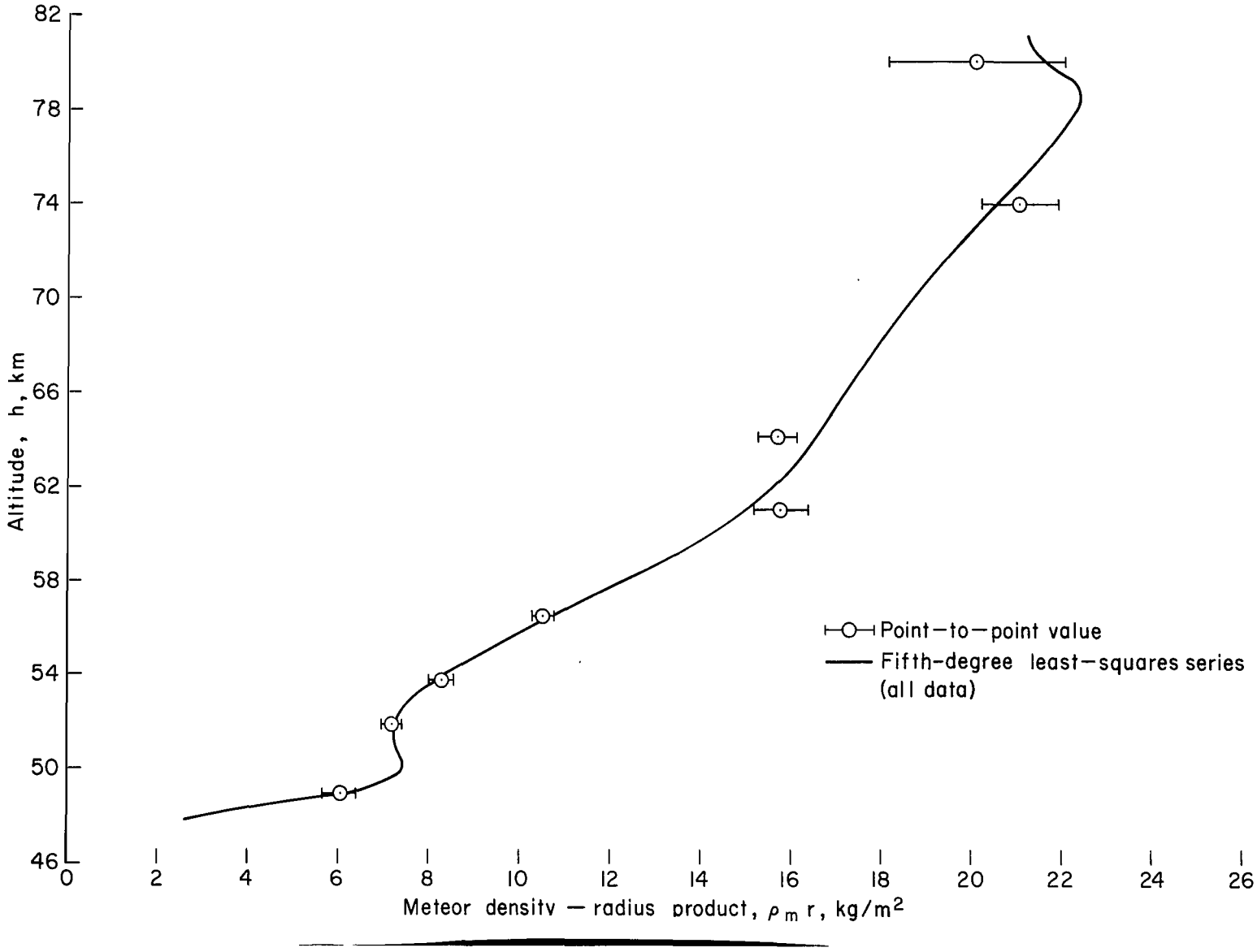

Figure 31.- Results of dynamical analyses of meteor density-radius product for Sacramento Peak meteor 19816.

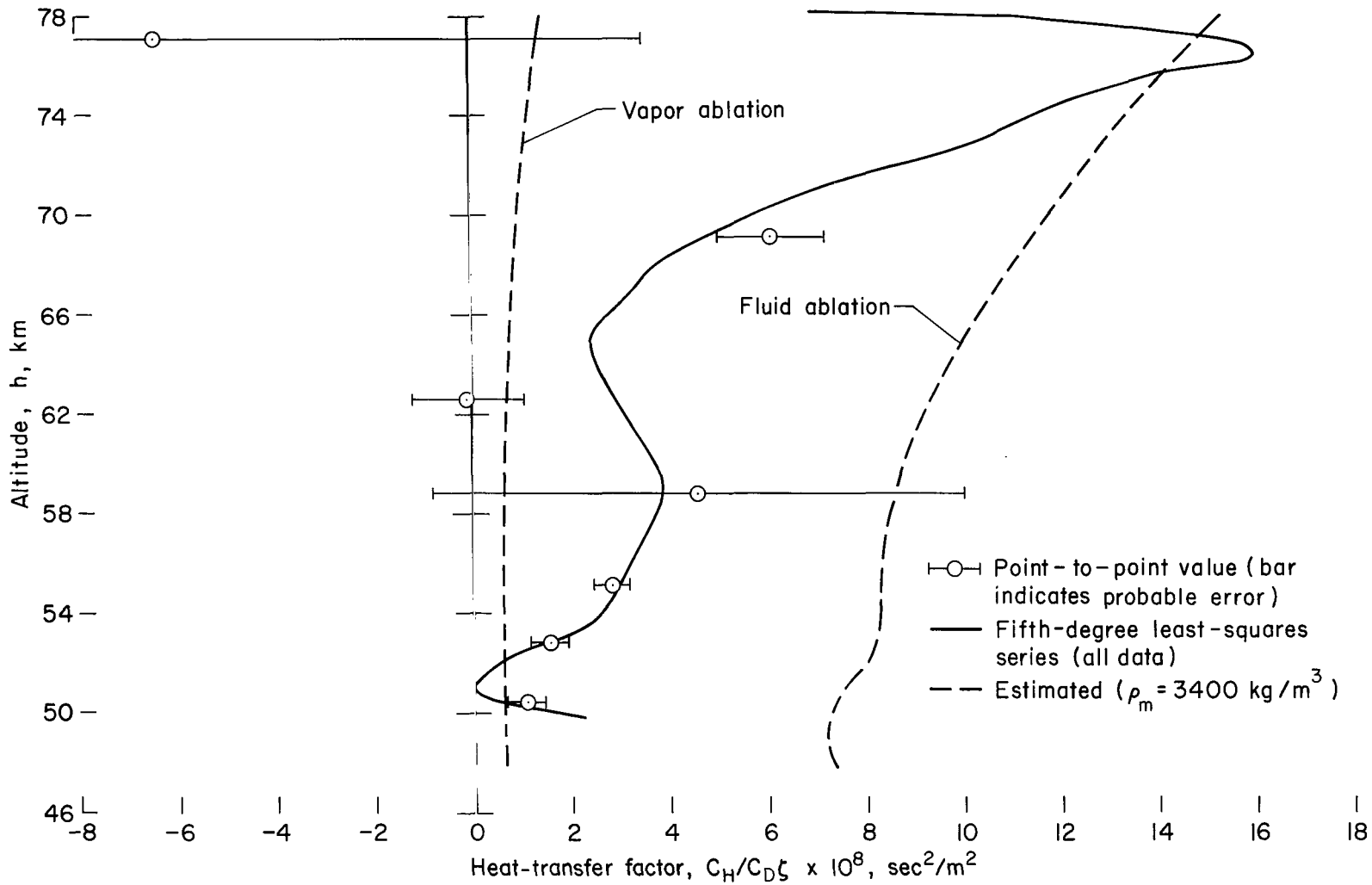

Figure 32.- Comparison of calculated heat-transfer factors obtained from dynamical analyses with fluid- and vapor-ablation estimates for Sacramento Peak meteor 19816.

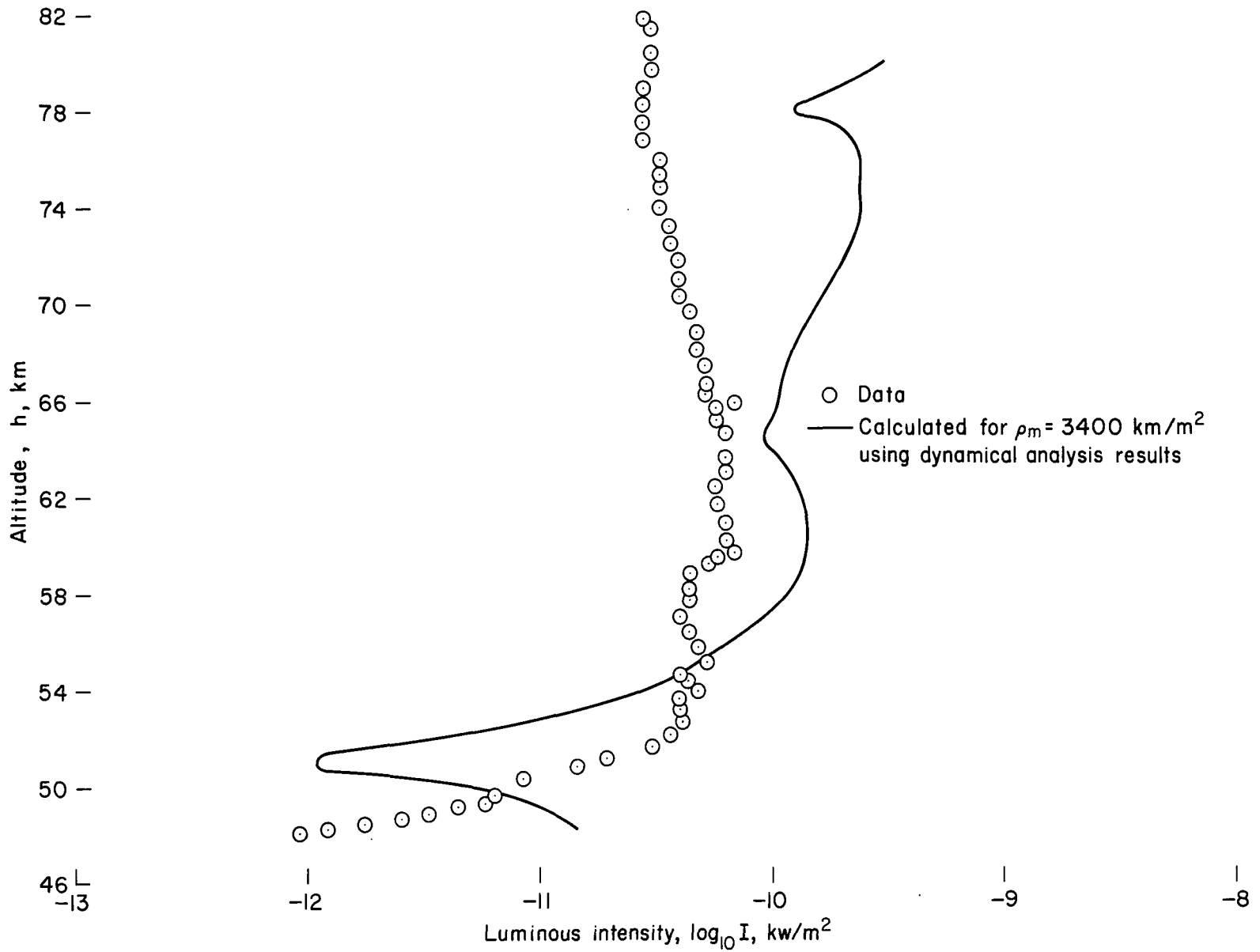

Figure 33.- Comparison of measured luminous intensity with that calculated using standard value of τ_o for Sacramento Peak meteor 19816.

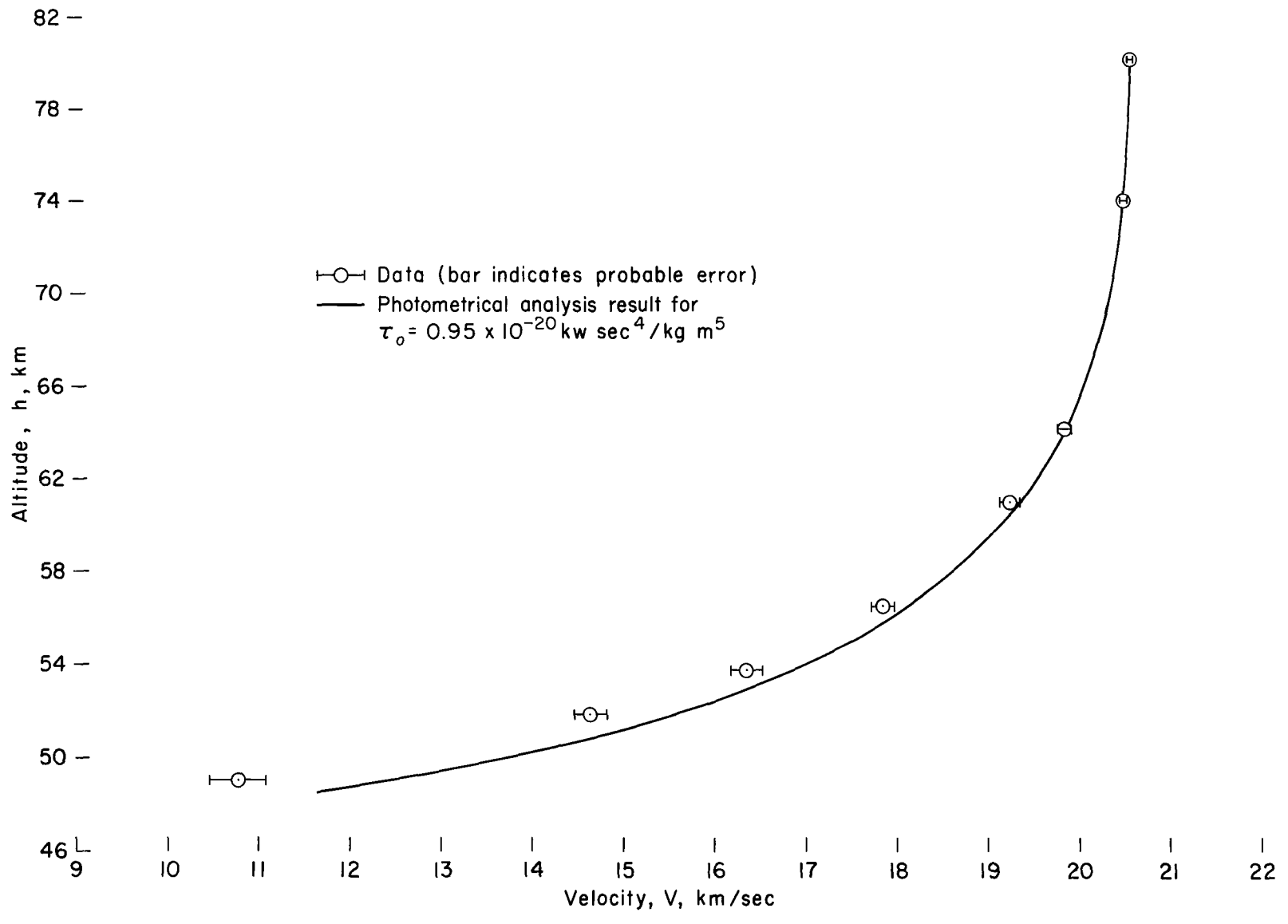

Figure 34.- Comparison of calculated velocity with data using asteroidal stone density and best-fit value of τ_o for Sacramento Peak meteor 19816.

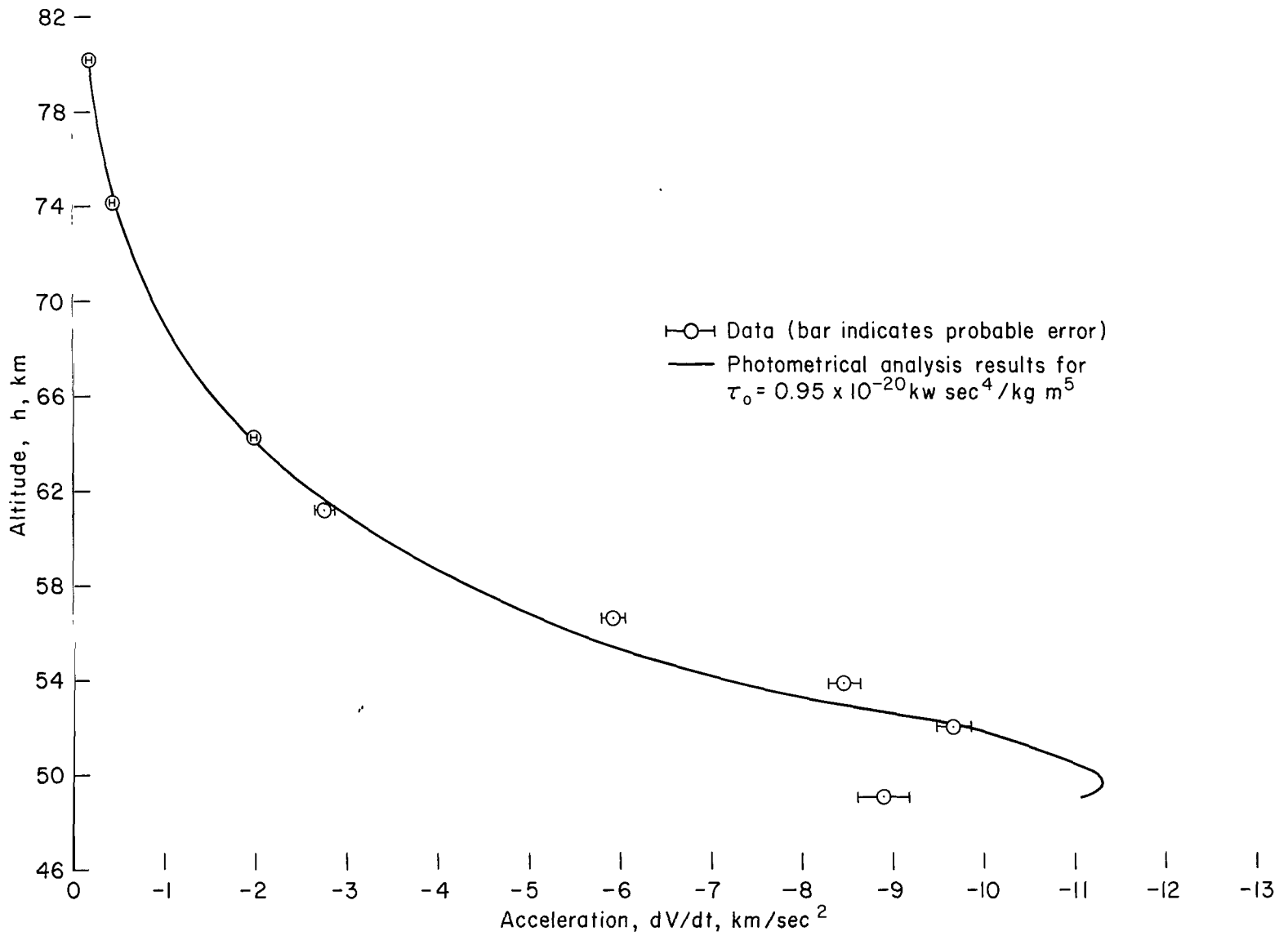

Figure 35.- Comparison of calculated acceleration with data using asteroidal stone density and best-fit value of τ_o for Sacramento Peak meteor 19816.

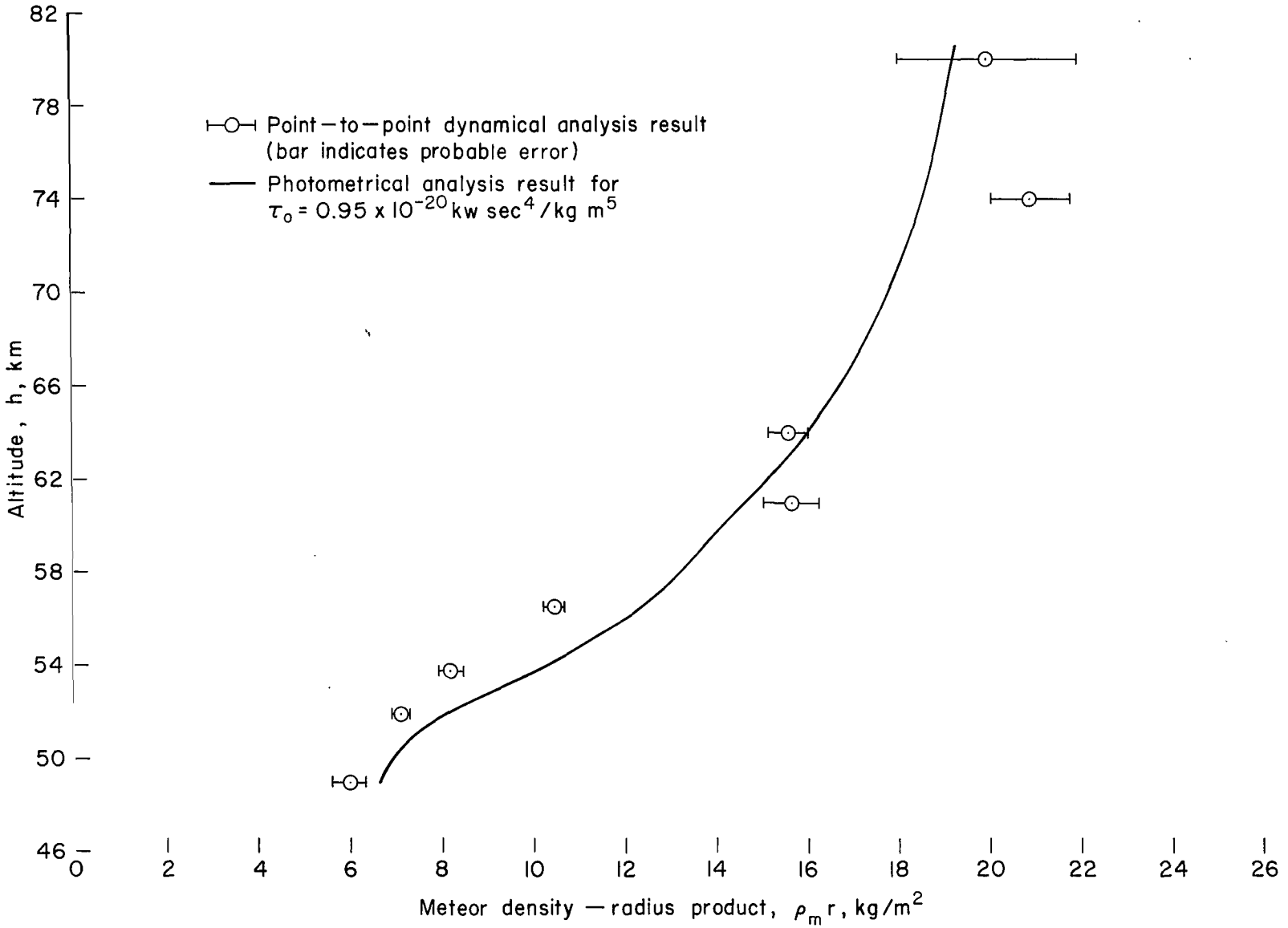

Figure 36.- Comparison of meteor density-radius product calculated from dynamical analysis and photometrical analysis using asteroidal stone density and best-fit value of τ_o for Sacramento Peak meteor 19816.

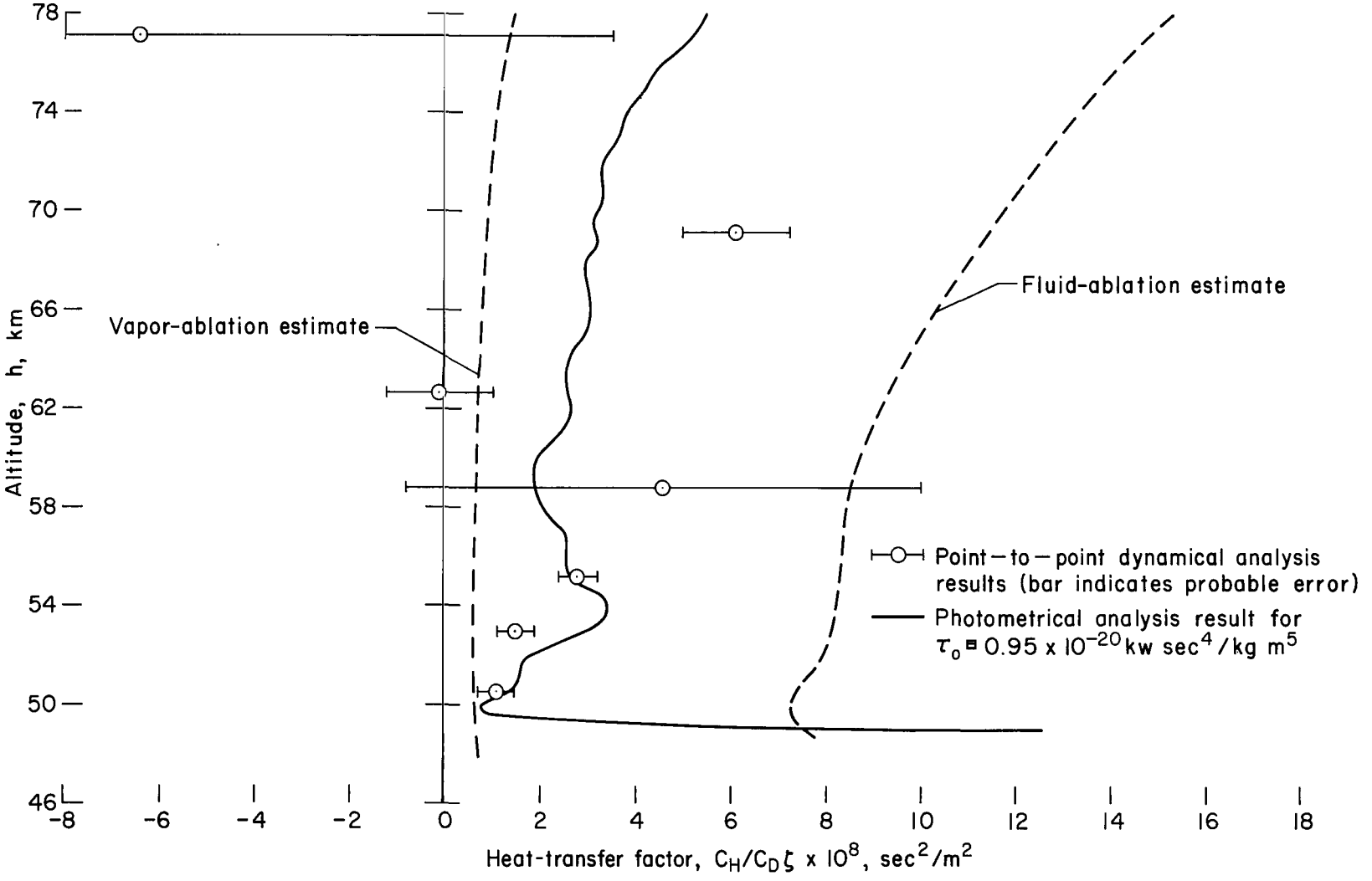

Figure 37.- Comparison of calculated heat-transfer factors obtained from dynamical and photometrical (best-fit τ_0) analyses with fluid and vapor estimates for Sacramento Peak meteor 19816.

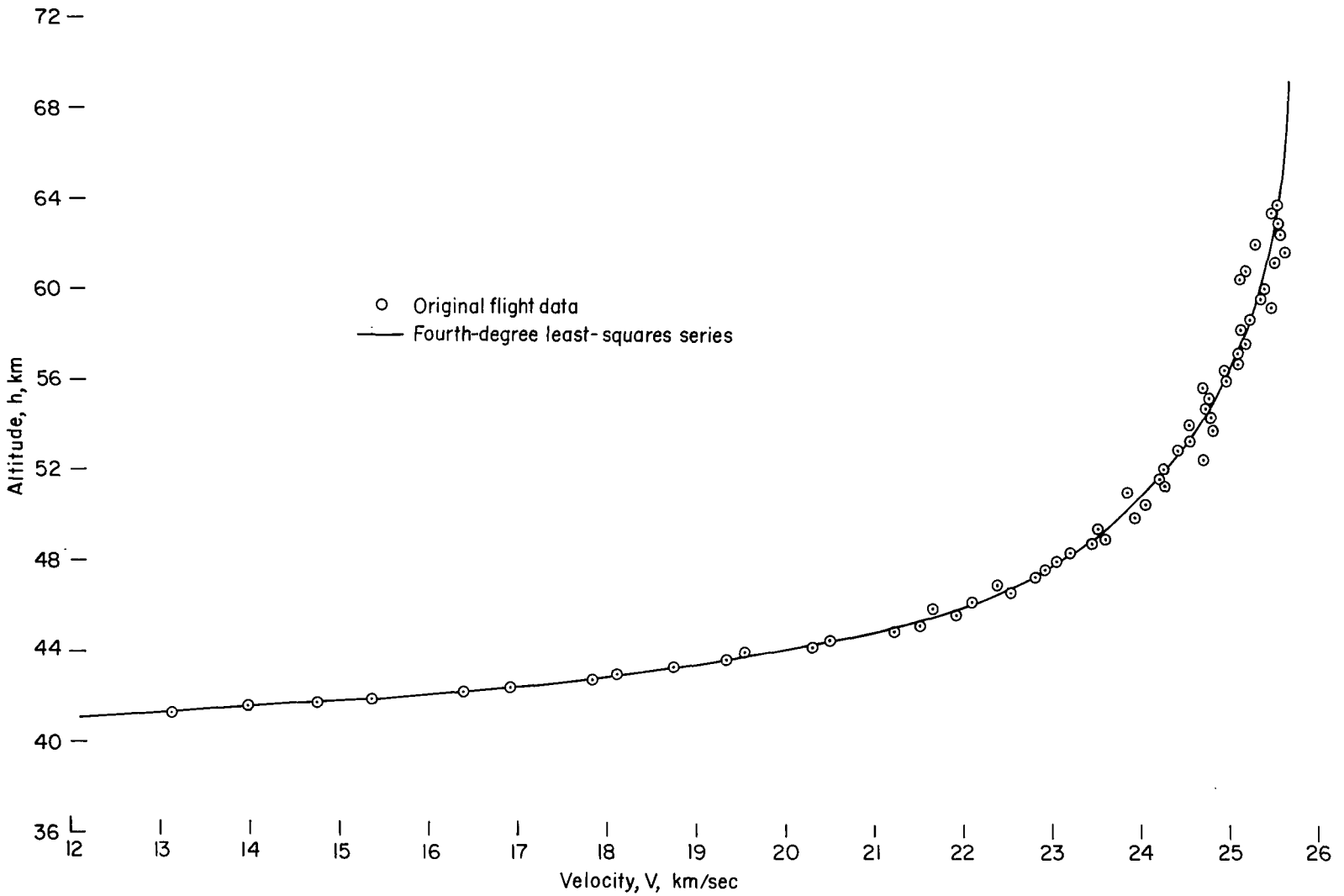

Figure 38.- Comparison of polynomial fit of velocity with original data for Ondřejov meteor 27471.

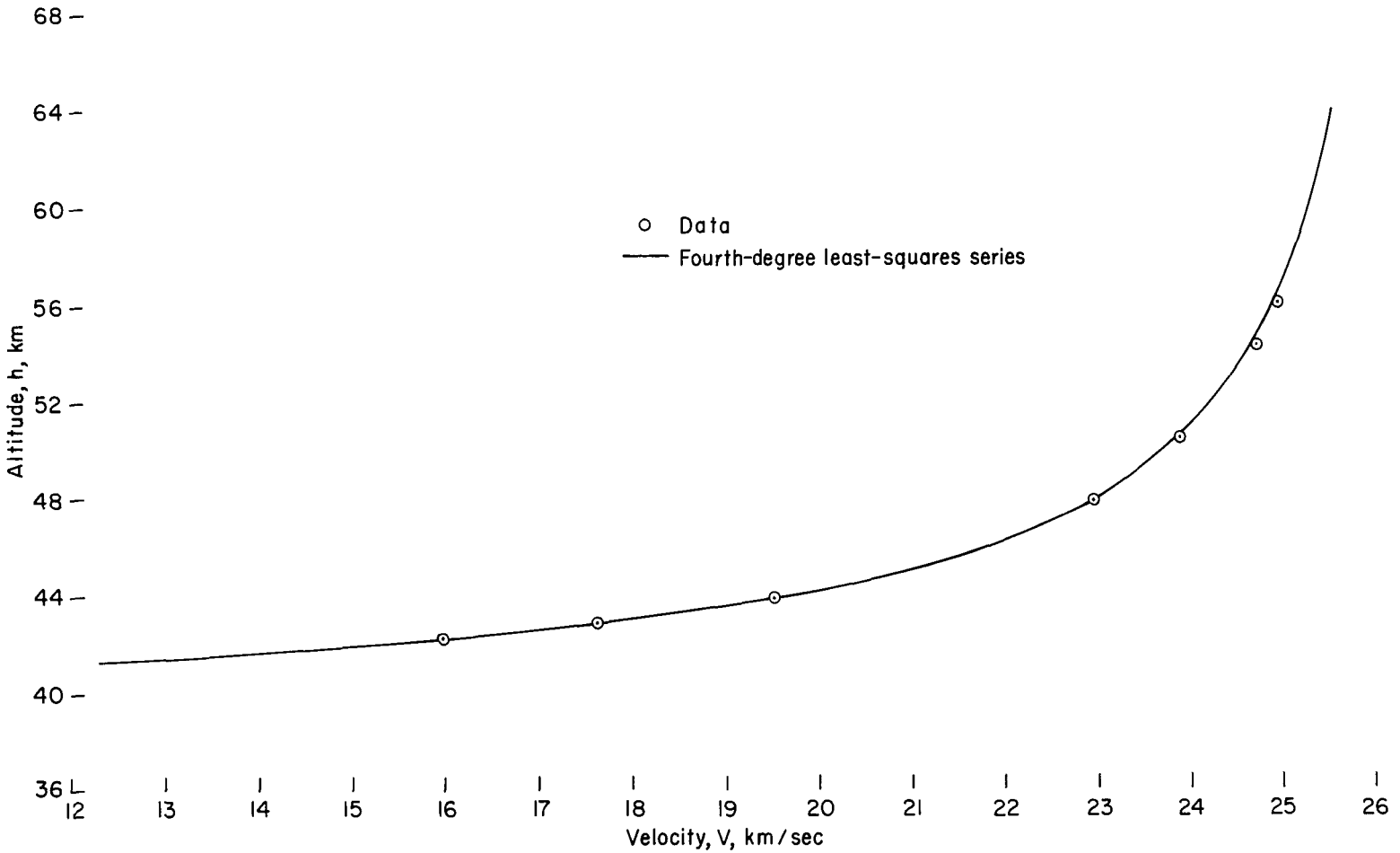

Figure 39.- Comparison of polynomial fit of velocity with reduced data for Ondřejov meteor 27471.

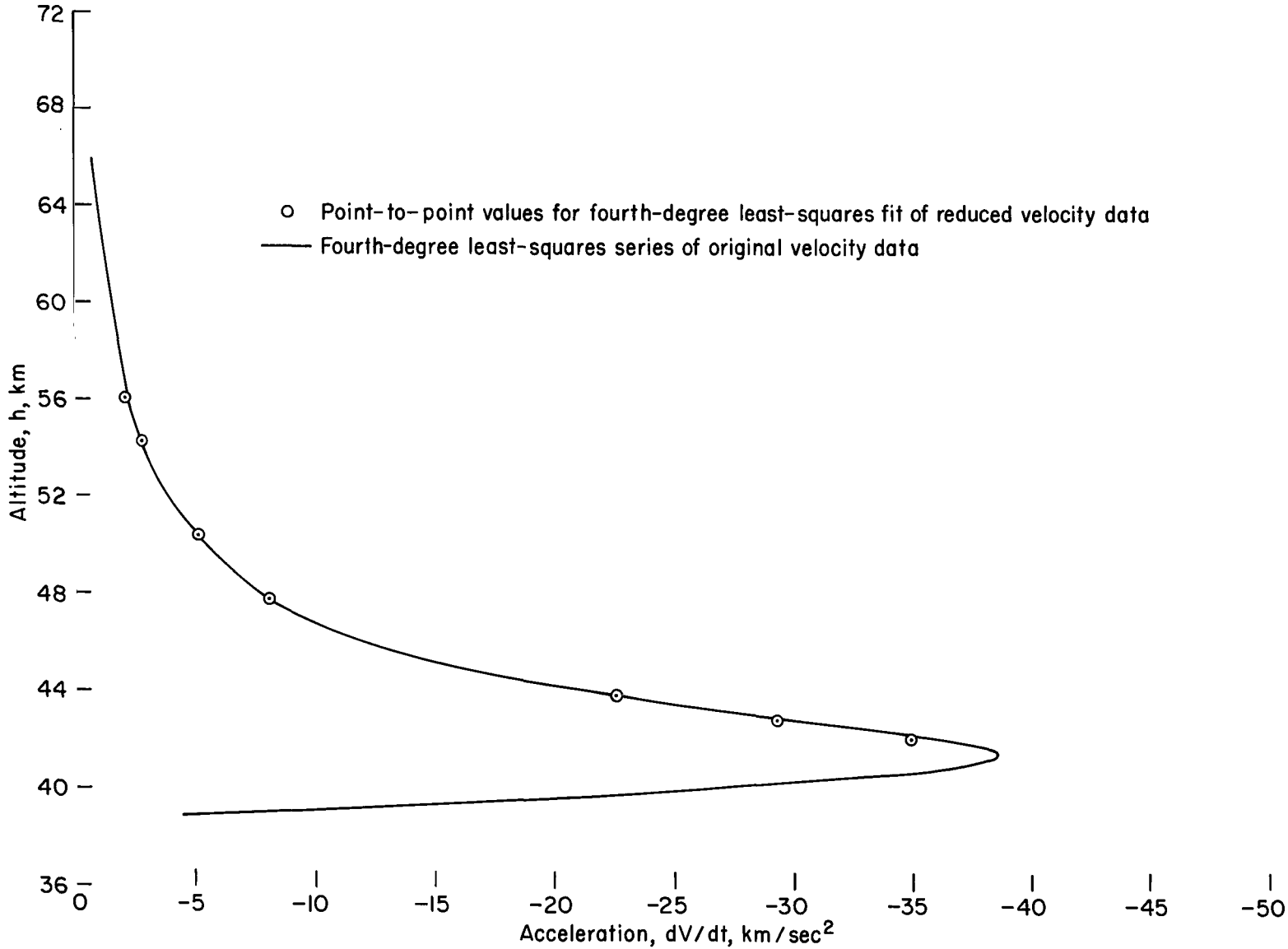

Figure 40.- Comparison of acceleration deduced from polynomial fit to original and reduced velocity data for Ondřejov meteor 27471.

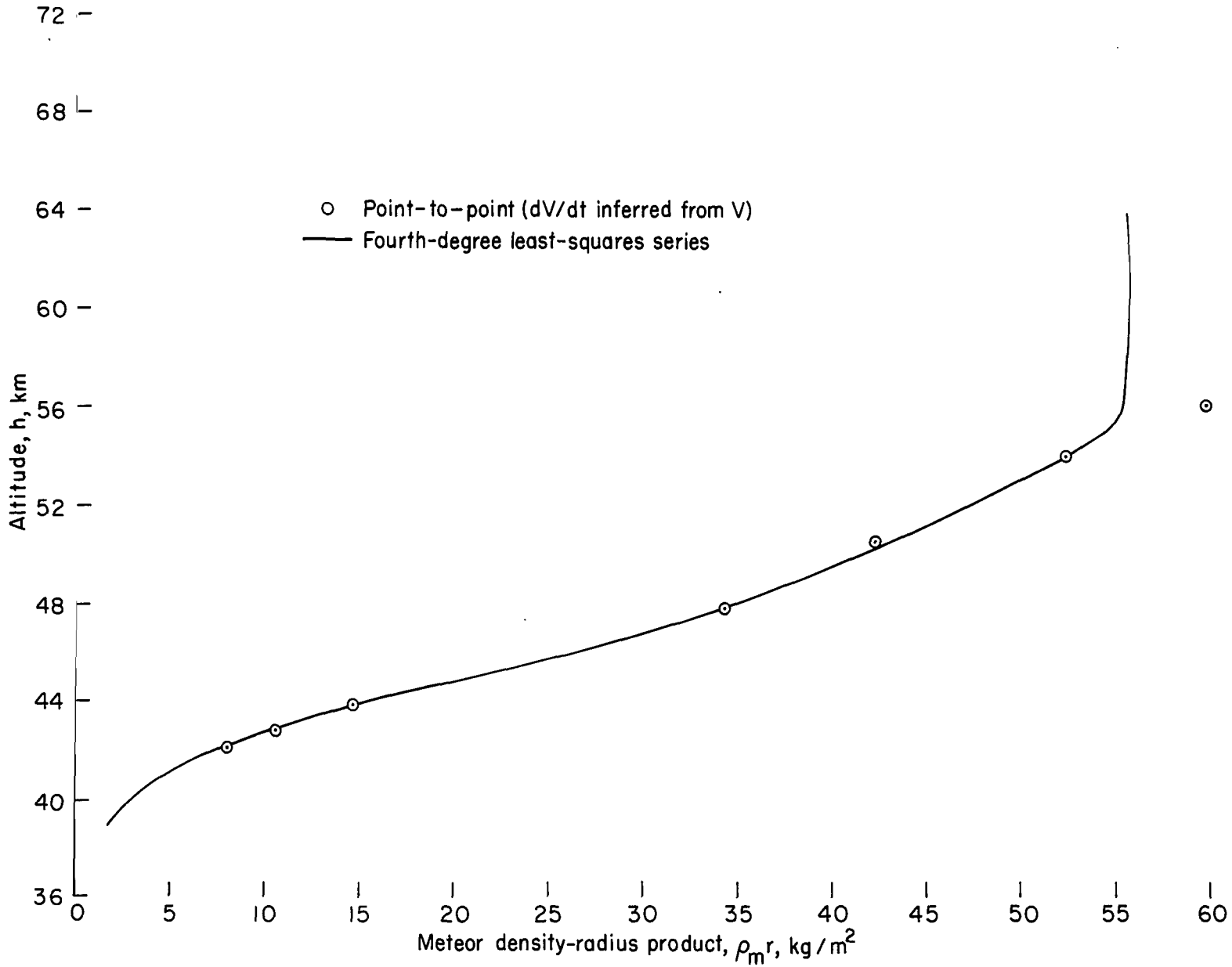

Figure 41.- Comparison of meteor density-radius product from dynamical analyses for Ondřejov meteor 27471.

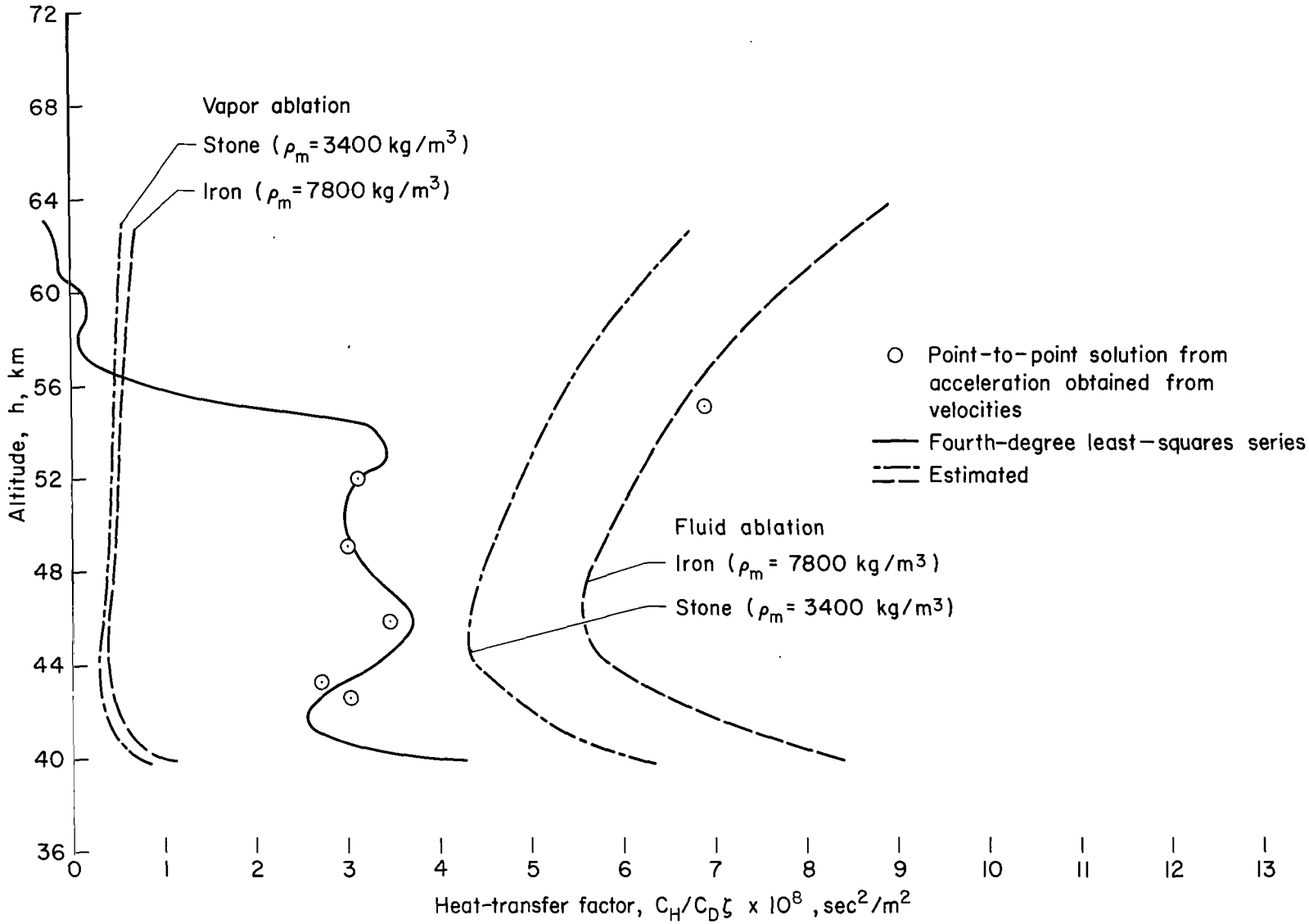

Figure 42.- Comparison of heat-transfer factors from dynamical analyses with fluid- and vapor-ablation estimates for Ondřejov meteor 27471.

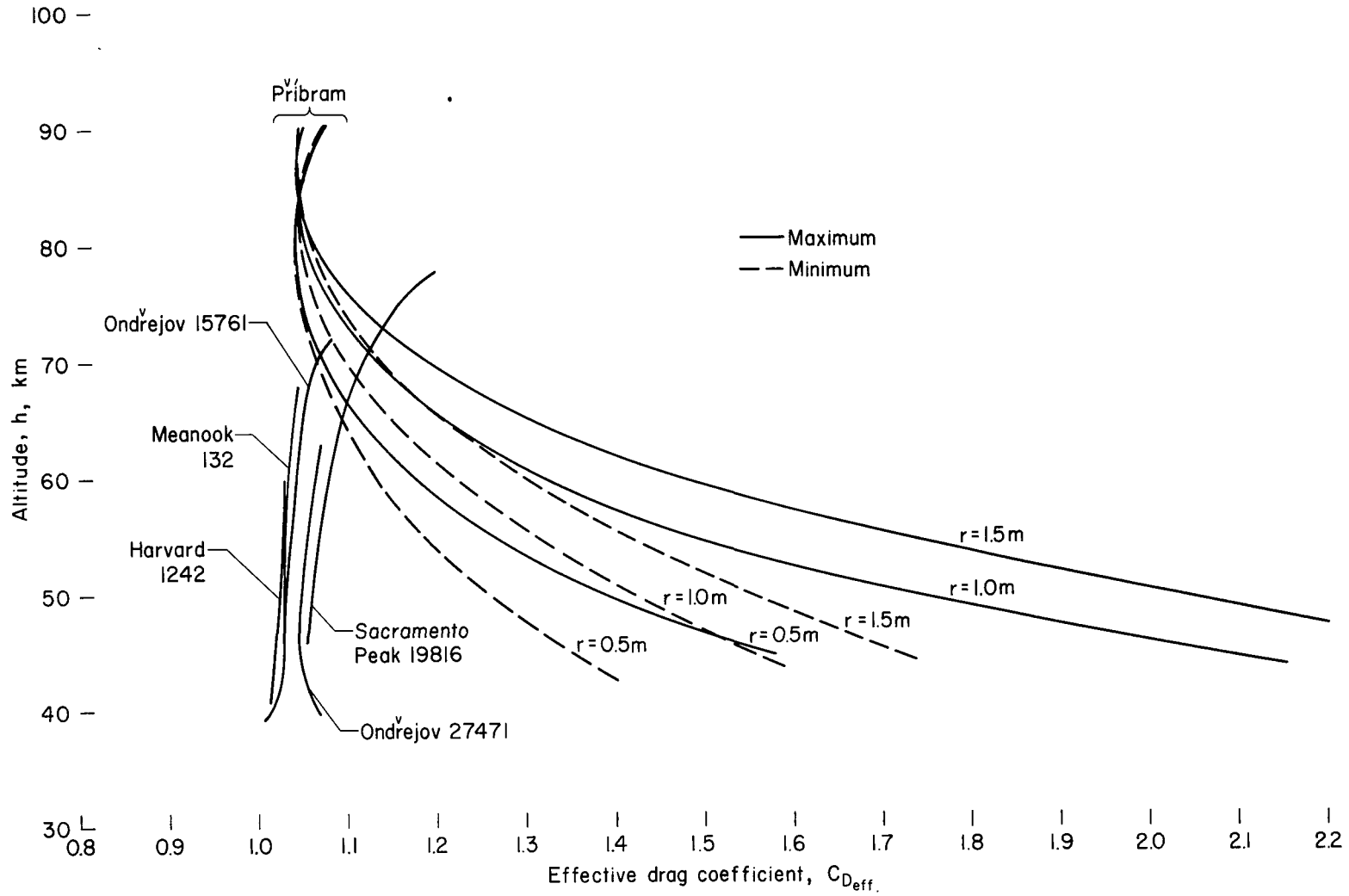

Figure 43.- Effective drag coefficients for all six meteors.

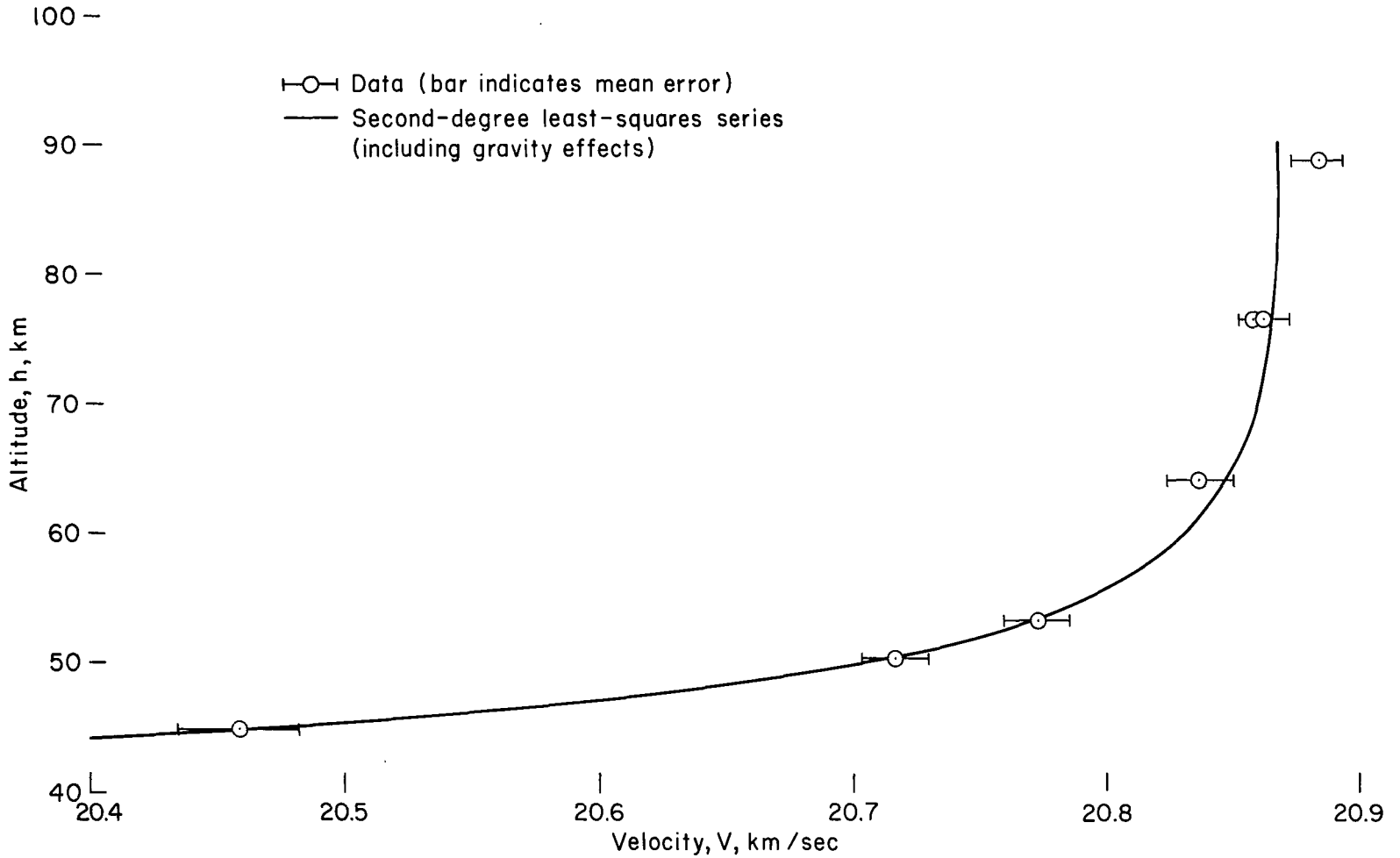

Figure 44.- Comparison of polynomial fit of velocity with data for Ondřejov meteor Příbram.

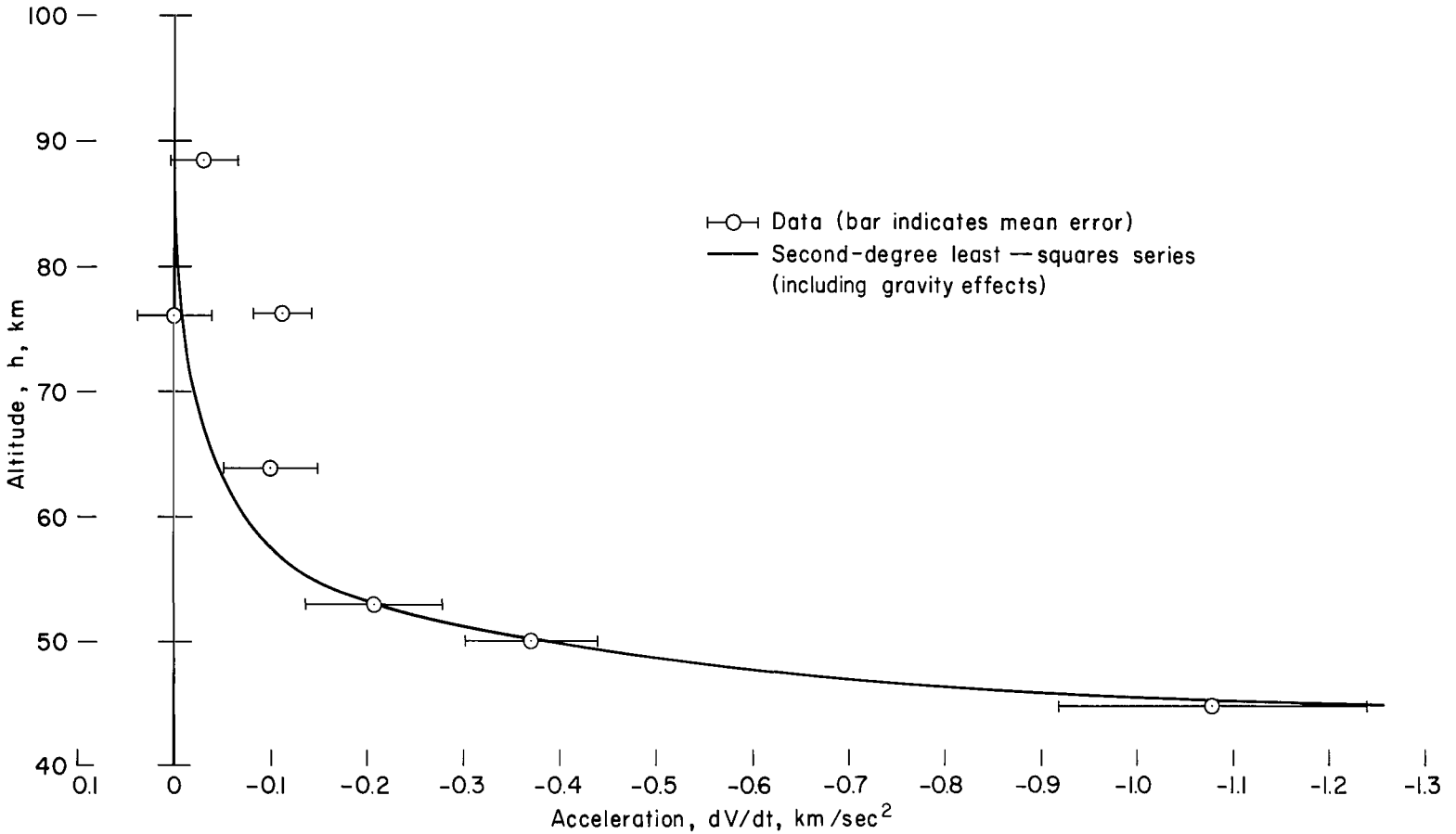

Figure 45.- Comparison of polynomial fit of acceleration with data for Ondřejov meteor Příbram.

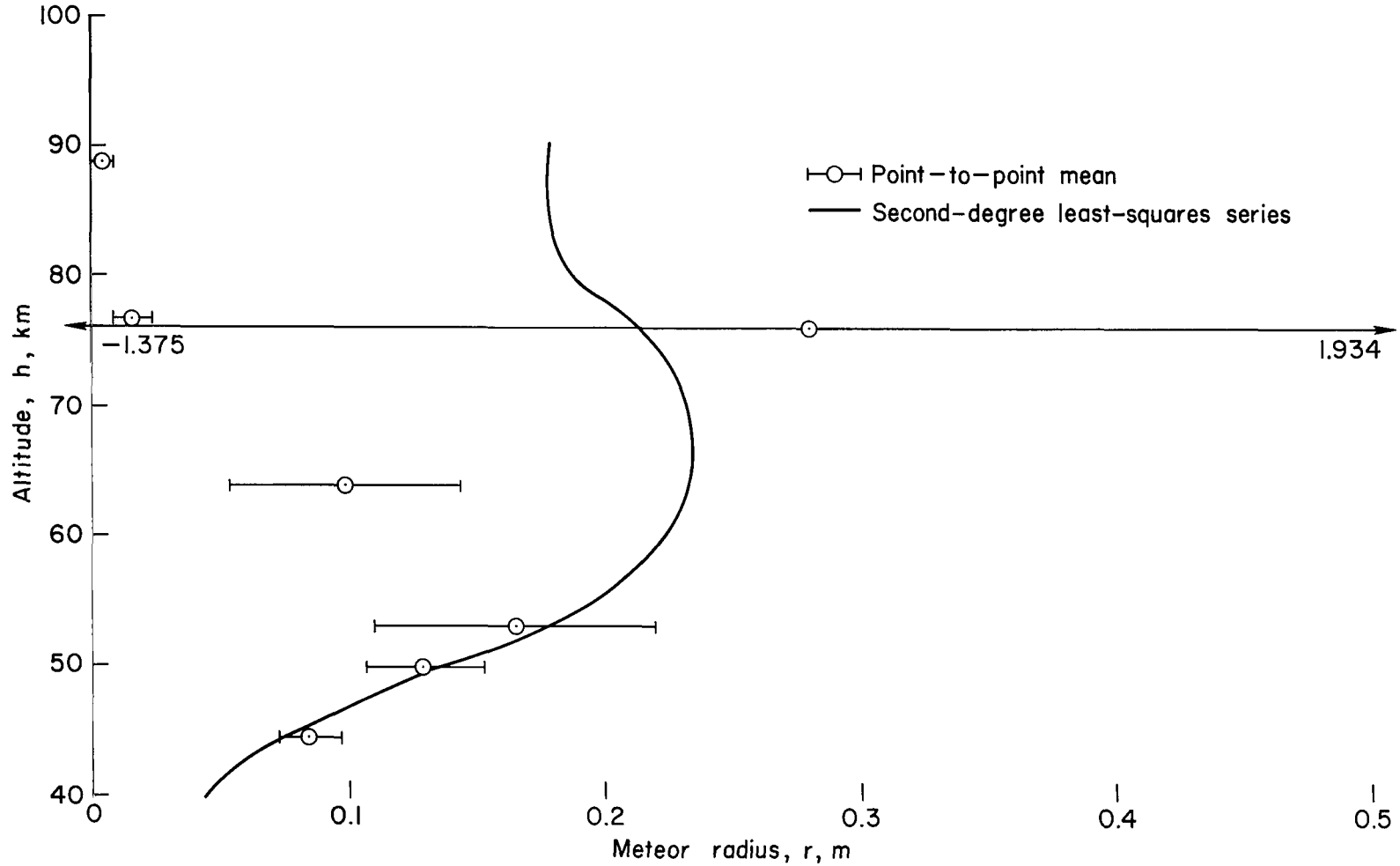

Figure 46.- Results of dynamical analyses of meteor density-radius product for Ondřejov meteor Příbram.

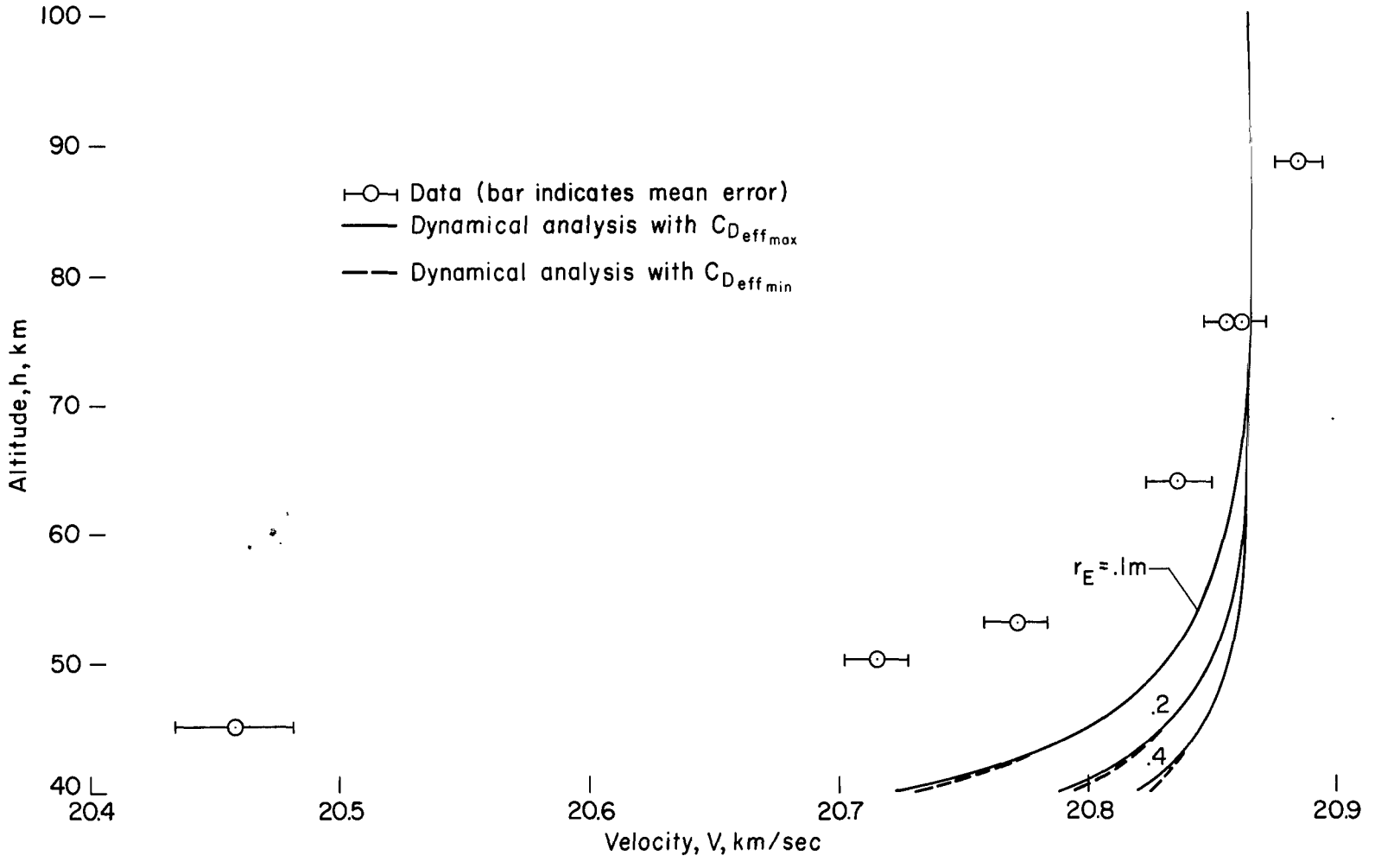

Figure 47.- Comparison of calculated velocity using estimated heating characteristics with data for Ondřejov meteor Příbram.

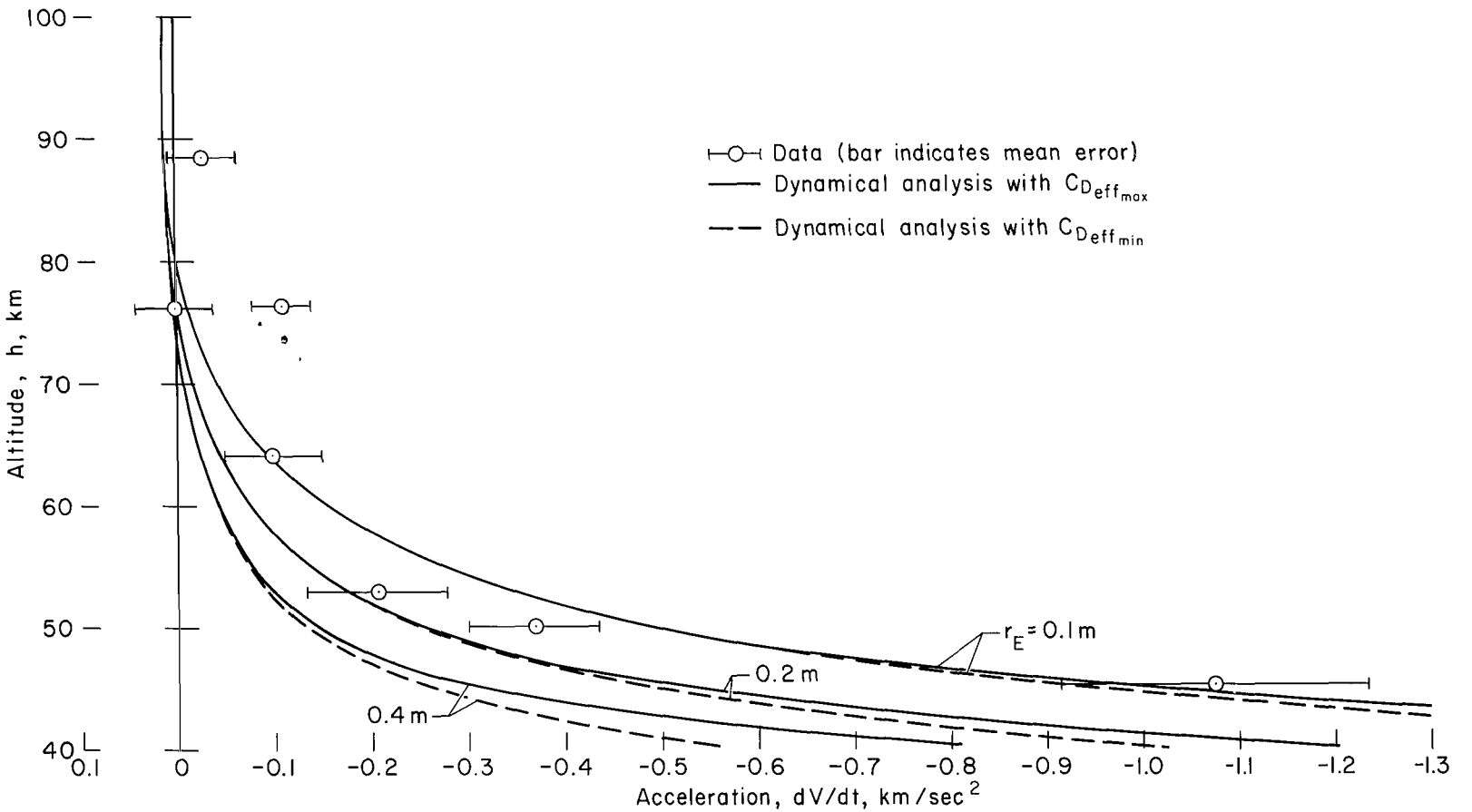

Figure 48.- Comparison of calculated acceleration using estimated heating characteristics with data for Ondřejov meteor Příbram.

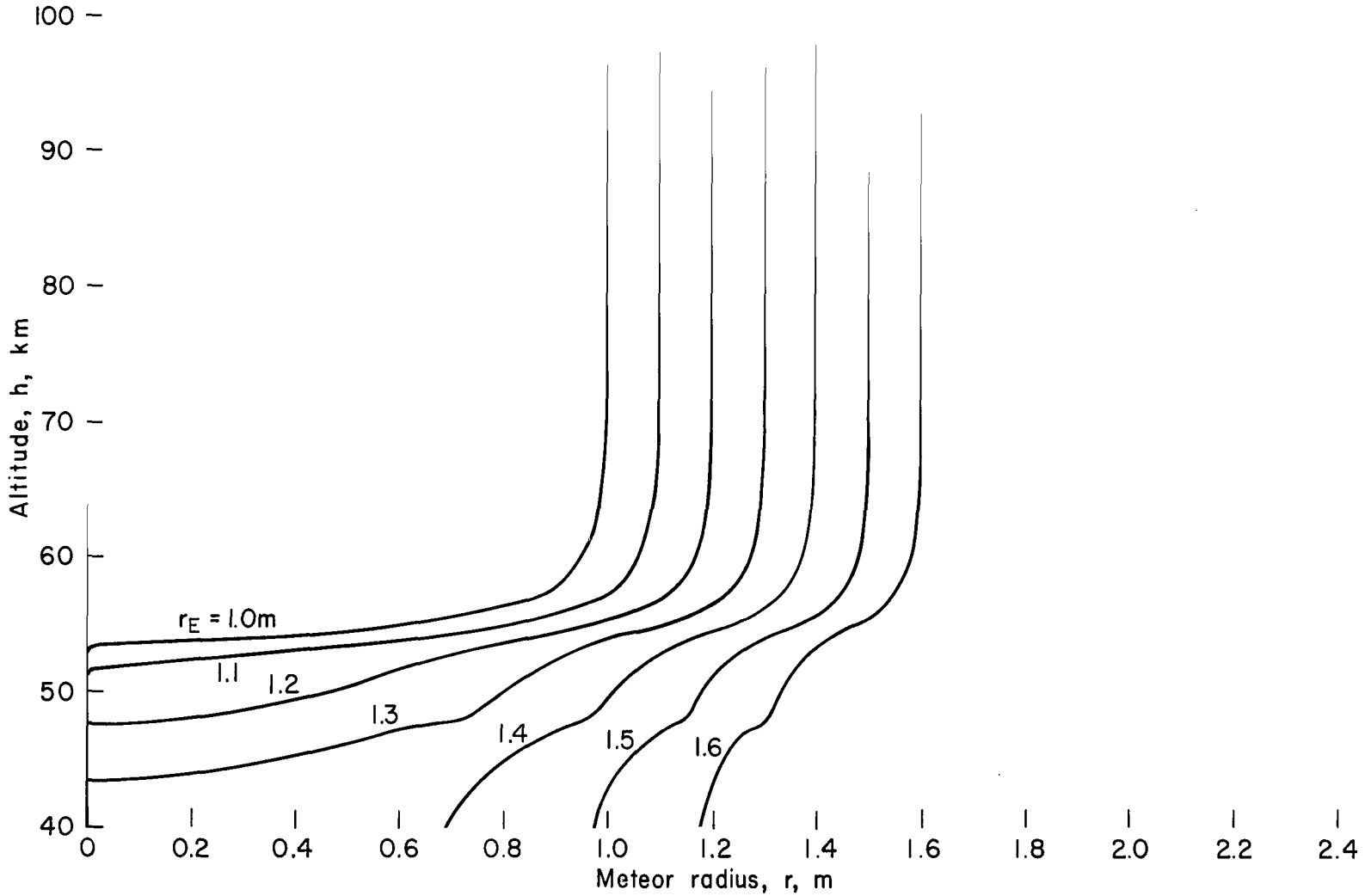

Figure 49.- Radius variation computed from photometrical analyses for Ondřejov meteor Příbram.

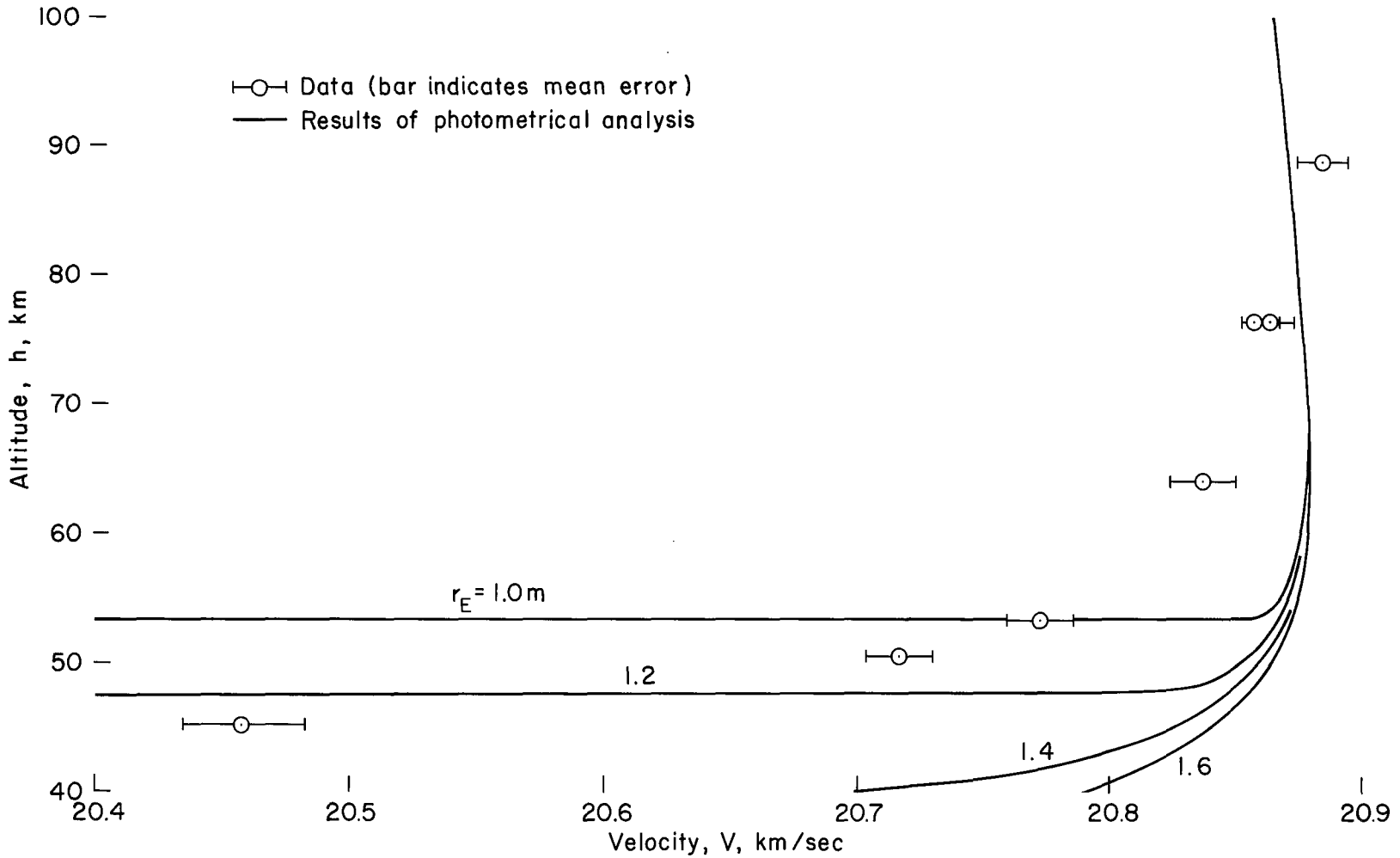

(a) For minimum effective drag.

Figure 50.- Comparison of calculated velocity from photometrical analysis with data for Ondřejov meteor Příbram.

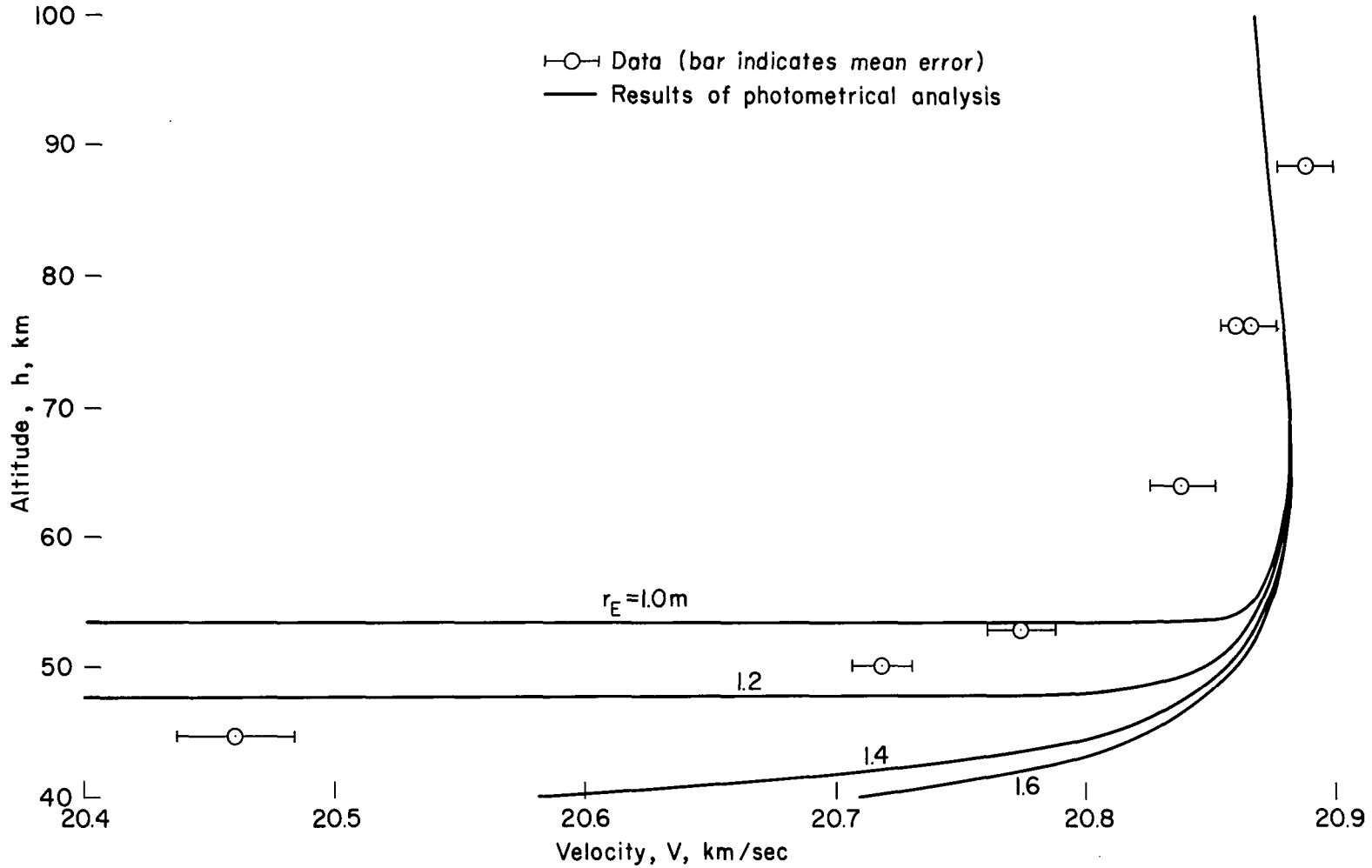

(b) For maximum effective drag.

Figure 50.- Concluded.

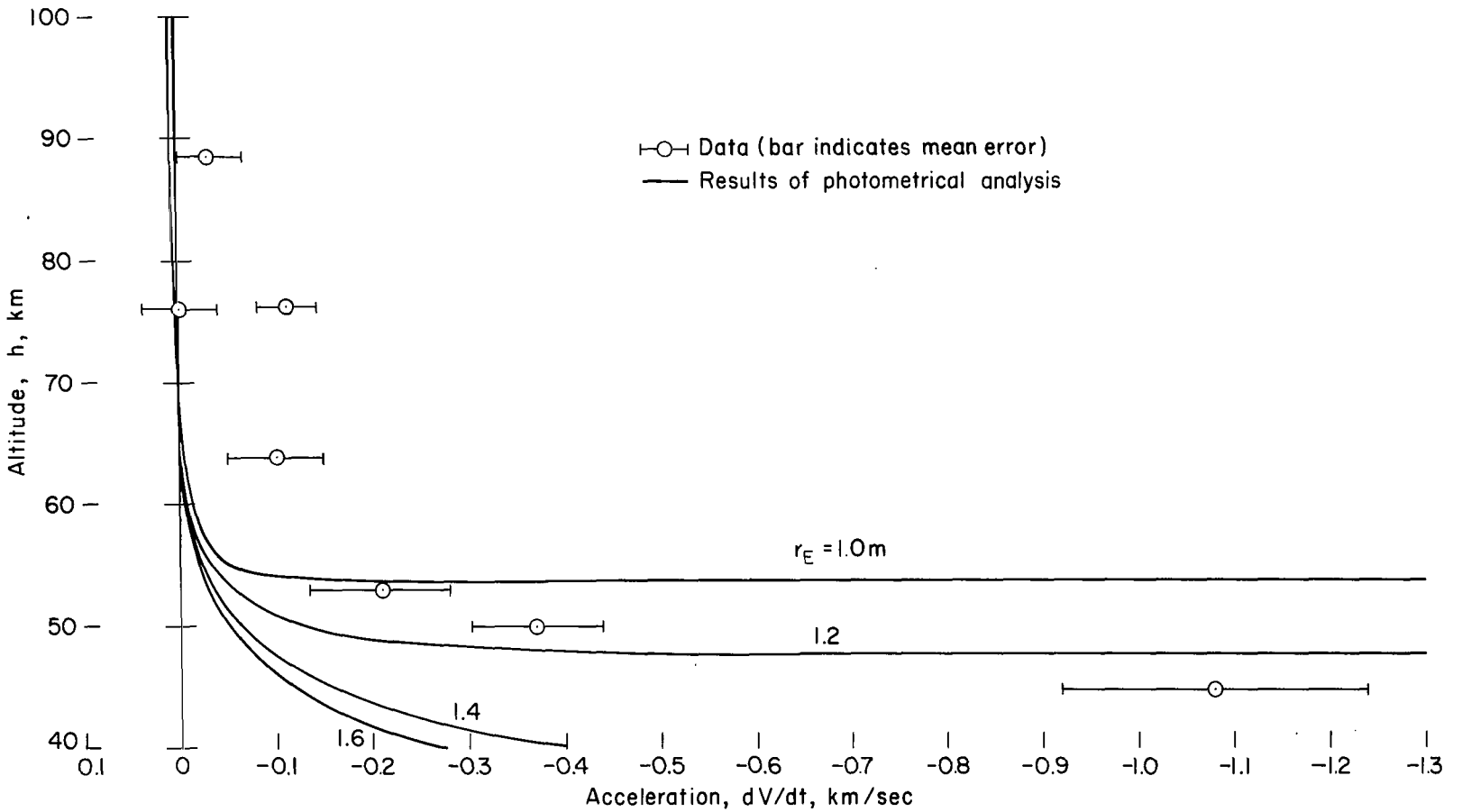

(a) For minimum effective drag.

Figure 51.- Comparison of calculated acceleration from photometrical analysis for Ondřejov meteor Příbram.

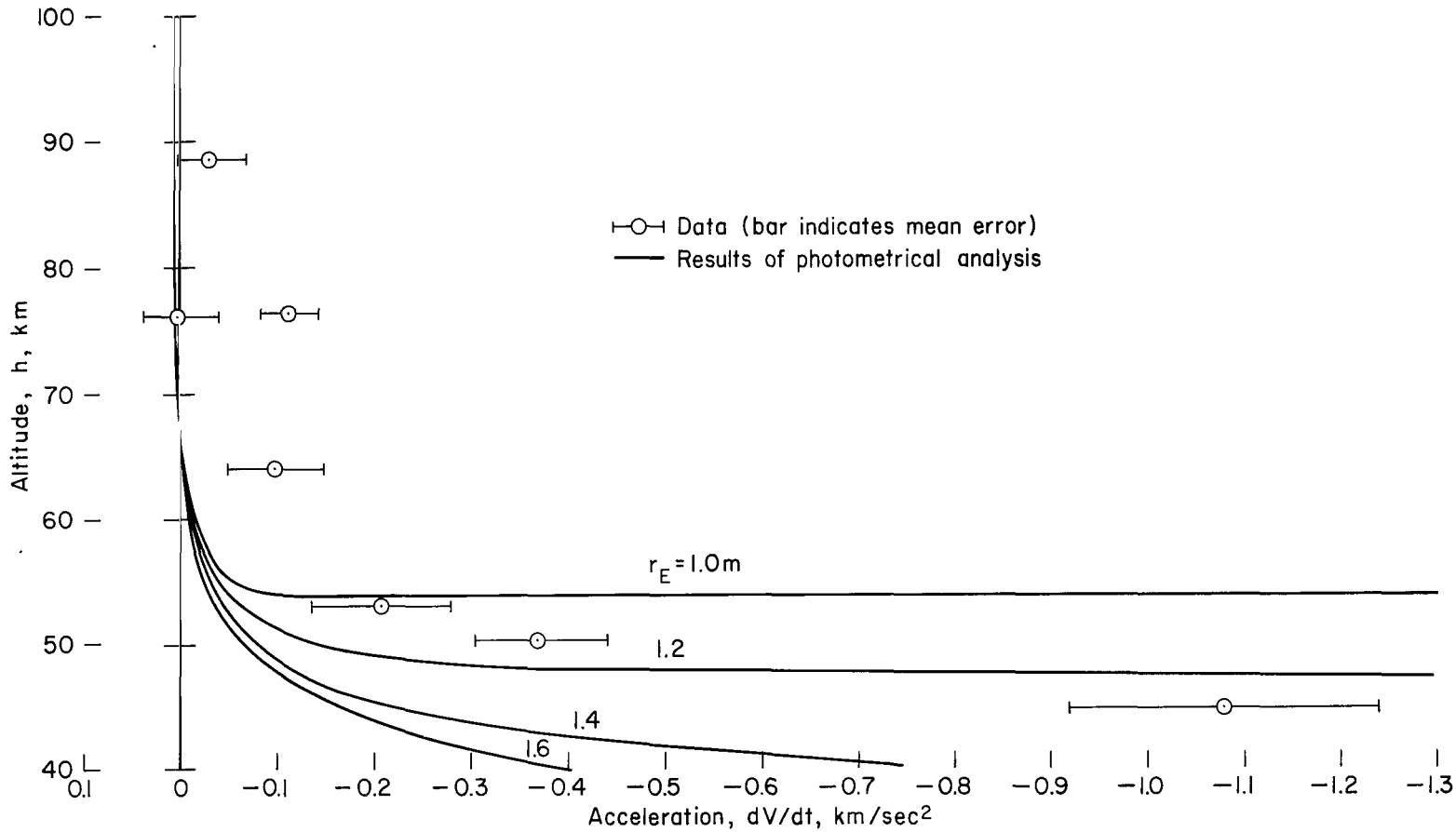

(b) For maximum effective drag.

Figure 51.- Concluded.

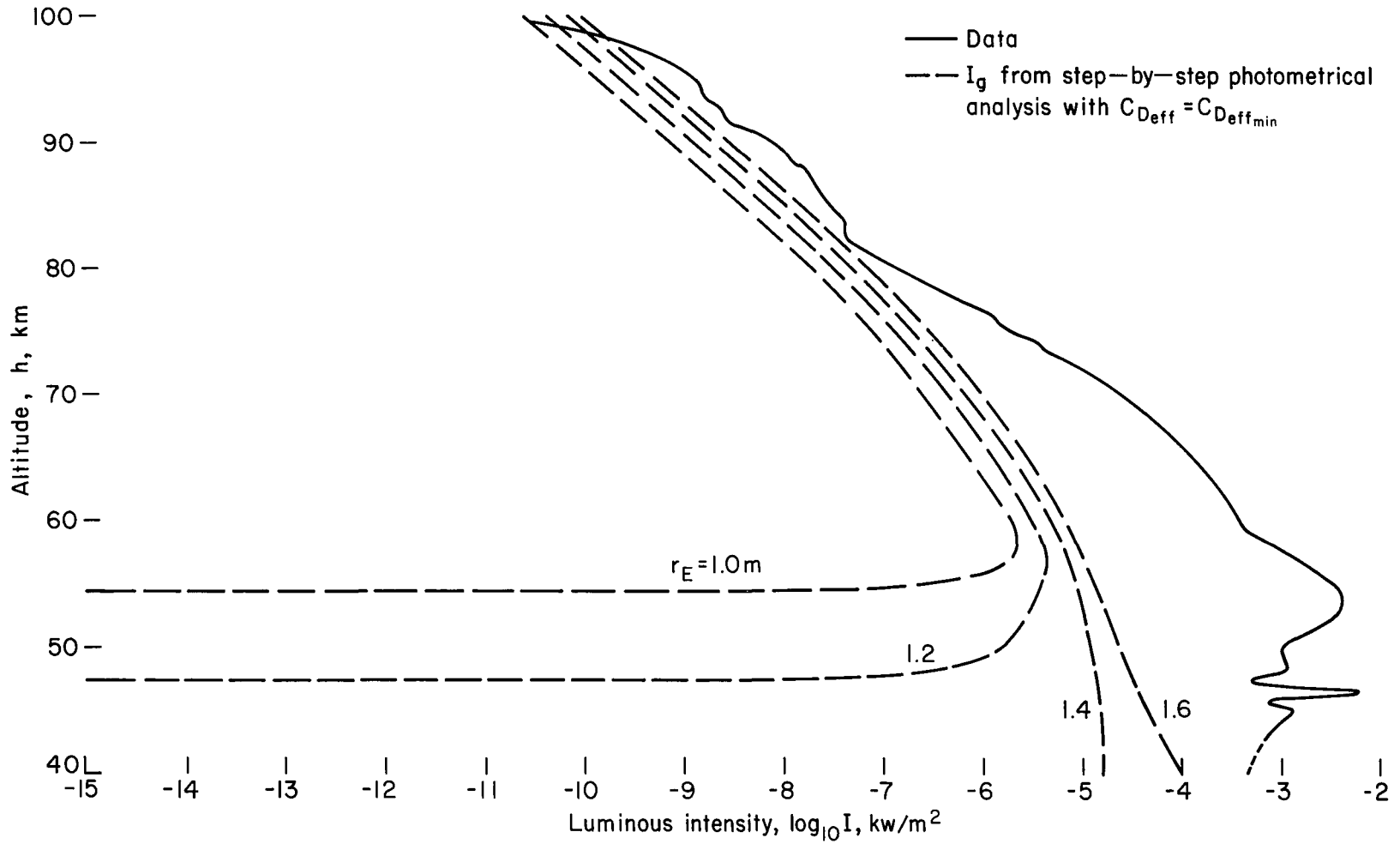

Figure 52.- Comparison of calculated gas-cap luminous intensity with total measured intensity for Ondřejov meteor Příbram.

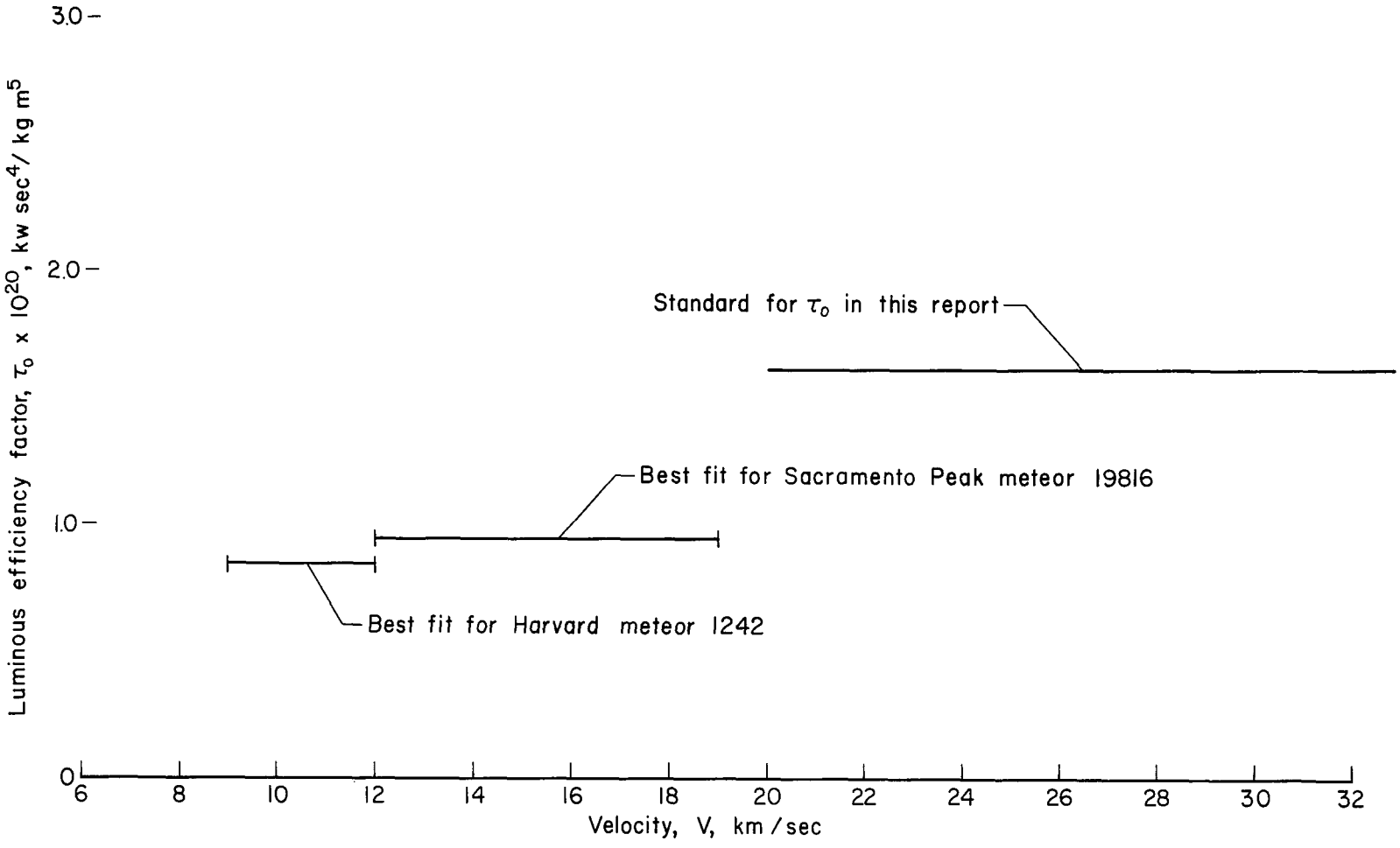

Figure 53.- Comparison of best-fit luminous efficiency factors with the standard.

Figure 54.- Photograph of an imitation meteoric body in flight.

A-31287

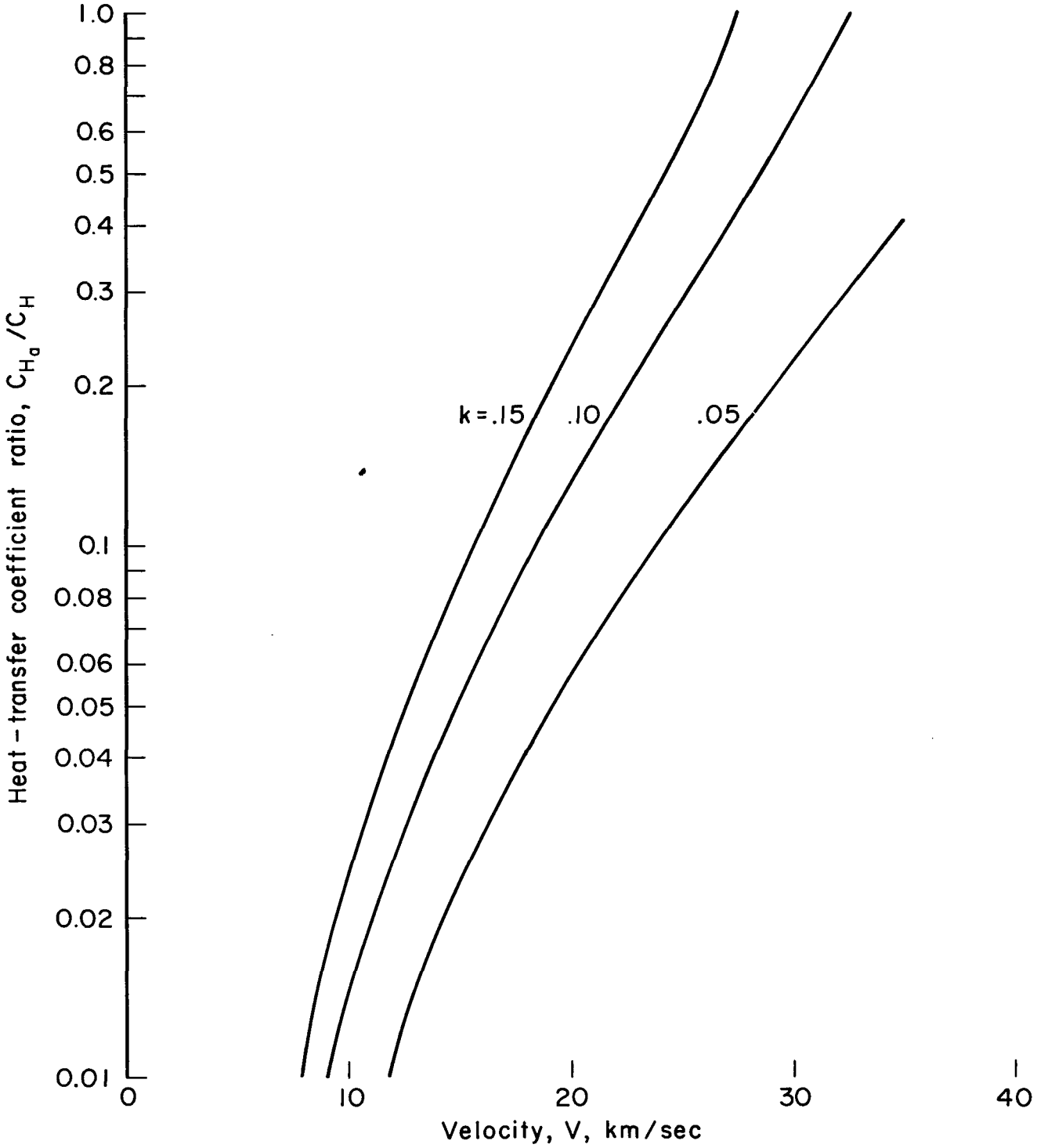

Figure 55.- Ratio of ablation radiation heat-transfer coefficient to total heat-transfer coefficient as a function of velocity.

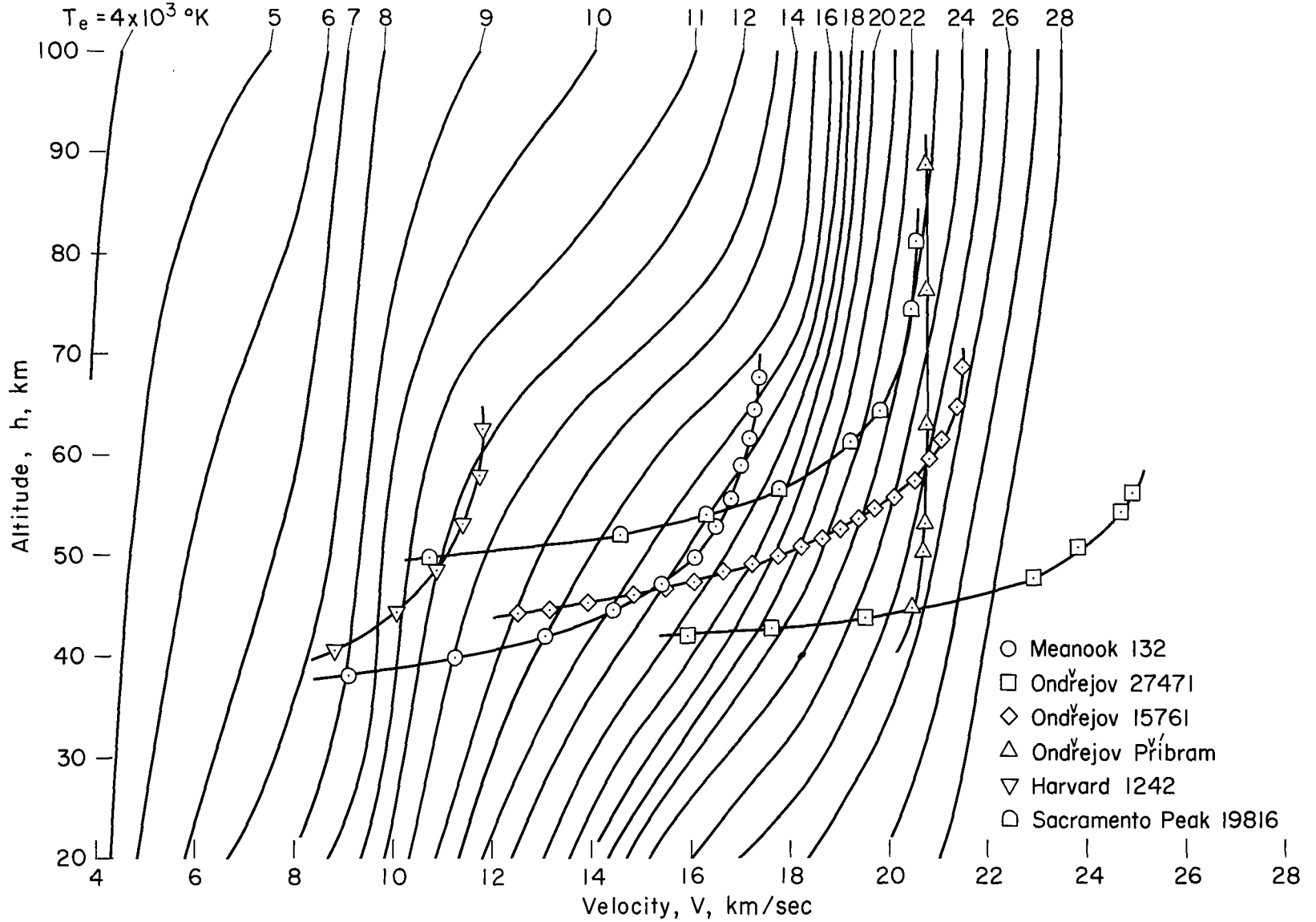

Figure 56.- Equilibrium gas-cap temperatures for the various meteors as a function of altitude and velocity.

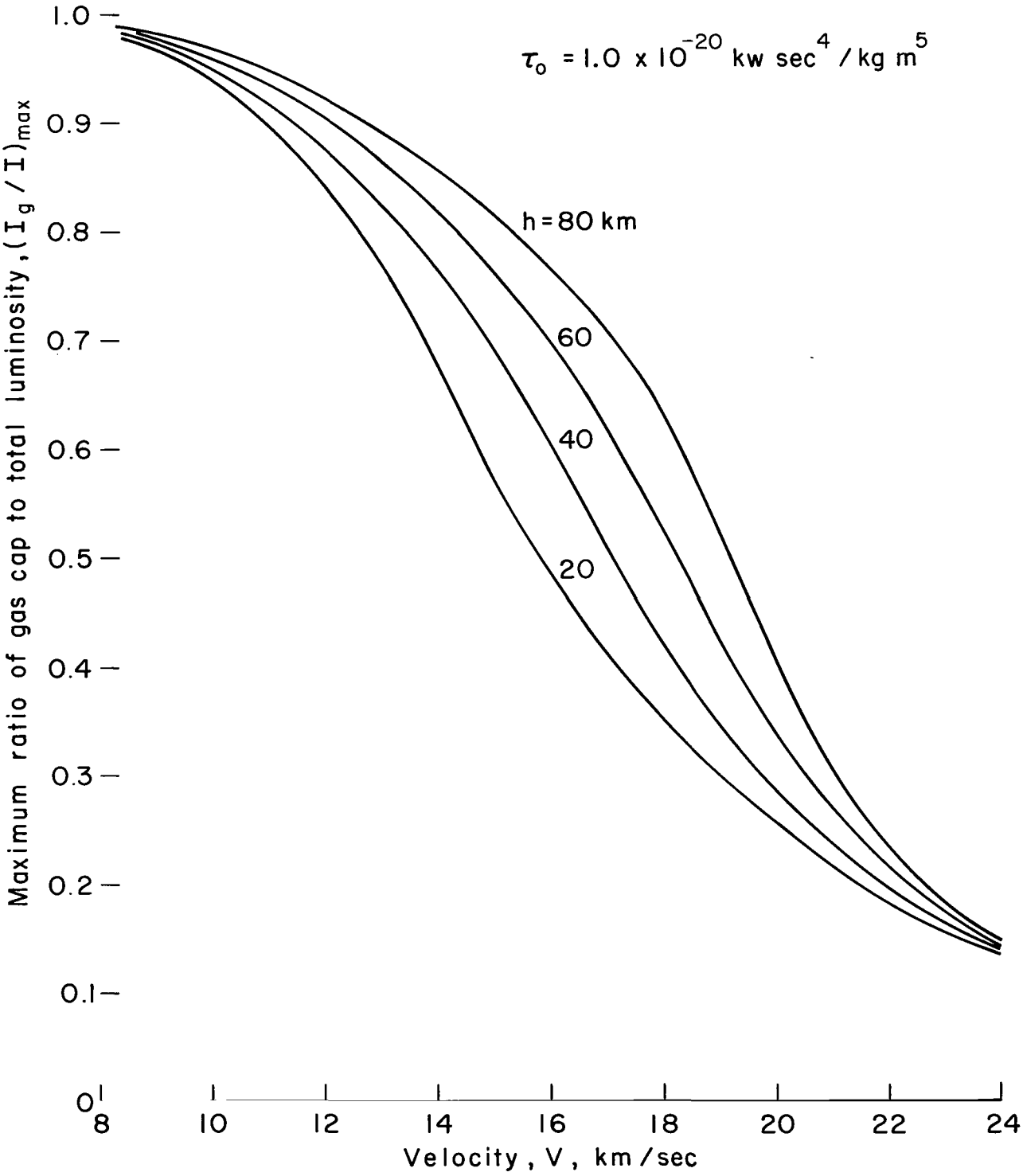

Figure 57.- Maximum ratios of gas-cap to total luminosity as a function of velocity.

"The aeronautical and space activities of the United States shall be conducted so as to contribute . . . to the expansion of human knowledge of phenomena in the atmosphere and space. The Administration shall provide for the widest practicable and appropriate dissemination of information concerning its activities and the results thereof."

—NATIONAL AERONAUTICS AND SPACE ACT OF 1958

NASA SCIENTIFIC AND TECHNICAL PUBLICATIONS

TECHNICAL REPORTS: Scientific and technical information considered important, complete, and a lasting contribution to existing knowledge.

TECHNICAL NOTES: Information less broad in scope but nevertheless of importance as a contribution to existing knowledge.

TECHNICAL MEMORANDUMS: Information receiving limited distribution because of preliminary data, security classification, or other reasons.

CONTRACTOR REPORTS: Technical information generated in connection with a NASA contract or grant and released under NASA auspices.

TECHNICAL TRANSLATIONS: Information published in a foreign language considered to merit NASA distribution in English.

TECHNICAL REPRINTS: Information derived from NASA activities and initially published in the form of journal articles.

SPECIAL PUBLICATIONS: Information derived from or of value to NASA activities but not necessarily reporting the results of individual NASA-programmed scientific efforts. Publications include conference proceedings, monographs, data compilations, handbooks, sourcebooks, and special bibliographies.

Details on the availability of these publications may be obtained from:

SCIENTIFIC AND TECHNICAL INFORMATION DIVISION

NATIONAL AERONAUTICS AND SPACE ADMINISTRATION

Washington, D.C. 20546